

Examination of the Neuroprotective Effects of URB597 in Young and Aged Rat Retina

by

Joanna Slusar

Submitted in partial fulfilment of the requirements  
for the degree of Master of Science

at

Dalhousie University  
Halifax, Nova Scotia  
September 2010

© Copyright by Joanna Slusar, 2010

DALHOUSIE UNIVERSITY

Department of Pharmacology

The undersigned hereby certify that they have read and recommend to the Faculty of Graduate Studies for acceptance a thesis entitled “Examination of the Neuroprotective Effects of URB597 in Young and Aged Rat Retina” by Joanna Slusar in partial fulfillment of the requirements for the degree of Master of Science.

Dated: September 23, 2010

Supervisor:

Readers:

---

---

---

DALHOUSIE UNIVERSITY

DATE: September 23, 2010

AUTHOR: Joanna Slusar

TITLE: Examination of the Neuroprotective Effects of URB597 in Young and Aged  
Rat Retina

DEPARTMENT OR SCHOOL: Pharmacology

DEGREE: MSc

CONVOCATION: May

YEAR: 2011

Permission is herewith granted to Dalhousie University to circulate and to have copied for non-commercial purposes, at its discretion, the above title upon the request of individuals or institutions.

---

Signature of Author

The author reserves other publication rights, and neither the thesis nor extensive extracts from it may be printed or otherwise reproduced without the author's written permission.

The author attests that permission has been obtained for the use of any copyrighted material appearing in the thesis (other than the brief excerpts requiring only proper acknowledgement in scholarly writing), and that all such use is clearly acknowledged.

## DEDICATION PAGE

This work is dedicated to Ben for always minimizing my failures and exaggerating my accomplishments.

## TABLE OF CONTENTS

LIST OF FIGURES.....	viii
ABSTRACT.....	x
LIST OF ABBREVIATIONS AND SYMBOLS USED.....	xi
ACKNOWLEDGEMENTS.....	xiv
<b>Chapter 1: Introduction.....</b>	<b>1</b>
1.1 Anatomy and Physiology of the Eye.....	1
1.2 The Retina.....	6
1.3 Anatomy of Blood Flow to the Eye.....	10
1.3.1 Choroidal Vasculature.....	13
1.3.2 Retinal Vasculature.....	16
1.4 Ocular Blood Flow Autoregulation.....	20
1.5 The Aged Eye.....	21
1.6 Age-Related Eye Diseases.....	22
1.6.1 Age-Related Macular Degeneration.....	23
1.6.2 Diabetic Retinopathy.....	23
1.6.3 Glaucoma.....	24
1.6.4 Anterior Ischemic Optic Neuropathy.....	25
1.7 The Endocannabinoid System.....	25
1.8 Endocannabinoids in the Eye.....	32
1.9 Endocannabinoids as Therapeutic Targets in the Eye.....	34
1.10 The Rat As An Animal Model of Age-Related Eye Diseases.....	37
1.11 Research Objectives.....	38
<b>Chapter 2: Methods.....</b>	<b>40</b>
2.1 Animals.....	40
2.2 Physiological Baseline Parameter.....	40
2.2.1 Blood Pressure.....	40
2.2.2 Blood Glucose Levels.....	41
2.2.3 Intraocular Pressure.....	41
2.3 Labelling Cells of the Retina.....	42
2.3.1 Retrograde Labelling of RGCs with Fluorogold from the SC.....	43

2.3.2 Retrograde Labelling of RGCs with Fluorogold from the Optic Stump.....	43
2.4 Pharmacological Agents.....	44
2.5 Animal Models of Disease.....	45
2.5.1 Axotomy.....	45
2.5.2 Acute Ischemia-Reperfusion through Occlusion of the Pterygopalatine Artery.....	46
2.5.3 Chronic Ischemia through Occlusion of the Common Carotid Arteries.....	49
2.6 Visualizing the Vasculature of the Retina.....	49
2.6.1 Lectin Immunolabelling.....	49
2.6.2 ADPase Stain.....	51
2.7 Labelling of Activated MG.....	52
2.8 Imaging and Quantification of RGCs, MG, and Vascular Density.....	53
2.9 Statistical Analysis.....	54
<b>Chapter 3: Results.....</b>	<b>55</b>
3.1 Comparison of Physiological Parameters and Retinal Vasculature in Young and Aged Animals.....	55
3.2 Retinal Vascular Measurements in Young and Aged Retina.....	55
3.3 Retinal Ganglion Cell Density in Vehicle- and URB597-treated Young and Aged Retina Following 1 and 2 Weeks of Axotomy.....	65
3.4 Phagocytotic Microglia Density in Vehicle- and URB597-treated Young and Aged Retina Following 1 and 2 Weeks of Axotomy.....	71
3.5 Capillary Intersection Density in Vehicle- and URB597-treated Young and Aged Retina Following 2 Weeks of Axotomy.....	74
3.6 Retinal Ganglion Cell and Phagocytotic Microglia Density in Vehicle- and URB597-treated Young and Aged Retina after Ischemia-Reperfusion.....	77
3.7 Capillary Intersections in Vehicle- and URB597-treated Young and Aged Retina Following 2 Weeks of Ischemia-Reperfusion Injury.....	80
3.8 Retinal Ganglion, Phagocytotic Microglia and Capillary Intersection Density Following Chronic Ischemia in Young Retina.....	83
<b>Chapter 4: Discussion.....</b>	<b>92</b>
4.1 Overview of Findings.....	92

4.2 Impact of Age and URB597 treatment on the Response of Retinal Neurons, Glia and Vasculature to Axotomy and Ischemic Insult.....	94
4.2.1 Retinal Vasculature.....	94
4.2.2 RGC.....	95
4.2.3 MG.....	98
4.2.4 Vasculature.....	99
4.3 Limitations and Future Directions.....	101
4.4 Clinical Implications and the Potential of URB597 as a Therapeutic Agents.....	103
4.5 Conclusion.....	104
<b>References.....</b>	<b>106</b>
<b>Appendix: Figures Licences.....</b>	<b>130</b>

## LIST OF FIGURES

Figure 1.1 The Eye and it's Light Processing Structures.....	2
Figure 1.2 Cells of the Retina.....	7
Figure 1.3 The Three Main Blood Systems to the Eye.....	11
Figure 1.4 Both the Retinal and Choroidal Vasculature Provide Blood to the Retina.....	14
Figure 1.5 Capillary-Free Zones Surround Retinal Arteries.....	18
Figure 1.6 Synthesis and Degradation of Anandamide.....	30
Figure 2.1 Animal Model of Ischemia-Reperfusion and Chronic Ischemia.....	47
Figure 3.1 Aging does not Impact Physiological Baseline Parameters.....	56
Figure 3.2 Age-Related Effects on Retinal Vasculature.....	58
Figure 3.3 Aged Rat Retinal Capillaries Show Differences in ADPase-Staining Compared to Young retinas.....	61
Figure 3.4 Aged Rat Retinal Capillaries Show Differences in Lectin-Staining Compared to Young.....	63
Figure 3.5 URB597 Provides Neuroprotection in Young Retina but not in Aged Retina Following 1 and 2 week Axotomy.....	66
Figure 3.6 URB597 Reduces Phagocytotic Microglia Density After 2 Weeks Axotomy in Young but not Aged Retina.....	69
Figure 3.7 URB597 Localized Iba1 Staining of Activated Microglia to the Ganglion Cell Layer in Young Rat Retina Following 1 Week of Axotomy.....	72
Figure 3.8 Age, Not Axotomy, Produces a Significant Effect on Capillary Intersection Density.....	75
Figure 3.9 URB597 Does Not Alter Retinal Ganglion or Microglia Cell Density in Young and Aged Rat Retina Following Transient Ischemia-Reperfusion.....	78
Figure 3.10 Transient Ischemia-Reperfusion Does Not Produce an Effect on Capillary Intersection Density.....	81
Figure 3.11 URB597 Provides Neuroprotection Following Chronic Ishemia in Young Rat Retina.....	84



Figure 3.12 URB597 Reduces phagocytotic Microglia in Young Rat Retina Following Chronic Ischemia.....	86
Figure 3.13 URB597 Promotes Retinal Capillary Stability Following Chronic Ischemia.....	89

## **ABSTRACT**

Anandamide (AEA), a well characterized endocannabinoid that has actions at multiple targets in the eye, may have potential as a novel therapeutic in the treatment of retinal disease. However, AEA is rapidly degraded by fatty acid amide hydrolase (FAAH). Therefore this study examined the drug URB597, that inhibits FAAH degradation of AEA, to assess AEA effects in experimental models of retinal damage. The objectives were to: 1) evaluate changes present in the aging retina, 2) determine whether the aging retina is more susceptible to tissue damage, and 3) investigate whether increasing AEA can provide retinal neurovascular protection in young and aged retina following damage. The results from this study showed that URB597 had protective effects on retinal ganglion cells and retinal capillaries and inhibited phagocytotic MG in models of retinal damage in young, but not the aged retina.

## LIST OF ABBREVIATIONS AND SYMBOLS USED

Abn-CBD	abnormal cannabidiol
ADPase	adenosine diphosphatase
AEA	anandamide
AH	aqueous humour
AMD	age-related macular degeneration
BCCAO	bilateral common carotid artery occlusion
Ca <sup>2+</sup>	calcium
CBR	cannabinoid receptors
CB1	cannabinoid subtype 1 receptor
CB2	cannabinoid subtype 2 receptor
CBx	novel vascular cannabinoid receptor
CNS	central nervous system
CRA	central retinal artery
CRV	central retinal vein
DAG	diacylglycerol
DAGL	diacylglycerols-lipase
diAPC	di-arachidonoylphosphatidylcholine
DMSO	dimethyl sulfoxide
DR	diabetic retinopathy
eCBS	endocannabinoid system
eCB	endocannabinoid
ET-1	endothelin
FAAH	fatty acid amide hydrolase

FG	fluorogold
GABA	$\gamma$ -Aminobutyric acid
GCL	ganglion cell layer
ION	ischemic optic neuropathy
IOP	intraocular pressure
I.P.	intraperitoneal
I-R	ischemia-reperfusion
K <sup>+</sup>	potassium
MAGL	monoacylglycerol lipase
MG	microglia
NAPE	N-arachidonyl phosphatidyl ethanolamine
NAT	N-acyltransferase
NBF	neutral buffered formalin
NMDA	N-methyl-d-aspartate
NO	nitric oxide
NT	neurotransmitter
ONH	optic nerve head
ONL	outer nuclear layer
PBS	phosphate buffered solution
PE	phosphatidylethanolamine
PPA	pterygopalatine artery
PTX	pertussis toxin
RGC	retinal ganglion cell

RPE	retinal pigment epithelium
SC	superior colliculus
SMC	smooth muscle cell
THC	delta-9-tetrahydrocannabinol
TNF $\alpha$	tumour necrosis factor alpha
TRPV1	transient receptor potential vanilloid 1
1W	1 week
2-AG	2-arachidonoylglycerol
2W	2 weeks

## **ACKNOWLEDGEMENTS**

First and foremost, I would like to thank my supervisor Dr. Melanie Kelly for all her advice and direction during these last 2 years. Nova Scotia Health Research Foundation student research award provided financial support that was invaluable to the completion of this project. The Optic Nerve and Retina Research Laboratory has been an amazingly supportive environment. Spring Farrell, Michele Archibald, Jeannette Nason and Kelly Stevens provided advice on everything from animal models to pumpkin cheesecake, and everything in between. I would like to thank Brian Hudson, Alex Dong, Jessica MacIntyre, and Anna Szczesniak for their invaluable insight and support throughout my time with the Kelly Lab. Over the last 2 years there were trying times but the support and friendship of these people ensured I made it to the end! Thank you!

# Chapter 1

## Introduction

### 1.1 Anatomy and Physiology of the Eye

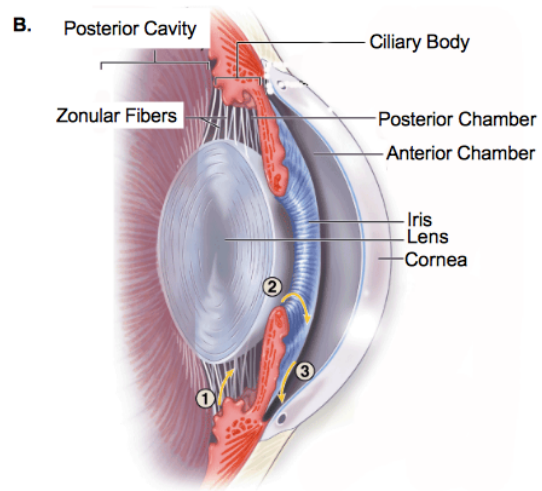
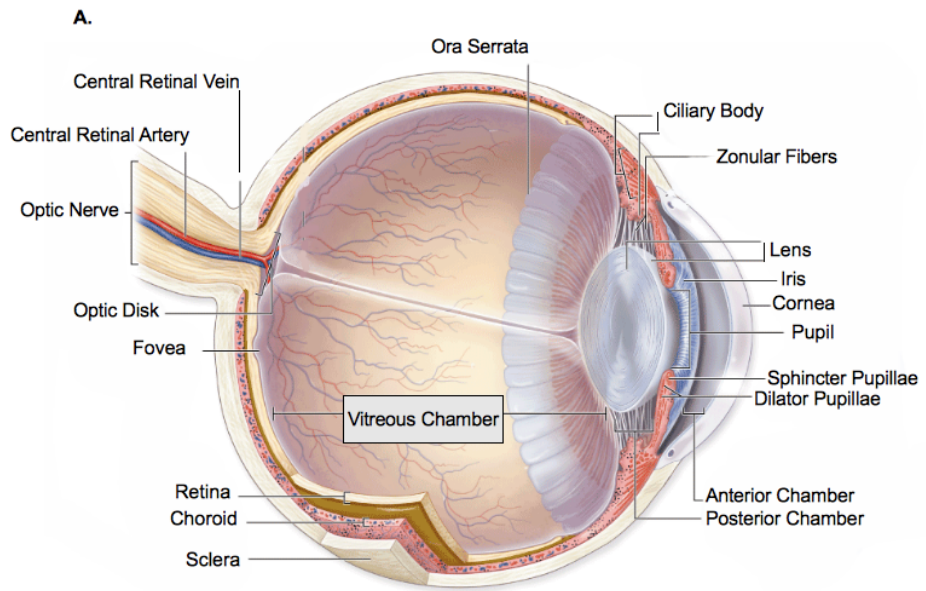
The eye is a specialized sensory organ that detects, processes and transmits light stimuli to the brain where it is interpreted as vision. The overall design of the eye and its individual components is to optimize the transmission and focusing of light onto the retina, a light-sensitive neuronal tissue where light is converted into an electrochemical signal before being relayed to the visual centre of the brain (See Section 1.2). The general anatomy of the eye and surrounding structures are shown in Figure 1.1. The outer-most part of the eye is the sclera; a tough, usually white, fibrous protective layer that contains collagen and elastic fibres. The sclera maintains the shape of the eye globe and offers resistance to internal and external forces. It is also perforated by a number of different blood vessels, nerves and muscles. There are six extraocular muscles within the sclera that enable the eye to move within the skull, which enables focusing in different directions without having to move the head. The extraocular muscles remain concealed by the conjunctiva, a tissue that connects the eye to the eye lid.

The cornea is a transparent, avascular structure and the site where light first makes contact with the eye (Figure 1.1A); therefore, the cornea is very important in ensuring light is refracted appropriately and accounts for approximately two thirds of the total refractive power of the eye (Bear et al., 2001). The cornea receives nutrients and exchanges waste with the tear film at the front of the cornea and the aqueous humor behind the cornea. The aqueous humor (AH) is a water-like substance that provides

**Figure 1.1 The Eye and its Light Processing Structures**

**A.** Sagittal section of the human eye depicting the sclera, choroid and cornea. The image shows the anterior portion of the eye housing the pupil, iris, dilator pupillae, sphincter pupillae, the zonular fibers, ciliary body, anterior chamber and the ora serrata. The posterior portion of the eye contains the optic nerve, optic disk, retina, fovea, central retinal vein and central retinal artery. **B.** Sagittal section of the anterior chamber of the eye showing the structures involved in aqueous humour production and outflow. This image depicts aqueous humour production by the ciliary body of the eye. (1) Aqueous humour flows from the posterior chamber to the anterior chamber (2) and drains through Schlemm's canal into the ciliary veins (3). The posterior cavity, zonular fibers, ciliary body, iris, lens and cornea are shown in reference to the anterior portion of the eye. Adapted from **Vaughan & Asbury's General Ophthalmology** with permission from McGraw-Hill Education.





immune activity, nutrients and waste removal to both the avascular lens and cornea. The AH is also vital in maintaining the intraocular pressure (IOP), which is determined by AH production and outflow. AH production is a dynamic process: AH is constantly being produced by the ciliary body of the posterior chamber at the base of the cornea, where it flows from the posterior to anterior cavity of the eye (Figure 1.1B). The AH is then drained into Schlemm's canal through the trabecular meshwork into the ciliary veins (Figure 1.1B). Alterations in AH production and outflow can have profound effects on cells of the retina as seen in various forms of glaucoma, in which elevated IOP is a primary risk factor for development of the disease (See Section 1.6).

The pupil is the aperture of the eye and is regulated by two muscles of the iris (Figure 1.1A) that have opposing effects on pupil size. The contraction of the sphincter pupillae, causes the pupil to constrict and reduces its opening, while the contraction of the dilator pupillae causes the pupil opening to increase, thus increasing the amount of light entering the eye. These muscles are a part of the pupillary light reflex which involves connections between the retina, neurons in the brain stem, and the muscles of the iris, to communicate the amount of incoming light and adjust the size of the pupil accordingly (Bear et al., 2001). Various pharmacological agents, such as atropine and marijuana, have the ability to influence pupil diameter. Atropine and atropine-like drugs which block muscarinic receptors, for example, are commonly used during ophthalmic examinations to dilate the pupils.

Directly behind the iris is the lens. The lens separates the eye into two chambers, the anterior cavity, which houses the AH in front of the lens, and the posterior cavity, which houses the vitreous humour immediately behind the lens (Figure 1.1A). The lens is an

avascular, transparent, biconvex structure suspended in the vitreous humour by ligaments called zonule fibres. These ligaments are attached to the ciliary bodies, which are embedded in the sclera, and form a ring within the eye, becoming an anatomical landmark referred to as the ora serrata (Figure 1.1A). When the ciliary muscles of the ciliary body contract, the diameter of the ring becomes smaller, the ligaments attached to the lens are relaxed, and the lens is thicker and more rounded due to its naturally elastic properties. The opposite holds true when the ciliary muscles are relaxed, the ring's diameter is larger, increasing the tension on the ligaments, and stretching the lens to make it more flat. The ability of the lens to stretch and become thinner, or to relax and become more round, helps process objects from different viewing distances, by refracting light, and adjusting the focusing power. Focusing on an object further away, such as a stop sign, requires relaxation of the ciliary muscles, increasing tension on zonules fibres, which flattens the lens, increasing the focal distance. In contrast, reading a book causes the contraction of ciliary muscles, decreasing tension on the zonule fibres allowing the lens to become more rounded, increasing the refractive power of the lens (Bear et al., 2001).

The vitreous humour is a transparent, gelatinous material that fills the eye from the lens to the retina (Figure 1.1A). It ensures the retina stays against the back of the eye, gives the eye globe shape, and further refracts light. Unlike the dynamic production of AH, the vitreous humour is stagnant and not constantly replenished. At the back of the eye lies the multi-cellular, light-sensitive retina. The photoreceptors that are activated by photons of light are at the very back of the eye, so light has to transverse all the cell layers of the retina before reaching the photoreceptors. This is necessary as the photoreceptors need to be in contact with the retinal pigment epithelium (RPE) to recycle

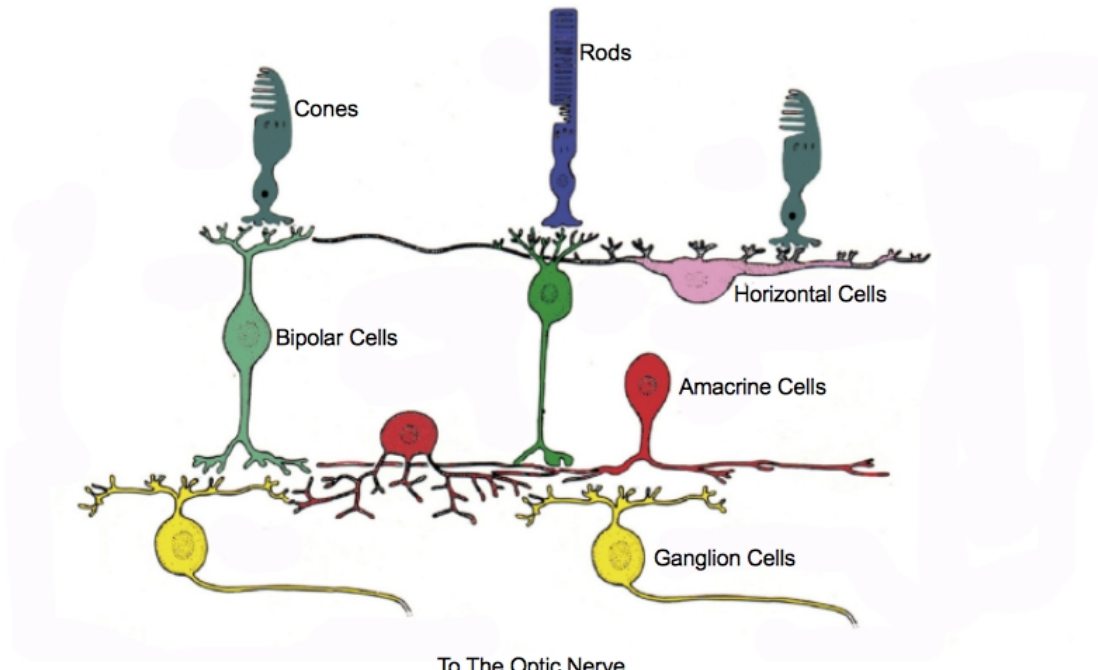
photopigments necessary to convert light into an electrochemical signal. The pigmented RPE also serves to absorb stray photons of light, to prevent light from bouncing off the back of the eye, activating retinal photoreceptors and blurring vision (Kolb et al., 2001). The RPE is also in contact with Bruch's membrane, a connective tissue that separates the RPE from the vascular choroid and the sclera.

## **1.2 The Retina**

The retina and the optic nerve are derived from the neuroectoderm during development, as are the brain and spinal cord, and thus are considered to be part of the central nervous system (CNS). The retina has a laminar organization, described by its position closest to the middle of the eye (Figure 1.2). These layers are characterized by the cell types that compose each layer and their specific function in intraretinal signalling. The retinal ganglion cell (RGC) bodies form the ganglion cell layer (GCL) and are at the front of the retina, while the light-activated photoreceptors are at the back of the retina. At the back of the retina in the outer nuclear layer (ONL), are the photoreceptors which are composed of two different segments; the outer segment containing stacks of membranous discs where light-sensitive opsins absorb light, and the inner segment housing mitochondria (Kolb et al., 2001). There are two different types of photoreceptors, rods and cones. Rods have a greater number of membranous discs and therefore have a high proportion of opsin, increasing their sensitivity to light. Thus, rods are considered to be the photoreceptors responsible for the ability to see in dim light. Although cones have less opsin than rods, there are 3 different types of cones, each of which contain a different type of opsin sensitive to different wavelengths of light. This sensitivity of cones to

**Figure 1.2 Cells of the Retina**

This schematic of the vertebrate retina shows the photoreceptors, rods and cones, bipolar cells, horizontal cells, amacrine cells, ganglion cells and the formation of the optic nerve by ganglion cell axons. The schematic also depicts the direction of light transmission through the retina. Adapted from **Physiology and Pathophysiology of Somatostatin in the Mammalian Retina: A Current View** with permission from Elsevier.



different wavelengths of light provide colour vision.

In the human eye, the macula is the region of the retina that facilitates central vision and permits high resolution visual acuity due to its dense concentration of photoreceptors resulting in a low ratio of cones to retinal ganglion cells (Kolb et al., 2001). The fovea is in the centre of the macula, an area of the retina identified by its absence of large blood vessels and trajectory of the optic nerve, which both arc around the fovea to prevent their shadows from disrupting light transmission. In contrast, the periphery of the retina has the lowest number of cones, highest number of rods and a high ratio of rods to RGCs. This results in greater light sensitivity, but poor resolution in high intensity light (Kolb et al., 2001).

In the inner nuclear layer lie the horizontal cells, bipolar cells and amacrine cells. Bipolar cells have a central body from which two sets of processes arise and can synapse with either rods or cones and transmit signals to the RGCs (Kolb, 2001). Bipolar cells also receive input from horizontal cells, which provide feedback from other bipolar cells and photoreceptors. Amacrine cells lie in the layer of the retina where bipolar cells synapse with RGCs. Amacrine cells provide feedback onto bipolar cells, RGCs and other amacrine cells. Each synaptic relay response is modified by lateral connections of horizontal and amacrine cells to produce a localized response (Kolb, 2003) (Figure 1.2).

Photoreceptors are influenced directly by light while most other cells of the retina are activated by direct or indirect synaptic interactions. RGCs are the only cells of the retina that can produce action potentials, as all other retinal cells generate graded membrane potentials (Kolb, 2001). The RGCs are also the only source of output from the retina, with their axons leaving the retina to form the optic nerve. It is this collection of signals

from individual cells of the retina that provide vision.

The axons of RGCs gather and exit the eye at the optic nerve head (ONH), and then travel behind the eyes to pass through the optic foramen (Bear et al., 2001). The optic nerve from each eye combines to form the optic chiasm where the axons originating in the left eye cross to the right side of the optic chiasm and vice versa. Thus, the information about the left visual hemifield is directed to the right side of the brain and the right visual hemifield to the left side of the brain (Bear et al., 2001). Upon crossing at the optic chiasm, these axons have now formed the optic tract. Most axons from the optic tract terminate in the lateral geniculate nucleus where information is relayed to the primary visual cortex and the signals are interpreted as vision. Other axons terminate in the pretectal nucleus or suprachiasmatic nucleus, where these signals are involved in the pupil-light reflex and circadian rhythms, respectively (Hattar et al., 2002).

### **1.3 Anatomy of Blood Flow to the Eye**

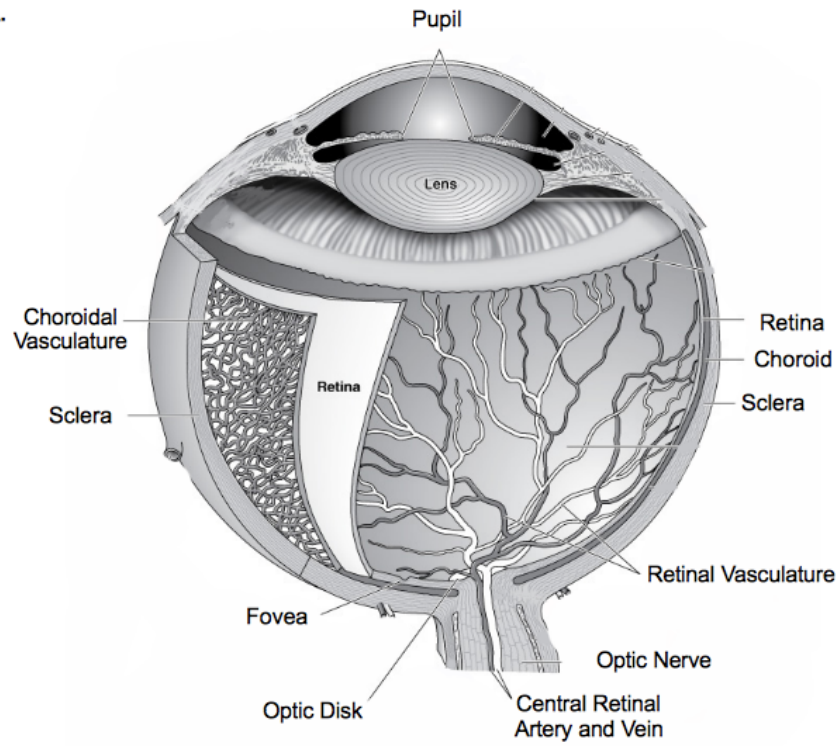
The blood supply to the eye is derived from the ophthalmic artery, which is a branch of the internal carotid, a major artery found in the neck and head and the main source of blood supply to the brain. The ophthalmic artery gives rise to ciliary arteries, that provide the ONH and choroidal circulation, in addition to the central retinal artery (CRA). The CRA runs within the optic nerve sheath before entering the eye to branch into 4 major intraretinal arteries in a pattern that is unique to each individual (Hardy et al., 2005). The retinal arteries and larger vessels are in the innermost part of the retina and travel within the layer of RGC axons, with their walls in close proximity to glial cells (Rungger-Brandle et al., 1993) (Figure 1.3A). These arterioles branch into two capillary plexuses



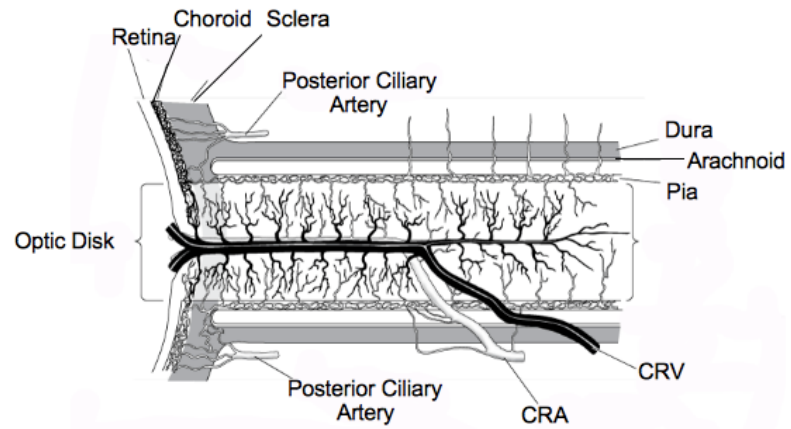
**Figure 1.3 The Three Main Blood Systems to the Eye**

**A.** The illustration depicts a normal human eye with its light processing structures and includes the pupil, cornea, and iris at the anterior of the eye. The image depicts the choroid and its vasculature which provide the avascular photoreceptors, macula and periphery of the retina with paracrine support. The central retinal artery is shown entering the eye and branching into a number of arterioles, providing the retina, with the exception of the periphery and macula, with blood. The central retinal vein (CRV) is shown exiting the eye with the optic nerve. **B.** The illustration shows the optic nerve head (ONH) posterior to the optic disk, retina, choroid and sclera. The ONH derives its major blood supply from the posterior ciliary arteries and branches from the central retinal artery (CRA). The image also shows the CRV, optic nerve, and the membranes that surround the optic nerve such as the pia, arachnoid and dura mater. Adapted from **Vaughan & Asbury's General Ophthalmology** with permission from McGraw-Hill Education.

A.



B.



which extend throughout the eye. Towards the periphery, the deep capillary network disappears leaving a single layer of wide-mesh capillaries. This capillary network services the rest of the eye until the extreme periphery, where there is a 1.5 mm wide avascular zone. The capillaries feed into venules which collect into the central retinal vein (CRV), which leaves the eye to drain into the cavernous sinus. Avascular regions of the retina, such as the periphery, photoreceptors and macula, receive paracrine support from the choroidal vasculature (Parver, 1991), which lies between the sclera and retina (Figure 1.3A). The ONH is supplied with blood from the posterior ciliary artery, with the exception of the ONH nerve fibre layer, which receives blood supply from the CRA (Figure 1.3B).

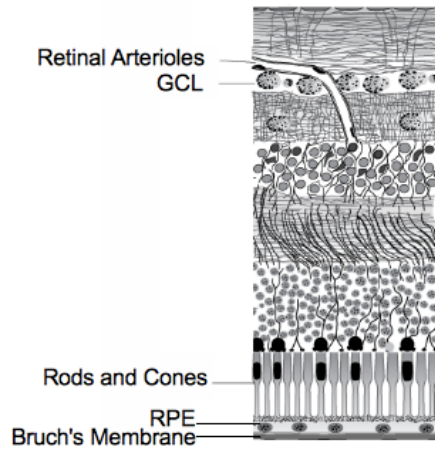
### *1.3.1 Choroidal Vasculature*

The choroidal vasculature, which is characterized by its high flow rate and low oxygen content, receives significant autonomic innervation and is subject to alterations in blood flow by local circulating systemic factors such as hormones (Ryan et al., 2005). The choroid is composed of three layers, with its largest arteries and veins found closest to the sclera, at the back of the eye, in Halley's layer (Figure 1.4C). The middle layer of the choroid, Sattler's layer, has arteries that branch into smaller arterioles and a few venules that carry deoxygenated blood to the cavernous sinus, where most of the blood supply from the choroid drains. The innermost layer of the choroid, closest to the retina, is termed the choriocapillaris, where fan-shaped sections of large (20-50 $\mu$ m) capillaries reside (Hayreh, 1975). The choriocapillaris are fenestrated and lack pericytes (Ryan et al., 2005) (Figure 1.4D). These factors make the choroid less capable of controlling localized tissue responses, thus rendering the choroid more dependent upon perfusion pressure and

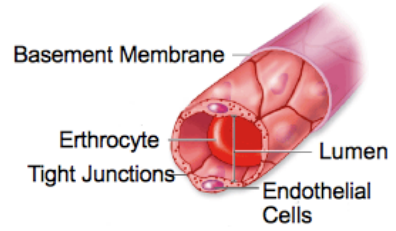
**Figure 1.4 Both the Retinal and Choroidal Vasculature Provide Blood to the Retina**

**A.** Schematic depicting the retina showing small arterioles that enter the retina through the ganglion cell layer (GCL), move posteriorly into the retina to branch into capillaries. The retina is shown with Bruch's membrane, retinal pigment epithelium (RPE) and photoreceptors. **B.** The image depicts capillaries of the retina that are characterized by tight junctions formed between endothelial cells lining the vessel lumen. The image shows the basement membrane and lumen of the capillary with an erythrocyte flowing through. **C.** The schematic depicts the choroidal vasculature layers, the choriocapillaris and larger choroidal vessels, shown posterior to the RPE, and Bruch's membrane. **D.** The image shows the choriocapillaris of the choroid as large (20-50 $\mu$ m), fenestrated capillaries with large intercellular clefts. Adapted from **Junqueira's Basic Histology: Text & Atlas, 12e** and **Vaughan & Asbury's General Ophthalmology** with permission from McGraw-Hill Education.

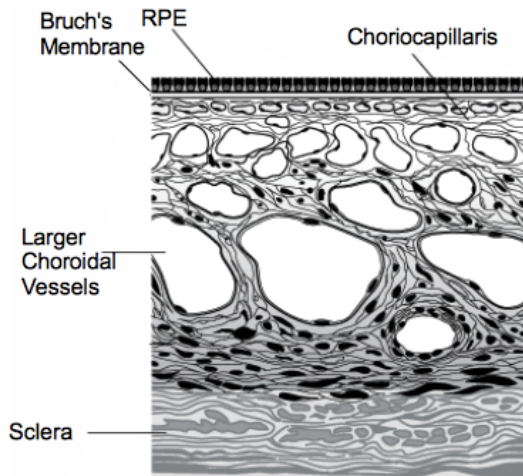
A.



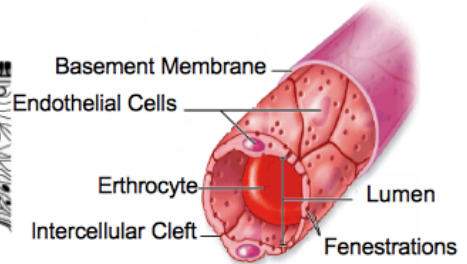
B.



C.



D.



circulating vasoactive compounds (Hayreh, 1975; Delaey and Van De Voorde, 2000).

### *1.3.2 Retinal Vasculature*

In contrast to the choroidal vasculature, the retinal vasculature is characterized by a low flow rate and high oxygen content and does not receive autonomic innervation; retinal blood flow is tightly regulated by local vasoactive compounds and neuronal activity (Ehinger and Falck, 1966; Laties, 1967; Harris et al., 1998; Yu and Cringle, 2001; Metea and Newman, 2007).

The retina is an end-arteriole system, meaning that arteries feed into arterioles, which branch into capillaries, which flow into venules then veins. This results in an absent collateral input other than the initial artery. This lack of anastomose and collaterals has significance in disease states that affect blood supply, as most other major organs of the body have a collateral blood supply to ensure adequate perfusion in disease states. In addition, as the only connection between the retinal arterial and venous system is through the capillary network, no connections exist between the capillary beds derived from the individual branched retinal arteries (Cogan, 1974). This morphological characteristic creates capillary-free areas where no capillary bed directly supplies blood. These capillary-free areas may be at increased risk during ischemia (Ryan et al., 2005). A capillary-free zone is also present around retinal arteries and arterioles and is thought to be due to high oxygen concentration (Pournaras, 1995). As the concentration of oxygen decreases further from arteries and arterioles, capillary density increases (Ryan et al., 2005) (Figure 1.5). Retinal arteries differ from arterioles of the same size found in other tissues as retinal arterioles have more developed layers of smooth muscle cells (SMC) and do not have an elastic lamina. SMC are important in providing mechanical

stimulation to encourage blood flow, while elastic lamina ensure arteries remain limber against the force of blood being pumped. In the retina, arteries can have as many as 5-7 layers of SMC on arteries closest to the optic disc and are progressively reduced to 1-2 layers in the periphery of the retina. Instead of an elastic lamina present in arteries of similar size elsewhere in the body, retinal arterioles have a single layer of endothelial cells that form tight junctions along the surface of the lumen (Shakib and Cunha-Vaz, 1966). This reduces the exposure of underlying tissues to circulating molecules and maximizes local regulatory mechanisms of blood flow (Yu and Cringle, 2001; Metea and Newman, 2007).

Capillaries are the smallest vessels in the body's blood supply and vital components in the microcirculation. The microcirculation, in contrast to the macrocirculation which transports blood to and from organs, is responsible for distribution of blood within the tissue. The retinal capillary wall is composed of three distinct layers: endothelial cells, intramural pericytes and a basement lamina (Figure 1.4B). Similar to arterioles, retinal capillaries have a layer of endothelial cells oriented along the lumen that react uniquely to various stimuli and are involved in the clearance of specific circulating hormones (Pohl and Kaas, 1994). Endothelial tight junctions also result in a tight blood-brain-like barrier to ensure selective exchange of substances between blood and retina.

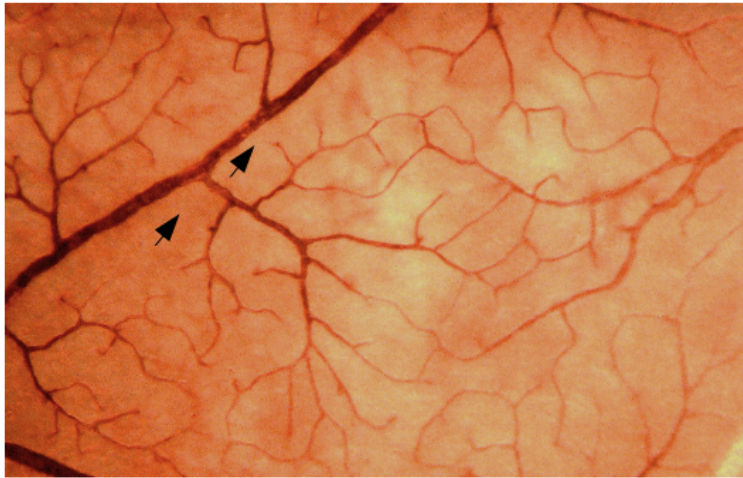
Endothelial cells are covered in a 1:1 ratio by intramural pericytes and encompassed by a basement membrane (Figure 1.4B). Pericytes provide the capillaries with mechanical support and vascular tone (Haefliger et al., 1994); they contain contractile proteins (Shepro and Morel, 1993 ; Pohl and Kaas, 1994 ) that enable the retinal vasculature to respond to vasoactive compounds and metabolic changes. The

**Figure 1.5 Capillary-Free Zones Surround Retinal Arteries**

**A.** Photomicrograph of an ADPase-stained flat-mounted retina depicting retinal arteries. Capillary-free zones surrounding the artery are indicated by an arrow.

Scale Bar= 20  $\mu\text{m}$





capillary basement membrane in the retinal capillaries is thought to act as a mechanical barrier and help the exchange of metabolites and waste from the blood.

#### **1.4 Ocular Blood Flow Autoregulation**

Autoregulation is defined as the ability of retinal vessels to keep blood flow constant despite changes in blood perfusion pressure or the ability of the tissue to adapt blood flow to metabolic needs (Flammer et al., 2002). The retina maintains a constant blood flow over a wide range of perfusion pressures that can range from 45-145 mmHg (Robinson et al., 1986). Alterations in metabolic parameters such as  $pO_2$  and  $pCO_2$  have also been shown to have effects on retinal blood flow. Both retinal arterioles and venules respond to blood gases, with vasoconstriction during decreased  $pO_2$  and vasodilation during increased  $pCO_2$  (Venkataraman et al., 2006). As metabolic demands increase, retinal arterioles dilate, resulting in a substantial increase in retinal perfusion (Riva et al., 1991). Several metabolic mediators and mechanisms have been proposed to be involved in this communication including  $K^+$  siphoning by glial cells (Kofuji and Newman, 2004). As neuronal activity increases,  $K^+$  is released into the extracellular space. Glial cells are capable of taking up this  $K^+$  and releasing it on to neighbouring arterioles to induce vasodilation (Kofuji and Newman, 2004). Also in a similar manner, activity-driven release of transmitters and compounds from retinal neurons, induces a rise in calcium levels in neighbouring glial cells. This rise in calcium is thought to mediate vasomotor responses in neighbouring vessels. This coupling of neuronal activity to vasomotor response has been termed, neurovascular coupling (Nedergaard, 1994; Schipke and Kettenmann, 2004; Newman, 2005).

## 1.5 The Aged Eye

Aging has been described as the progressive accumulation of physiological changes with time that are associated with, or responsible for, the ever-increasing susceptibility to disease and death (Harman, 1981). In the retina, alterations in vessel structure, vasculature reactivity and blood flow have been associated with aging. These include a number of morphologic abnormalities of the microvasculature including vessel tortuosity, glomerular looping, as well as spiralling of arterioles, venules and capillaries (Hughes et al., 2006). These alterations have also been detected in the CNS of aging humans and are thought to retard blood supply to the brain (Fang, 1976). Peripheral capillaries show increased thickness of their basement membranes, which may result in reduced endothelial-pericyte communication leading to cell death or loss of capillaries (Hughes et al., 2006). In support of this, significantly more acellular capillary remnants in the periphery of the retina have been observed in the aged population in comparison to their younger counterparts (Kuwabara et al., 1961; Lai et al., 1978).

The choriocapillaris have also shown reduced choriocapillary density and decreased lumen diameter with age (Ramrattan et al., 1994). The major arteries that serve the choroidal blood supply have exhibited increased resistance with age (Salter et al., 1998), and a total overall reduction in blood flow and perfusion in the aged eye (Ravalico et al., 1996). Similarly, the CRA has shown a progressive decrease in blood flow and increase in resistive index of approximately 6-11% per decade (Groh et al., 1996).

The primary function of blood is to provide cells with nutrients and removal of wastes, therefore cumulative alterations in structures that carry and disperse blood to cells, over time, may alter cellular function. This is observed in age-related decreases in RGC and

axon density (Weinreb et al, 1995; Tjon-Fo-Sand et al., 1996; Lovasik et al., 2003).

## **1.6 Age-Related Eye Diseases**

In Canada, 13% of those over the age of 65 have some form of visual impairment with >8% having severe impairment (blindness in both eyes or the inability to read).

Legal blindness (<20/200) increases from 3% at age 60 to 11% at age 80. While 15% of blindness is accounted for by cataracts, diseases with a component of vascular dysregulation are the leading causes of new cases of blindness in the aging population (Patterson, 2008). In addition to the direct cost of treating these diseases to preserve vision, indirect costs such as lower employment rates, increased care giver requirements and a lower quality of life for the visually impaired are things to be considered. With the increase in age of North American populations, treating visual impairment in the elderly is a relevant concern for the future.

In the Western world 75% of blindness and vision loss is attributable to retinal diseases with a vascular component (Yu et al., 2003). Alterations in retinal blood flow and vessel tone are known to occur in aging (See Section 1.5) and may lead to retinal ischemia and neurodegeneration. Furthermore, reduced ocular blood flow has also been reported to contribute to various ocular pathologies in which aging is also a recognized risk factor, including age-related macular degeneration (AMD), diabetic retinopathy (DR), glaucoma, and anterior ischemic optic neuropathy (AION).

### *1.6.1 Age Related Macular Degeneration*

According to the National Eye Institute, AMD in its various forms and progressions has a 40% prevalence in those over 80 years (National Eye Institute, 2007). Exudative

AMD is characterized by choroidal neovascularization, where abnormal vessels in the choriocapillaris, break through into Bruch's membrane. These vessels have a greater tendency of leakage and bleeding into the macula, leading to irreversible damage to the photoreceptors if left untreated. This choroidal neovascularization accounts for the most significant vision loss from AMD (Ciulla et al., 2001). Another form of AMD, non-exudative, results in the accumulation of debris, metabolic waste and engorgement of the cells in the RPE which leads to drusen formation and dysfunction of remaining retinal cells (Young, 1987).

### *1.6.2 Diabetic Retinopathy*

DR is one of the most common retinal microangiopathies and involves the development of abnormal vasculature. DR is a leading cause of blindness and visual impairment in the working age population in the industrialized world (Rahmani et al., 1996; Kocur and Resnikoff, 2002). The mechanisms leading to vascular disturbances in the retina and progression of the disease are still largely unknown. Evidence suggests that in DR, endothelial cells of the microvasculature do not produce appropriate autoregulatory mechanisms in response to persistent exposure to high glucose levels, producing lesions in the vasculature (Gillow et al., 1999). DR eyes also exhibit changes in the capillary basement membrane (Cai and Boulton, 2002), show pericyte loss (Hammes, 2005) and changes in blood flow (Chung et al., 1993). Ultimately, these changes in the vascular wall of the vessels in the eye lead to capillary occlusion, retinal ischemia and dysfunction of existing cells. In fact, there is correlation between pericyte loss and microaneurysm formation during DR (Dodge and D'Amore, 1992). In addition, the extent of blood flow dysregulation in DR patients is proportional to visual problems

(Aren et al., 1995; Harris et al., 1996). Interestingly, a decrease in total retinal blood flow has been observed in diabetics without DR, yet a marked increase in retinal blood flow in diabetics that have developed DR (Kohner et al., 1975; Cunha-Vaz et al., 1978; Grunwald et al., 1986). Age-related changes in autoregulatory components may lead to vascular dysregulation and hypoxia which may initiate angiogenesis (Hughes et al., 2006). Eventually, as observed in DR, unstable vessels develop that leak or interfere with the transmission of light leading to vision loss.

### *1.6.3 Glaucoma*

Glaucoma is a progressive eye disease characterized by cupping of the optic nerve, elevated IOP and progressive loss of RGCs resulting in vision loss (Weinreb and Khaw, 2004). There are two prominent theories regarding the progression of glaucoma: the mechanical and the vascular theories (Fechtner and Weinreb, 1994). The mechanical theory suggests an elevation in IOP damages the ONH and neural axons, leading to RGC loss (Yan et al., 1994). Therefore, glaucoma treatments have traditionally been targeted at reducing IOP. However, in some cases, despite a reduction in IOP, the disease progresses (Werner and Drance, 1977; Tezel et al., 2001). The vascular theory suggests glaucoma is a result of insufficient blood supply due to increased IOP or other risk factors that alter blood flow (Flammer, 1994). These risk factors, including hypertension and age, as well as compromised autoregulatory mechanisms, make the eye more susceptible to alterations in IOP and RGC loss (Flammer et al., 1994).

### *1.6.4 Anterior Ischemic Optic Neuropathy*

AION is the most frequent optic ischemia in individuals over the age of 50. It is caused by a sudden ischemic event, which leads to vision loss, with variable recovery

(Kerr et al., 2009). The pathophysiology is not well understood, but sudden vision loss often occurs upon waking, suggesting nocturnal arterial hypotension may play a role (Hayreh et al., 1997). AION is characterized by ONH swelling together with visible paleness of the ONH as the disease progresses (Quigley and Anderson, 1977; Kerr et al., 2009).

Despite earlier diagnosis and treatment for many of these retinal diseases, progressive vision loss continues with age, underscoring the need to understand age-related changes in the retina and how these contribute to disease process. As age-associated alterations occur at every level of the blood supply, from alterations in ophthalmic artery, to thickening of capillary walls, identifying compounds that can promote blood flow to the eye, in addition to targeting other risk factors, may provide the aged eye with enhanced protection.

### **1.7 The Endocannabinoid System**

The medicinal uses of cannabinoids and cannabis have been known for over a millennium, although it was not until relatively recently that the active compounds in the cannabis plant, including the primary psychoactive phytocannabinoid delta-9-tetrahydrocannabinol (THC), have been identified (Mechoulam and Gaoni, 1964). In 1990, Matsuda et al., eventually cloned the receptor through which THC exerts its many cellular effects (Matsuda et al., 1990; Munro et al., 1993). These findings have led to extensive research focused on the cannabinoid receptors, their endogenous ligands, endocannabinoids (eCBs), and the enzymes involved in their production, hydrolysis and transport, collectively called the endocannabinoid system (eCBS) (Piomelli, 2003; Bari et

al., 2006).

There are currently two cloned receptors, cannabinoid subtype 1 receptors (CB1) and cannabinoid subtype 2 receptors (CB2), shown to have cannabinoid actions. Both CB1 and CB2 are activated by THC and structurally similar compounds. CB1 are found within the CNS and periphery (Herkenham et al., 1990; Kaminski et al., 1992; Bouaboula et al., 1993; Schatz et al., 1997). CB2 are found primarily on cells in the periphery, particularly those involved in immune responses (Skaper et al., 1996; Van Sickle et al., 2005) and has been identified within the CNS, on support cells such as astrocytes (Pazos et al., 2005; Martinez-Orgado et al., 2007; Cabral et al., 2008), microglia (Nunez et al., 2004) as well as some neurons in the brainstem and cerebellum, although at much lower levels than CB1 (Van sickle et al., 2005; Ashton et al., 2006).

The cannabinoid receptors are seven transmembrane G-protein coupled receptors. Both CB1 and CB2 preferentially activate  $G_{i/o}$  pathways (Munro et al., 1993), but may also couple to  $G_s$  and  $G_q$  proteins to initiate distinct cellular signalling cascades (Glass and Felder, 1997; Lauckner et al., 2005; MacIntosh et al., 2007; Mackie, 2008). In general, CB1 coupling to  $G_{i/o}$  pathways leads to an increase in opening of voltage-gated potassium channels and reduced activity of N- and P/Q-type voltage-gated calcium channels, resulting in an overall reduction of neurotransmitter (NT) release, in the CNS this is most commonly  $\gamma$ -Aminobutyric acid (GABA) and glutamate (McAllister and Glass, 2002; Pertwee and Ross, 2002; Straiker and Mackie, 2007; For Review See Hudson et al., 2010). CB1 agonists have also been shown to inhibit the activity of adenylyl cyclase and activate mitogen-activated protein kinase-mediated cascades (Pertwee, 2008; Hudson et al., 2010). CB2 also signals through  $G_{i/o}$  pathways (Howlett et



al., 1986; Munro et al., 1993), although evidence shows that it is also capable of interacting with a number of different signalling cascades including mitogen-activated protein kinase (Bayewitch et al., 1995; Slipetz et al., 1995) and is associated with cell migration and immune responses (Bouaboula et al., 1996).

The discovery of THC and cannabidiol, the two most well characterized constituents of marijuana, preceded discovery of the receptors they activated. Similarly, there is increasing evidence to suggest that a number of endogenous and synthetic cannabimimetic compounds exert their effects through a CB1/CB2-independent mechanism. The most convincing evidence thus far for additional cannabinoid receptor targets is the persistence of cannabinoid-mediated effects in CB1/CB2 knockout mice (Zimmer et al., 1999; Breivogel et al., 2001; Begg et al., 2005), including effects in the CNS and peripheral sites, such as the vasculature (Jarai et al., 1999; Begg et al., 2005) and immune cells (Lambert et al., 2002). In addition, the highest levels of the eCB, anandamide (AEA), are found in the brain stem, yet this region has one of the lowest densities of CB1 (Bisogno, 1999; Di Marzo, 2000), suggesting that AEA may have actions at other, yet unidentified receptors. For example, several lines of evidence now suggest the presence of a potential vascular AEA-sensitive CBR (CBx); endothelial-dependent AEA relaxation of murine mesenteric arteries persisted in the presence of AM251 and AM630, CB1 and CB2 specific antagonists respectively, although the response was sensitive to pertussis toxin (PTX), suggesting  $G_{i/o}$  involvement (Jarai et al., 1999). The cannabidiol analogue, abnormal cannabidiol (Abn-CBD), has no action at CB1 or CB2 receptors, but like AEA, is able to produce vasorelaxation. The cannabinoid, O-1918, has been shown to be a selective antagonist of Abn-CBD action (Jarai et al., 1999; Hiley and

Kaup, 2007). The effects of both Abn-CBD and O-1918 are thought to be mediated by CBx. Activation of CBx in some vascular beds results in release of nitric oxide (NO) and hyperpolarization through activation of SMC K<sup>+</sup> channels, leading to vasorelaxation and vasodilation (Jarai et al., 1999; Offertaler et al., 2003; Hiley and Kaup, 2007; Pertwee, 2008).

The two most well characterized eCBs, 2-arachidonoylglycerol (2-AG) and AEA, have independent biosynthesis, selectivity, efficacy and degradation. 2-AG and AEA are both synthesized on-demand from membrane phospholipids through calcium-dependent phospholipases and released from post-synaptic membranes independent of synaptic vesicles (Piomelli, 2003).

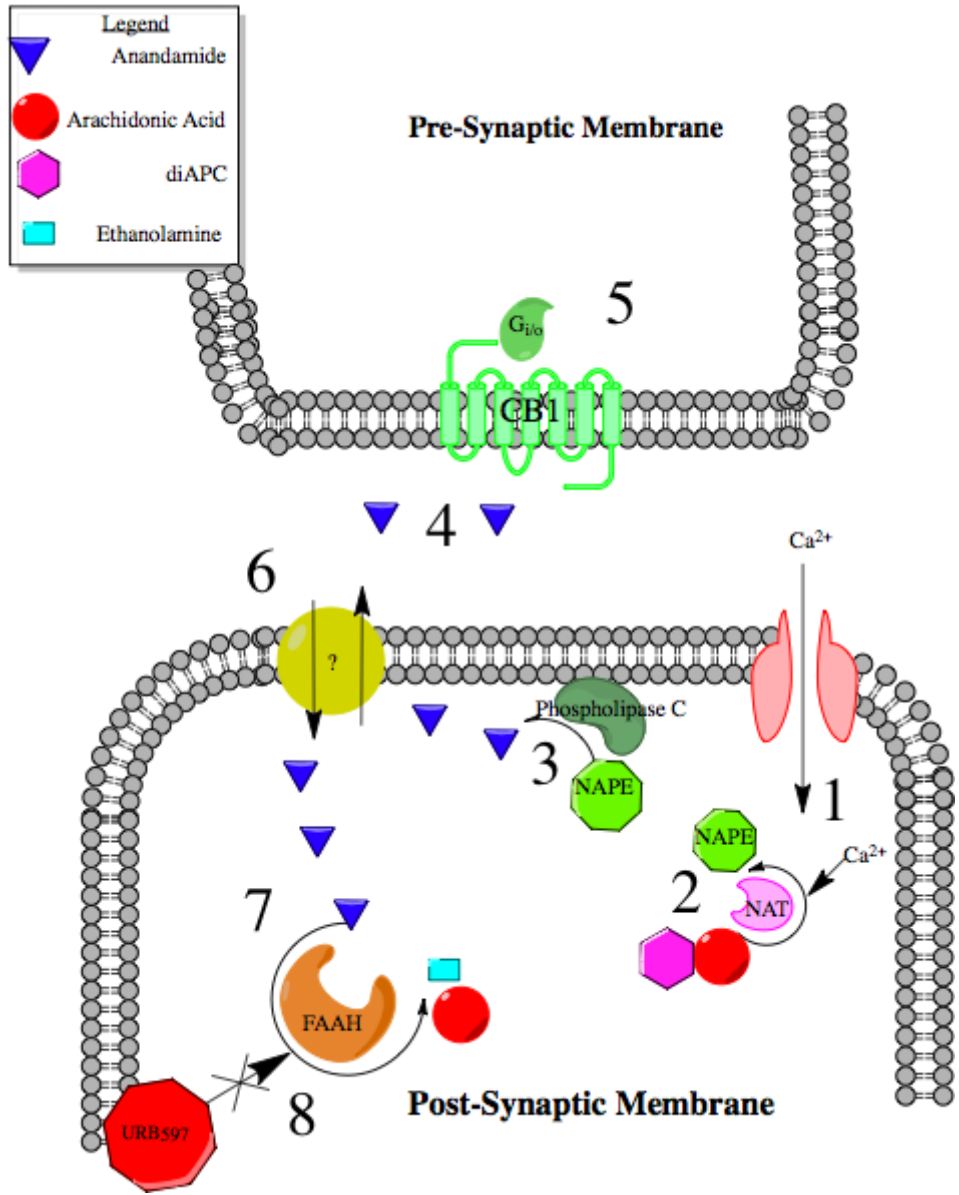
The primary pathway of 2-AG synthesis appears to be hydrolysis of diacylglycerols (DAG) by two different DAG-lipase isozymes (DAGL), alpha and beta. 2-AG levels in the CNS are higher than those of AEA, however evidence suggests CNS levels of 2-AG may be reciprocally regulated by AEA (Maccarrone et al., 2008). 2-AG can bind to both CB1 and CB2, but mainly activates pre-synaptic CB2 receptors. This is reflected in the localization of synthesizing and degrading enzymes of 2AG; DAGL are expressed in the dendritic post-synaptic compartment (Bisogno et al., 2003), while enzymes responsible for 2-AG degradation are found in pre-synaptic cytosolic regions (Gulyas et al., 2004). 2-AG can be degraded by fatty acid amide hydrolyze (FAAH) releasing arachidonic acid and glycerol, but 2-AG is mainly hydrolyzed by monoacylglycerol lipase (MAGL) to release these same metabolites.

The precursor of AEA is a membrane phospholipid, N-arachidonyl phosphatidyl ethanolamine (NAPE) (Figure 1.6). NAPE is formed from changing the position of

arachidonic acid on di-arachidonoylphosphatidylcholine (diAPC) to phosphatidylethanolamine (PE), a process catalysed by the calcium-dependent N-acyltransferase (NAT). There are several different pathways that have been shown to convert NAPE into AEA using either a 1 or 2 step process (Liu et al., 2008). In the two step process, NAPE is hydrolyzed by phospholipase A1/A2 to N-Acyl-lyso-PE before being catalysed by phospholipase D to release AEA. This pathway is thought to be involved in the production of basal AEA levels (Liu et al., 2008), while the one step process where NAPE is cleaved by phospholipase C to generate phosphoanandamide before being dephosphorylated to release AEA, is implicated in “on-demand” synthesis (Liu et al., 2008). AEA is synthesized in the cytosol and shown to exert its effects through retrograde transmission in which postsynaptic release of AEA results in activation of CBR, primarily CB1, on the pre-synaptic membrane (Devane et al., 1992; Schlicker and Kathmann, 2001) to inhibit the release of NT. This process occurs through modulation of both  $Ca^{2+}$  or  $K^{+}$  channels (Mackie and Hille 1992; Daniel and Crepel 2001) (Figure 1.6). AEA may also act postsynaptically, at CBR and non-CBR. For example, in addition to actions at CBx, AEA has also been shown to activate the transient receptor potential vanilloid 1 (TRPV1). TRPV1 is a non-specific cation channel found in peripheral sensory fibres, several nuclei of the CNS as well as other peripheral tissues (Marinelli et al., 2003; Maccarrone et al., 2008). TRPV1 is characterized by its activation by capsaicin, the spicy component in peppers. FAAH (McKinney and Cravatt, 2005) degrades AEA to arachidonic acid and ethanolamine (Deutsch and Chin, 1993; Yu et al., 1997; Goparaju et al., 1998) although AEA is not the only substrate of FAAH, which degrades other long

### **Figure 1.6 Synthesis and Degradation of Anandamide**

As intracellular calcium increases in post-synaptic membrane (1), calcium dependent N-acyltransferase (NAT) transfers arachidonic acid to di-arachidonoylphosphatidylcholine (diAPC) (2), forming N-arachidonyl phosphatidyl ethanolamine (NAPE), the precursor of AEA. NAPE is then hydrolysed by phospholipase C (3) to form AEA. AEA transverses the cell membrane in a manner independent of synaptic vesicles due to its lipophilic nature (4). AEA acts primarily on pre-synaptic cannabinoid subtype 1 receptor (CB1) which preferentially activates  $G_{i/o}$  signalling cascades (5). AEA is then taken up by the post-synaptic membrane, although the mechanisms are still unclear (6), to be degraded by fatty acid amide hydrolase (FAAH) into ethanolamine and arachidonic acid (7). URB597, a FAAH specific enzyme inhibitor, increases AEA levels (8).



fatty acid chains (Ho and Hillard, 2005, Ahn et al., 2007). Cox-2 is capable of oxidizing arachidonic acid by-products to prostamides or prostaglandins glyceryl esters, leading to prostaglandins, that are also biologically active (Yu et al., 1997; Kozak et al., 2000).

## **1.8 Endocannabinoids in the Eye**

Since the first reported observation of marijuana producing vasodilation and reducing IOP (Adams et al., 1978; Green, 1979), there has been an increasing body of evidence validating a role for the eCBS in ocular pharmacology. Studies have shown CB1 mRNA in the human trabecular meshwork (Stamer et al., 2001), ciliary body and retina of both rat and human (Buckley et al., 1998; Porcella et al., 1998; Stamer et al., 2001), although CB1 mRNA was found to be 10 times higher in the ciliary body than the retina in both rat and humans. CB1 mRNA has also been found in the retina of human and rat at the synaptic terminals of cones, the synaptic cleft between bipolar and RGCs, and on the RGC cell body (Straiker et al., 1999a; Straiker et al., 1999b). These suggest a role of cannabinoid receptors in everything from aqueous humour production to signal transduction in the retina.

The presence of eCBs in ocular tissues has been identified in the ciliary body, iris, choroid, and trabecular meshwork in a number of different species including humans (Gawienowski et al., 1982; Matsuda et al., 1997; Stamer et al., 2001; Chien et al., 2003; Lograno and Romano, 2004; Chen et al., 2005; Stumpff et al., 2005; Njie et al., 2008). Gas chromatography has shown AEA in all human ocular tissue with the exception of the lens (Chen et al., 2005; Matias et al., 2006). The hydrolysis of AEA has been measured in the porcine iris, choroid, lacrimal gland and optic nerve (Matsuda et al., 1997) suggesting

a functional endocannabinoid system in the eye.

Both cannabinoids and endocannabinoids exert a number of actions in the eye; in the retina, cannabinoid agonists modulate voltage-dependent membrane currents in photoreceptors, bipolar cells and ganglion cells (Straiker et al., 1999b; Yazulla et al., 2000; Straiker and Sullivan, 2003; Fan and Yazulla, 2004; Fan and Yazulla 2005; Lalonde et al., 2006). THC and other cannabinoids, including AEA, reduce IOP by local actions on CB1 and possible non-CB1 targets in anterior ocular tissues including the ciliary body and the trabecular meshwork (Straiker et al., 1999a; Song and Slowey, 2000; Porcella et al., 2001; Stamer et al., 2001). In the ocular vasculature, AEA has also been shown to cause vasodilation in bovine ophthalmic artery (Romano and Lograno, 2006) and in human subjects, where the administration of cannabinoid agonists enhanced retinal perfusion (Plange et al., 2007).

Taken together, evidence of the presence of receptors, eCBs, their hydrolysing enzymes and the ability of this system to alter blood flow and signal transduction in the eye suggests the endocannabinoid system plays an active role in retinal and ocular physiology.

## **1.9 Endocannabinoids as Therapeutic Targets in the Eye**

There are a number of different age-related progressive eye diseases that have components of vascular dysregulation and loss of RGCs (See Section 1.6). Therefore, compounds with multiple therapeutic targets may be beneficial in addressing several of the mechanisms implicated in disease pathology.

In animal models of glaucoma, glutamate excitotoxicity is thought to play a role in the degeneration of RGCs that is characteristic of this disease. This retinal excitotoxicity is mediated by over stimulation of the N-methyl-d-aspartate (NMDA) and non-NMDA glutamate receptors (Lam et al., 1999). As more glutamate is released, there is increased cell activation (excitation) causing an influx of  $Ca^{2+}$  into RGCs (Sucher et al., 1991). This in turn leads to activation of NO synthase and excess accumulation of NO, causing mitochondrial dysfunction and eventual cell death (Coyle and Puttfarcken, 1993; Dreyer et al., 1996).

AEA has been shown to activate CB1, thus modulating neuronal membrane permeability to  $Ca^{2+}$  and  $K^{+}$  and reducing the activity of adenylyl cyclase, with the final outcome being decreased NT release (Pertwee, 1997). Specifically, CB1 are found on presynaptic nerve endings of glutamatergic synapses (Twitchell et al., 1997; Davies et al., 2002) and activation of CB1 inhibits presynaptic release of both glutamate and GABA (Kim and Thayer, 2000; Gilbert et al., 2007). It has been shown that in high IOP-induced ischemia, a glutamate channel blocker not only prevented RGC death, but also reduced the high-IOP induced elevation of FAAH (Nucci et al., 2007). Exogenous cannabinoids, natural and synthetic, have also been shown to exert neuroprotective effects in several models of neurotoxicity (Mechoulam et al., 2002; van der Stelt et al., 2002; Croxford, 2003; Veldhuis et al., 2003 ), possess antioxidant properties and protect various cell types against oxidative stress (Hampson et al., 1998; Chen and Buck, 2000). The neuroprotective role of eCBs is not without its controversy as AEA binding to TRPV1 triggers the opening of non-selective cation channels that can lead to increased intracellular  $Ca^{2+}$ , mitochondrial uncoupling and cytochrome c release (Maccarrone and



Finazzi-Agro, 2003; Yamaji et al., 2003).

The role of microglia (MG) and immune response within pathological states is controversial. Although traditionally viewed as passive cellular by-standers in cell death and degeneration, there has been an increasing body of evidence to suggest that MG have an active role in degeneration of RGCs in various animal models of disease. In a mouse model of retinitis pigmentosa, where the photoreceptor layer in the retina spontaneously degenerates, MG activation and migration was observed prior to the initiation of photoreceptor loss (Zeng et al., 2005). Although MG have an important role in phagocytosing debris of dead and dying RGCs to prevent release of their toxic intracellular components, MG also release various chemoattractants and noxious stimuli including NO, glutamate and tumour necrosis factor (TNF), all of which may be deleterious to the surviving RGCs (Weinred and Khaw, 2004). Experimentally-induced glaucoma has shown to be associated with an increased activation of astrocytes, Müller cells and MG (Weinred and Khaw, 2004). Therefore, compounds that can reduce or modify the activation of MG and/or reduce gliosis may provide some support in chronic eye diseases.

Activation of CB1 and CB2 has been associated with the modulation of MG activation and migration, resulting in inhibition of the production of inflammatory cytokines and NO (Walter and Stella, 2004; Jackson et al, 2005; Stella, 2010). AEA has been suggested to have an inhibitory role in immune cell migration (Joseph et al., 2004; Oka et al., 2004). In contrast, increased 2-AG levels, have been shown to activate the migration of MG following excitotoxicity (Walter et al., 2003). Although AEA itself may inhibit migration of MG, it's metabolites may have stimulatory effects on immune response. It has been

speculated that increased FAAH activity in astrocytes serves to release arachidonic acid from AEA, thus leading to pro-inflammatory mediators (Paradisi et al., 2006). Alterations in the inflammatory response may be of particular importance in the aged eye, where it has been documented that activated MG are observed in a resting, unaltered retina of aged rat suggesting a low level of constant inflammation (Xu et al., 2009).

AEA has also been shown to have vasorelaxant effects via both CB1 and non-CB1 targets and by endothelium-dependent and -independent mechanisms (Randall et al., 1996; Plane et al., 1997; Chaytor et al., 1999). AEA's vasoactive effects through CB1 include inhibition of Ca<sup>2+</sup> entry through L- type Ca<sup>2+</sup> channels and inhibition of NT release (Gebremedhin et al., 1999) including the endogenous potent vasoconstrictor endothelin (ET-1). ET-1 has been shown to be elevated in low-pressure glaucoma patients (Emre et al., 2005; Kim et al., 2006; Wang et al., 2006) and AEA is able to promote blood flow and inhibit vascular damage through inhibition of ET-1 release (Dogulu et al., 2003; Ronco et al., 2007).

Overall it is thought that eCBs, in particular the action of AEA, can exert neuroprotective effects through a number of different mechanisms including inhibition of excitotoxicity (Maccarrone et al., 1998; Shen and Thayer, 1998; Marsicano et al., 2003), actions on MG cells and other invading immune cells by regulating their migration (Walter et al., 2003) and promotion of blood flow by inducing hypotension and decreasing edema (Parmentier-Batteur et al., 2002).

### **1.10 The Rat as an Animal Model of Age-Related Eye Diseases**

Anatomically, the rodent and human eyes have very similar structures, as light

travels through the rat's cornea and focuses images on the macular area of the light-sensitive retina in a manner similar to humans. There are, however, some key differences between the rat and human eye: the rodent lens is substantially larger than the human eye and the rat has poorly developed ciliary muscles (Woolf, 1956) and therefore may not be able to alter the shape of the lens to the same degree as humans. This results in rodents having limited focusing power or visual acuity. Compared to other animal models, the rodent visual system is most similar to humans. The ophthalmic artery supplies blood to the eye in both rat and human and the retinal vasculature pattern in both these species is classified as holangiotic, characterized by a direct blood supply from major arteries or cilioretinal network providing blood to the retina (Ryan et al., 2005).

Since the vasculature and overall structure and function of the rat eye is similar to humans, it makes it a relevant model when examining age-related alterations in the retina. The rat retina, like the human retina, has been shown to exhibit a number of age-related alterations in its vasculature (Leuenberger 1973; Nagata et al., 1986; Weisse, 1995) and retinal cell loss with age (Weinreb et al., 1995; Tjon-Fo-Sand et al., 1996; Lovasik et al., 2003). Furthermore, the rat is used in a number of animal models representing human age-related eye diseases such as glaucoma (Sawada and Neufeld, 1999) and DR (Rosenmann et al., 1975). The rat retina has been shown to have receptors, enzymes responsible for eCB synthesis and degradation (Buckley et al., 1998; Porcella et al., 1998, 2000; Stamer et al., 2001; Yazulla et al., 1999; Yazulla and Studholme, 2001; Glaser et al., 2005) and eCBs have been shown to promote blood flow and vasodilation in the rat retina (Schwartz and Yoles, 1999; Crandall et al., 2007; Oltmanns et al., 2008). In addition, administration of eCBs in the rat provides neuroprotection in a variety of animal

models of damage (Belayev et al., 1995; Ramírez et al., 2005; Shouman et al., 2006; García-Arencibia et al., 2007), including high IOP-induced ischemia (Nucci et al., 2007). These factors make the rat retina an excellent model to examine the potential of compounds that modulate eCBs to protect the retinal vasculature of the aged eye.

### **1.11 Research Objectives**

A number of progressive eye-diseases have both age and vascular dysregulation as major risk factors, suggesting that alterations that occur with age may make the aged eye more susceptible to ischemic and retinal damage. However, it is difficult to understand the interaction of vascular damage and neuronal cell loss. Therefore, examining a model of primarily neuronal insult, axotomy, and a model of primarily vascular insult, ischemia, in both young and aged animals may provide insight into what factors make the aged retina more susceptible to damage. Since the eCB system has shown to have an integral role in ocular pharmacology in addition to multiple therapeutic targets, modulation of this system may exert varying levels of neuronal and vascular protection depending on the model of retinal damage. URB597 inhibits degradation of AEA by FAAH and thus can promote physiological relevant concentrations of AEA on-demand, at the site of action. The objectives of the present study were to 1) evaluate changes present with aging in the rat retina, 2) to determine whether the aging retina is more susceptible to insult (ex. ischemia, axotomy) and 3) investigate whether modulation of the eCBs can provide retinal neurovascular protection in young and aged in models of retinal damage (ex. ischemia, axotomy).

## Chapter 2

### Materials and Methods

#### 2.1 Animals

Fischer-344 young (8-12 weeks) and aged ( $\geq 20$  months) rats were obtained from Charles River Laboratories International Inc. (USA). All animals were maintained in the Carleton Animal Care Facility at Dalhousie University under a 12 hour light-dark cycle with food and water *ad libitum*. All experiments were carried out in accordance with the guidelines set out by the Canadian Council for Animal Care (<http://www.ccac.ca/>). Approval for the described experiments were obtained from Dalhousie University Committee on Laboratory Animals, and all efforts were made to minimize the number of animals required and their distress.

#### 2.2 Physiological Baseline Measurements

Blood pressure, blood glucose levels and elevated IOP have been shown to have effects on vasculature and may contribute to observed age-related changes in retinal vasculature (Hayreh et al., 1994; Fuchsjäger-Mayrl et al., 2004; Tirsi et al., 2009). Therefore, measures of these physiological parameters were obtained for all animals that were used for age-related vascular analysis.

##### 2.2.1 Blood Pressure

The CODA non-invasive blood pressure system (Kent Scientific Corp., USA) was used to obtain blood pressures from both young and aged animals. The awake animal was placed in clear acrylic holder with a built-in nose cone. The tail remained outside the

holder and two cuffs were placed on the tail, recording the occlusion and volume-pressure. For each session, the blood pressure ran through 5 trial cycles to accustom the animal to the process, followed by 15 cycles in which the systolic and diastolic pressures were recorded. Each animal had their blood pressure measured at the same time every day for at least one week. The measurements were averaged per day, then again for the week to obtain a single value per animal.

### *2.2.2 Blood Glucose Levels*

To assess fasting blood glucose levels, the rats were fasted for least 4 hours prior to blood glucose measurements. Prior to testing blood glucose levels, the blood glucose monitoring system's (TRUEtrack, Home Diagnostics Inc., USA) accuracy was calibrated with a glucose control solution of 6 mmol/L. Once accuracy of the system had been established, non-anaesthetized rats were immobilized in a towel and blood samples were obtained from their tail vein. The blood was collected on blood glucose test strips, these strips were then placed in the monitoring system and a blood glucose value (mmol/L) was obtained. A single sample was taken per animal.

### *2.2.3 Intraocular Pressure*

IOP was assessed using the rebound tonometer Tonolab (Colonial Medical Supply, USA). Non-anaesthetized animals were gently restrained and 1 drop of a topical anaesthetic (0.5% Alcaine) was placed in the eye. The Tonolab was brought in close proximity to the eye, and gently placed in contact with the cornea to obtain a reading. Ten readings per day for 5 consecutive days were obtained for each animal. Values from each day were averaged, then mean daily measurements were averaged over the 5 day period

to obtain a single value for each animal.

### **2.3 Labelling Cells of the Retina**

Approximately 98% of all RGC axons terminate in the contralateral superior colliculus (SC) and these axons are able to retrogradely transport dye from the SC back to the RGC cell bodies (Forrester and Peters, 1967; Vidal-Sanza et al., 1988). Since RGCs are the only axons from the retina that have access to the SC, this procedure enables RGC-specific labelling. In addition, this method also enables identification and quantification of phagocytotic MG, which fluoresce as a result of digesting dying or injured RGCs (Vidal-Sanza et al., 1988). Aged animals showed significant delays in recovery from retrograde labelling from the SC in comparison to the young animals. Therefore, aged animals that underwent axotomy had retrograde labelling of RGCs with FG from the optic nerve stump. Retrograde labeling from the optic stump is considered inferior to SC labelling since the dye is placed on the optic nerve stump following transection of the optic nerve (eg. axotomy), which can damage RGCs (Thanos et al., 1992). Since RGC loss following axotomy was being assessed, this was not a confounding issue for the present study. Furthermore, results obtained in young animals with 2 days of FG labelling from the optic stump were comparable to labelling from the SC. Since RGC apoptosis is delayed until approximately 3-5 days post axotomy (Villegas-Perez et al., 1993) and FG has been shown to be taken up into RGCs cell body within 3 days (Vidal-Sanza et al., 1988), both RGCs and phagocytotic MG were labelled with FG after retrograde labelling. RGCs were labelled within 3 days and FG-positive

MG were present within 1 week.

### *2.3.1 Retrograde Labelling of RGCs with Fluorogold from the SC*

For all surgical procedures unless stated otherwise, animals were weighed and then placed under 5% isoflurane for anaesthetic induction. Buprenorphine (0.05mg/kg; CDMV, Canada) was given at the beginning of all surgical procedures to ensure the analgesics had taken effect upon the animal waking. Once the animal was non-responsive, it was placed in a stereotaxic holder and the isoflurane was reduced to 3% for the duration of the surgery. The surgical area was prepared with soap, ethanol and betadine. An incision was made mid-line on the rat head exposing the cranial land-marks bregma and lambda. A hole, 5 mm in diameter, was made 1 mm rostral to lambda and 1 mm lateral from the midline. Forceps and scissors were used to remove the skull and dura mater overlying the cortex. A blunt, 21-gauge needle attached to a pump, was used to aspirate the cortex until the SC was located. A blunt, 23-gauge needle was then used to ensure the SC was clearly exposed and all white matter was removed from the surface of the SC. Surgical gel foam soaked in 2% fluorogold (Fluorochrome Inc., USA) in sterile 0.9% NaCl was then placed on top of the SC. The incision was cleared of blood and closed with a wound clip. Animals were given 6 mL of sterile 0.9% NaCl to account for blood loss, and were then returned to a clean cage and placed on a heating pad. The animals recovered for at least 5 days before the next procedure.

### *2.3.2 Retrograde Labelling of RGCs with Fluorogold from the Optic Stump*

To label RGCs from the optic nerve stump an axotomy of the optic nerve was carried out. The animals were placed in a stereotaxic apparatus and a 5-0 polypropylene



suture (Ethicon Inc., USA) was used to exert tension on the conjunctiva to produce a downwards displacement of the eye, allowing easier access to the optic nerve. An incision was then made midline on the rat head at the same location used previously for FG labelling. The portion of tissue lateral to the midline, was sutured and pulled over to ensure the orbital rim was exposed on the same eye as the sutured conjunctiva. An incision was then made along the orbital rim, the orbital tissue was dissected and a portion of the lacrimal gland was pulled rostrally to increase the field of view. The extraocular muscles were then separated to expose the optic nerve. Taking care to ensure the blood supply to the eye was undisturbed, the overlying dura mater was dissected away to completely expose the optic nerve. A complete transection of the optic nerve was then carried out approximately 0.5-1mm behind the eye globe. FG soaked surgical gel foam was placed within the dura mater of the transected posterior portion of the optic nerve that remained attached to the eye globe. In this case, instead of RGCs retrogradely taking FG up from the SC, the FG was transported retrogradely through the optic nerve stump to the RGC cell bodies. Lastly, the wound was sutured closed and the animal placed in a clean cage on a heating pad.

## **2.4 Pharmacological Agents**

URB597 inhibits the degradation of the endocannabinoid, AEA, therefore prolonging its duration of action. It has been shown that URB597 is able to reduce AEA hydrolysis, and significantly increase AEA levels within 30 minutes of administration (Fegley et al., 2005). URB597 is an irreversible inhibitor of FAAH and has been shown

to produce more stable and persistent increases of AEA in comparison to other reversible and irreversible FAAH inhibitors (Piomelli et al., 2006). Therefore, either vehicle or 0.3mg/kg URB597 was given i.p. one hour prior to experimental insult. URB597 was dissolved in dimethyl sulfoxide (DMSO; Sigma Aldrich, Canada) in 1:3 ratio DMSO to saline (Kathuria et al., 2003). This ratio was mirrored in the vehicle group with a total injection volume for all animals of 500µl/kg body weight.

## **2.5 Animal Models of Disease**

### *2.5.1 Axotomy*

As above (section 2.3.2), the animals were placed in a stereotaxic apparatus and a 5-0 polypropylene suture (Ethicon Inc., USA) was used to exert tension on the conjunctiva to produce a downwards displacement of the eye, allowing easier access to the optic nerve. An incision was then made midline on the rat head at the same location used previously for FG labelling. The portion of tissue lateral to the midline, was sutured and pulled over to ensure the orbital rim was exposed on the same eye as the sutured conjunctiva. An incision was then made along the orbital rim, the orbital tissue was dissected and a portion of the lacrimal gland was pulled rostrally to increase the field of view. The extraocular muscles were then separated to expose the optic nerve. Taking great care to ensure the blood supply to the eye was undisturbed, the overlying dura mater was dissected away to completely expose the optic nerve. A complete transection of the optic nerve was completed at approximately 0.5-1mm behind the eye globe. The lacrimal gland was placed back in its original position, the incision was sutured, and the animals

began recovery. Animals were sacrificed at 1 or 2 weeks post-axotomy.

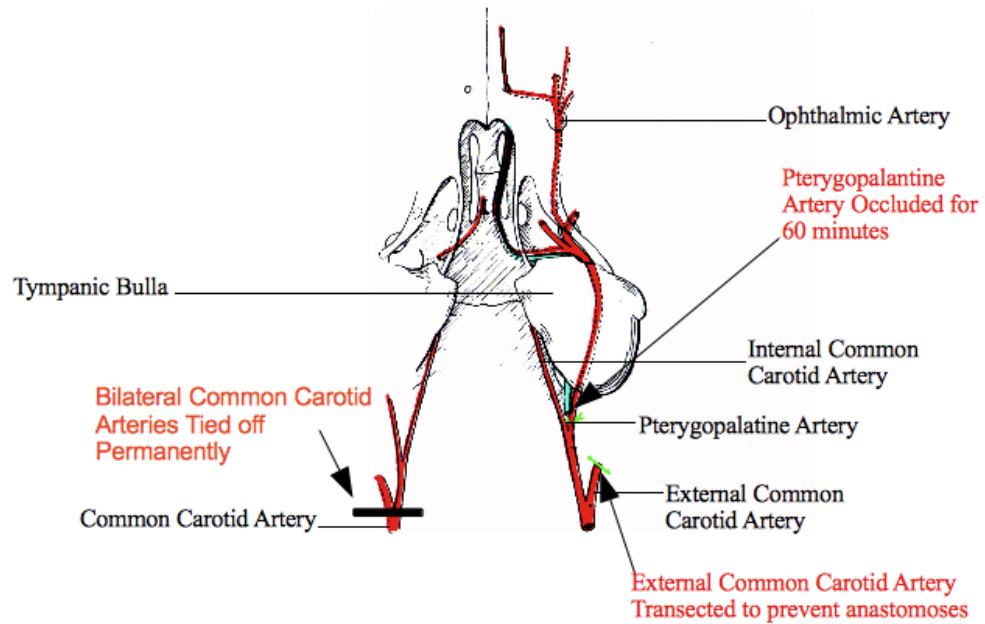
### *2.5.2 Acute Ischemia-Reperfusion through Occlusion of the Pterygopalatine Artery*

A number of animal models are available that reduce blood-flow to the retina such as transient occlusion of the CRA or elevated IOP-induced ischemia. However, temporary occlusion of the CRA can result in damage to the optic nerve and the procedure to increase IOP may produce pressure-related mechanical injury to the retina (Gehlbach and Purple, 1994). Therefore, these types of retinal ischemia models cannot eliminate optic nerve injury and may introduce additional confounding inflammatory effects independent of ischemia. In the rat circulatory system, the pterygopalatine artery (PPA) gives rise to the ophthalmic artery. Occlusion of the PPA, which resides in the neck of the rat, reduces the confounding damage to the retina and produces unilateral global retinal ischemia on the side of the occlusion (LeLong et al., 2007). In order to carry out occlusion of the PPA, animals were placed on their back, and a ventral midline incision was made in the animal's neck. Blunt dissection was used to separate muscle and the submaxillary glands until the common carotid artery was visible. The common carotid artery is easily identified due to its large size and observable pulsing. Arising from the common carotid artery, the internal and external carotid arteries were then identified. The internal carotid artery was subsequently dissected until the first branch of the internal carotid artery, the PPA, was located. Taking care not to disturb the vagus nerve while isolating the PPA, a 6-0 polypropylene suture (Ethicon Inc., USA) was tightened around the PPA. The external carotid artery was then ligated on two sites of the artery and transected to prevent anastomoses between the external and ophthalmic artery (LeLong et

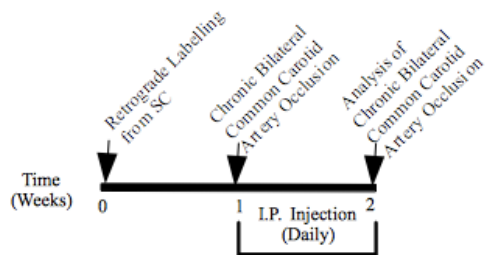
**Figure 2.1 Animal Model of Ischemia-Reperfusion and Chronic Ischemia**

**A.** The normal rat neck with anatomical reference point the tympanic bulla shown. The common carotid artery on the left hand side is ligated for the chronic ischemia model. The right hand side shows procedure for the transient I-R. The pterygopalantine artery, internal carotid artery and external carotid artery are all shown and ligation sites indicated. **B.** Surgical timeline schematic showing retrograde labelling of retinal ganglion cells from the SC followed by BCCAO for chronic ischemia model. **C.** Surgical timeline schematic for transient I-R. Adapted from **Novel Mouse Model of Monocular Amaurosis Fugax** with permission from Wolters Kluwer Health.

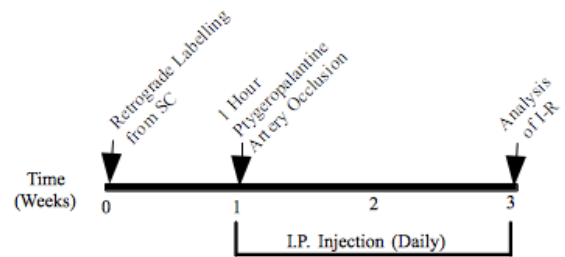
A.



B. Timeline For Chronic Ischemia



C. Surgical Timeline For Transient Ischemia Reperfusion (Monocular Amaurosis Fugax)



al., 2007). The PPA was ligated for 60 minutes after which the suture was removed and the wound sutured closed. The animals were allowed to recover for 2 weeks prior to sacrifice (Figure 2.1B).

### *2.5.3 Chronic Ischemia through Occlusion of the Common Carotid Arteries*

We also chose a chronic model of ischemia, where the common carotid arteries were permanently ligated, to compare with our chronic axotomy model of nerve damage. Similar to acute retinal I-R described in section 2.4.2, a ventral mid-line incision was made on the rat's neck and the tissue was dissected away from the mid-line. After separating the submaxillary glands and blunt dissecting through the muscles, the common carotid arteries became visible. Bilateral common carotid arteries were dissected away from the vagus nerve, and tied off with a 4-0 suture (Ethicon Inc., USA). The wound was then sutured closed with the common carotid arteries remaining ligated until the animals were sacrificed 1 week later (Figure 2.1A).

## **2.6 Visualizing the Vasculature of the Retina**

### *2.6.1 Lectin Immunolabelling*

The vascular endothelium forms a continuous layer that separates circulating blood from surrounding tissues. The endothelium and its surface contains specific domains with characteristic carbohydrate residues (Simionescu, 1982) that are selectively bound to by lectin. Therefore, lectin is a commonly used marker to distinguish endothelial cells from other tissue lining cells (Alroy et al., 1987). For lectin immunolabelling of the retinal vasculature, animals were sacrificed by an overdose of

sodium pentobarbital (240mg/kg body weight) via i.p. injection and the eyes were enucleated. A small incision was made in the cornea and the eyes were then placed in 4% paraformaldehyde solution for at least 3 hours. The eyes were then removed from the paraformaldehyde, placed in a phosphate buffered solution (PBS) under a dissecting microscope where the cornea and lens were removed. To release the retina from the eye-cup, the anterior portion of the eye was removed along the ora serrata and posteriorly the retina was released by cutting close to the optic nerve. Using small brushes, the retina was carefully mounted onto a glass slide, cut into four quadrants and flattened. Filter paper was then placed on the ganglion cell side of the retina to remove the vitreous. The retina with the attached filter paper was then placed in 4% paraformaldehyde solution for a minimum of 10 minutes. Next, the retina was gently peeled from the filter paper and placed in a 24-well plate containing PBS. After washing in PBS, the retinas were permeabilized with ice cold 100% methanol for 10 minutes. The retinas were then washed with PBS for 5 minutes before being washed with 1% tritonX (Sigma-Aldrich Canada Ltd., Canada) in PBS 3 times for 5 minutes. TRITC labelled lectin from *Bandeiraea simplicifolia* (Sigma-Aldrich Canada Ltd., Canada) was diluted in 1% tritonX in a ratio of 1/100. The container was then wrapped in aluminum foil and placed on a shaker table over night at room temperature. The next day, the tissue was rinsed 3 times in PBS then mounted on slides with anti-fade mounting media and imaged immediately.

### 2.6.2 *ADPase Stain*

Adenosine diphosphatase (ADPase) is a magnesium-activated endothelium cell

ectoenzyme that was first used to visualize the vasculature of the retina by Luty and McLeod (1992). The reaction product developed with ammonium sulfide yields a brown stain that is restricted to established endothelial cells and their precursors. It has been shown to have reduced staining in non-perfused areas, as seen with retinal tissue from individuals with diabetic retinopathy (Luty and McLeod, 1992). In addition, tissue samples are able to be left in fixative for prolonged periods of time and the reaction product does not fade with time, making this method conducive to analyzing a number of morphological parameters over time. However, the reagents and duration of staining for ADPase negatively impacted the ability to visualize FG labelled MG and RGC. Therefore, ADPase staining was used to assess vascular differences between young and aged retina, while lectin was used on animals that underwent surgery and required FG analysis. Animals were sacrificed by an overdose of sodium pentobarbital (240 mg/kg body weight) via i.p. injection and the eyes were enucleated. A small opening was made in the cornea and the eyes were then placed in 10% neutral buffered formalin overnight (NBF; Sigma-Aldrich Canada Ltd., Canada). Fixed eyes were placed in a PBS under a dissecting microscope and the cornea and lens were removed. To release the retina from the eye-cup, the anterior portion of the eye was removed along the ora serrata, and posteriorly the retina was carefully cut away where it joined the optic nerve. Using small brushes, the retina was mounted onto a glass slide, cut into four quadrants and flattened. Filter paper was then placed on the ganglion cell layer side of the retina to remove the vitreous and left in 10% NBF for at least 10 minutes. The retina was then washed in 50 mM TRIS 5 times for 15 minutes each. A fresh ADPase medium containing 6 mM



magnesium chloride and 3 mM lead nitrate in 2M TRIS was prepared, stirred, filtered and heated to 37 °C. Once the solution had warmed, 1 mg of ADP (Sigma-Aldrich Canada Ltd., Canada) was added per 1 mL solution, and the solution immediately placed on the retinas for 15 minutes. Following this incubation, the retinas were washed 5 times for 15 minutes with 50 mM TRIS following which ammonium sulphide, diluted in distilled water (1:10), was reacted with the retinas for 1 minute. The tissue was washed with 50 mM TRIS a further 3 times for 15 minutes. Stained retinas were then placed on a slide in an anti-fade mounting media and cover-slipped.

## **2.7 Labelling of Activated MG**

Animals were sacrificed by an overdose of sodium pentobarbital (240 mg/kg body weight) via i.p. injection following which the eyes were enucleated. A small opening was made in the cornea and the eyes were then placed in 4% paraformaldehyde solution overnight. The next day the cornea was removed and the remaining eye cup was placed in paraformaldehyde solution overnight. The following day, the eye cup was placed in 30% sucrose in PBS until the eye cup sank to the bottom of the solution, approximately 2 days. Twenty micrometer sagittal sections of the eye cup were made using the MICROM HM500 O cryostat (GMI Inc., USA), then placed on microscope slides (Fisherbrand Superfrost/Plus, USA). Slides were washed 3 times for 10 minutes in PBS at room temperature before being incubated in 3% normal goat serum (Jackson Laboratories, USA), in 0.3% Triton X (Sigma Aldrich, Canada) for one hour at room temperature. Iba1 (Wako Chemicals USA Inc., USA) antibody was then added to this solution in 1/200 for 2

days at room temperature. Slides were then again washed 3 times with PBS for 10 minutes, followed by incubation with the secondary antibody, CY3 goat anti-rabbit (Cedarline, USA) for 1 hour. Slides were then washed 3 times in PBS for 10 minutes before being coverslipped in an anti-fade mounting media.

## **2.8 Imaging and Quantification of RGCs, MG, and Vascular Density**

FG-labelled cells were visualized using an epifluorescence microscope (E800' Nikon, Canada) with filters for UV-2A (excitation 330-380 nm; barrier 420 nm; emission 400 nm). RGCs and phagocytotic MG were counted manually from digital micrographs taken at distances of 1, 2 and 3 mm from the optic disk in each retinal quadrant, for a total of 12 images over an area of 1 mm<sup>2</sup>. Because phagocytotic MG become labelled with FG by digesting fragments of dying RGCs, FG-labelled RGCs were differentiated from FG-labelled MG using size (>10µm) and shape (circular or oval) (Chauhan et al., 2004).

Lectin- labelled capillaries were visualized using an epifluorescence microscope (E800' Nikon, Canada) with filters for G1-B (excitation 541-551nm; barrier 590nm; emission 546nm). Capillaries were counted manually from digital micrographs taken at a distance of 1, 2 and 3 mm from the optic disk for each retinal quadrant. Capillaries were distinguished from arterioles based on their location within the retina (posterior) and size (<3 µm). The number of times capillaries crossed a grid presented at these points were averaged to obtain capillary intersections/mm<sup>2</sup> (Mutapcic et al., 2005).

ADPase stained retinas were visualized using bright-field illumination and

quantified with the same methodology as that for lectin-stained capillaries. To measure ADPase-stained retinal flat-mount density, images were first taken under bright-field illumination. Images were then imported into the image processing program that was capable of density slice analysis (Scion,USA). An upper and lower limit for pixel sensitivity was held constant between images, to produce a density of pixels per millimeter for each retina flat-mount.

## **2.9 Statistical Analysis**

Data and statistical analysis were performed using GraphPad Prism Version 4.0 (GraphPad Software Inc., USA). All data was presented as means  $\pm$  s.e.m. Unpaired Student's t-test was utilized to assess significance between 2 groups, while 3 or more groups were analyzed by one-way ANOVA with a Tukey post-test, or by two-way ANOVA with the Bonferroni method post-test. A p-value of less than 0.05 was considered to be significant.

## Chapter 3

### Results

#### 3.1 Comparison of Physiological Parameters in Young and Aged Animals

The incidence of hypertension, hyperglycemia and elevated IOP increase with age in the human population and have all been shown to contribute to retinal vasculature pathology (Hayreh et al., 1994; Fuchsjäger-Mayrl et al., 2004; Tirsi et al., 2009).

Therefore, these parameters were examined in aged rats to identify if they may be contributing to age-related alterations in retinal vasculature. Mean blood glucose levels in young rats ( $4.263 \pm 0.134$ ;  $n=10$ ) were not significantly different ( $p=0.11$ ) from blood glucose measurements obtained from aged rats ( $4.613 \pm 0.4893$ ;  $n=10$ ) (Figure 3.1A). IOP was also not significantly different ( $p=0.22$ ) between young ( $19.39 \pm 0.4893$ ;  $n=10$ ) and aged rats ( $18.56 \pm 0.4196$ ;  $n=10$ ) (Figure 3.1B). Similarly, systolic ( $129.0 \pm 2.04$ ;  $n=10$ ) and diastolic ( $89.86 \pm 2.837$ ;  $n=10$ ) blood pressure in young rats did not differ significantly from from systolic ( $135.5 \pm 2.71$ ;  $n=10$ ) ( $p=0.08$ ) or diastolic ( $3.80 \pm 1.773$ ;  $n=10$ ) ( $p=0.26$ ) blood pressure in aged rats (Figure 3.1C).

#### 3.2 Retinal Vascular Measurements in Young and Aged Retina

Retinal vasculature was then examined in young and aged animals that had undergone baseline physiological measurements (See Section 3.1). Figure 3.2A and B shows young and aged ADPase-stained flat-mount retinas, respectively. Reduced ADPase staining seen in the aged retina is suggestive of alterations in vascular morphology with age. The bar graph in figure 3.2C shows that the density of pixels/mm<sup>2</sup> in the aged retina

**Figure 3.1 Aging did not Impact Physiological Baseline Parameters**

**A.** Bar graph depicting mean values for blood glucose levels obtained in young (n=10) and aged animals (n=10) (p=0.11). **B.** Bar graph illustrating mean intraocular pressure (IOP) for young (n=10) and aged (n=10) rats (p=0.22). **C.** Bar Graph depicting mean systolic blood pressure (p=0.08) and diastolic blood pressure (p=0.26) in young (n=10) and aged (n=10) rats.

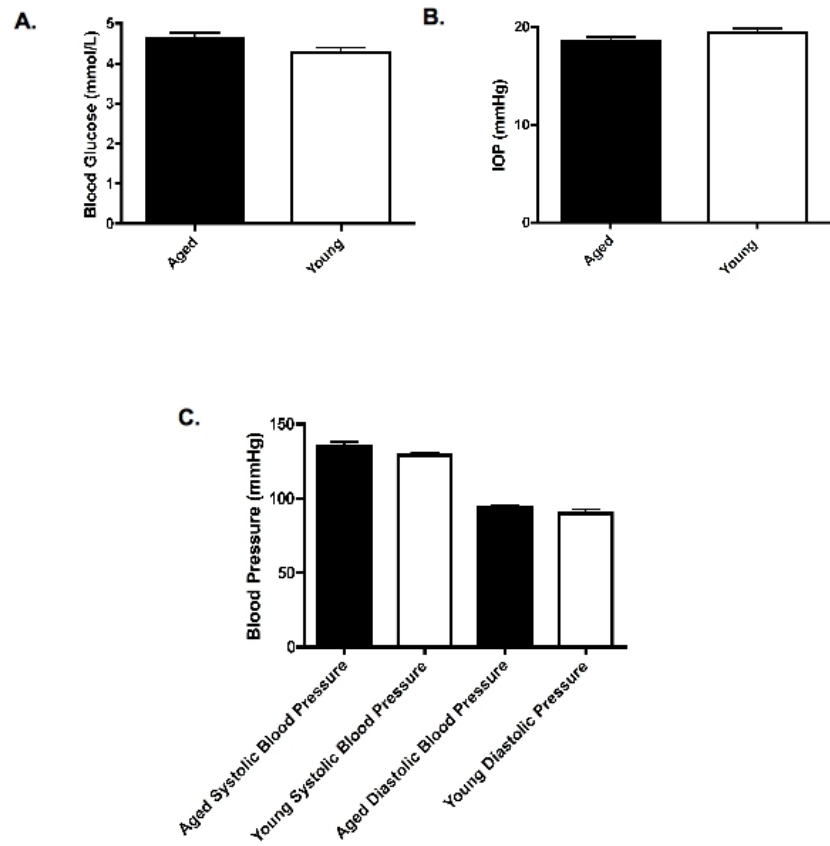
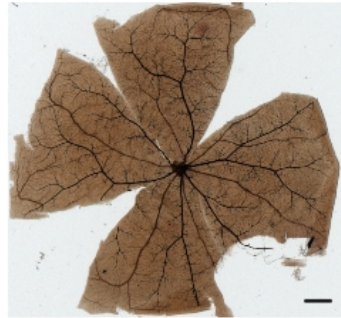


**Figure 3.2 Age-Related Effects on Retinal Vasculature**

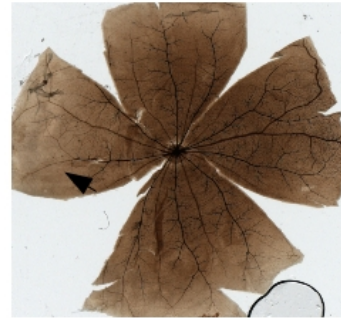
**A.** and **B.** Photomicrograph of ADPase-stained flat-mounted young and aged retina. A decrease in staining in the left quadrant and the periphery of the aged retina is indicated with an arrow. **C.** Bar graph representing ADPase-stained artery and arteriole staining density in young (n=8) and aged (n=10) rats (p=0.22). **D.** Bar graph representing lectin-stained capillary intersection density in young and aged retina from varying distance of 1, 2 and 3 mm from the optic disk in young (n=9) and aged (n=9) rat retinal capillaries. Scale Bar =1mm

A.



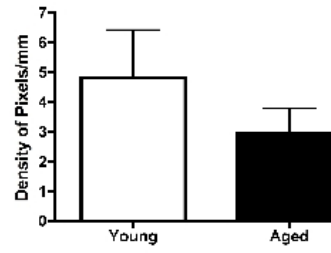
Young

B.

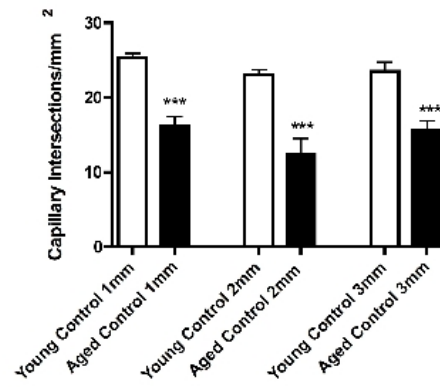


Aged

C.



D.





( $2.929 \pm 0.8662$ ;  $n=10$ ) appears to be reduced in comparison to the young retina ( $4.810 \pm 1.617$ ;  $n=7$ ) although this was not statistically significant ( $p=0.22$ ). When the capillary intersection density was measured at 1, 2 and 3 mm from the ONH, there was a significant reduction with age at all distances. Mean capillary intersection density in young retina at 1 mm from the optic disk ( $25.3 \pm 0.69$ ;  $n=9$ ) was significantly greater ( $p<0.001$ ) than that of the aged retina ( $16.17 \pm 1.35$ ;  $n=9$ ). A similar effect was seen at 2 mm from the optic disk where the density of mean capillary intersections ( $23.0 \pm 0.73$ ;  $n=9$ ) in young retina was significantly higher ( $p<0.001$ ) than those in the aged retina ( $12.33 \pm 2.23$ ;  $n=9$ ). This pattern of reduced capillary intersection density in aged retina ( $5.67 \pm 1.23$ ;  $n=9$ ) compared to the young retina ( $23.5 \pm 1.26$ ;  $n=9$ ) was also seen at 3 mm from the optic disk ( $p<0.001$ ). Figures 3.3A-C and 3.4A-C show representative photomicrographs of retinal vasculature stained with ADPase or lectin, respectively. At 1 mm (Figure 3.3A) and 2 mm (Figure 3.3B) from the optic disk, there is an overall reduction in ADPase staining in the aged retina compared to capillaries from the young retina. Aged capillaries appear to branch less often, have more area between capillaries and there is an overall reduction in staining in comparison to young retina. The most drastic effects of age are observed 3 mm from the optic disk where large areas of reduced staining make the capillaries difficult to visualize, and those that are visible, display an erratic branching pattern in comparison to the young ADPase-stained retina (Figure 3.3C). Lectin staining of capillaries at 1 mm from the optic disk showed broad capillary branching, with capillaries spread further from one another in aged retina in comparison to young retina (Figure 3.4A). Lectin-stained capillaries at 2 mm from the optic disk also

**Figure 3.3 Aged Rat Retinal Capillaries Show Differences in ADPase-Staining Compared to Young**

**A.-C.** Photomicrographs of young and aged flat-mounted ADPase-stained retinal capillaries at 1, 2 and 3 mm from the optic disk in young and aged rat retina. The aged retina shows fewer retinal capillaries that branch more erratically than those in the young rat retina.

Scale bar = 20  $\mu\text{m}$

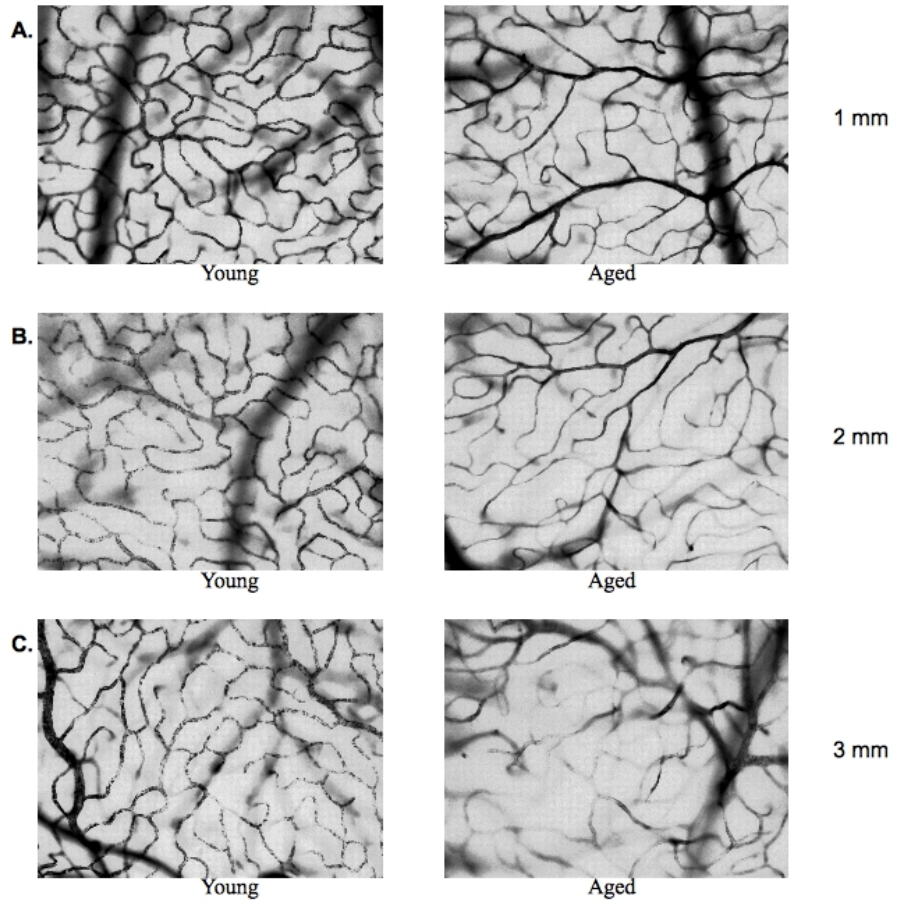
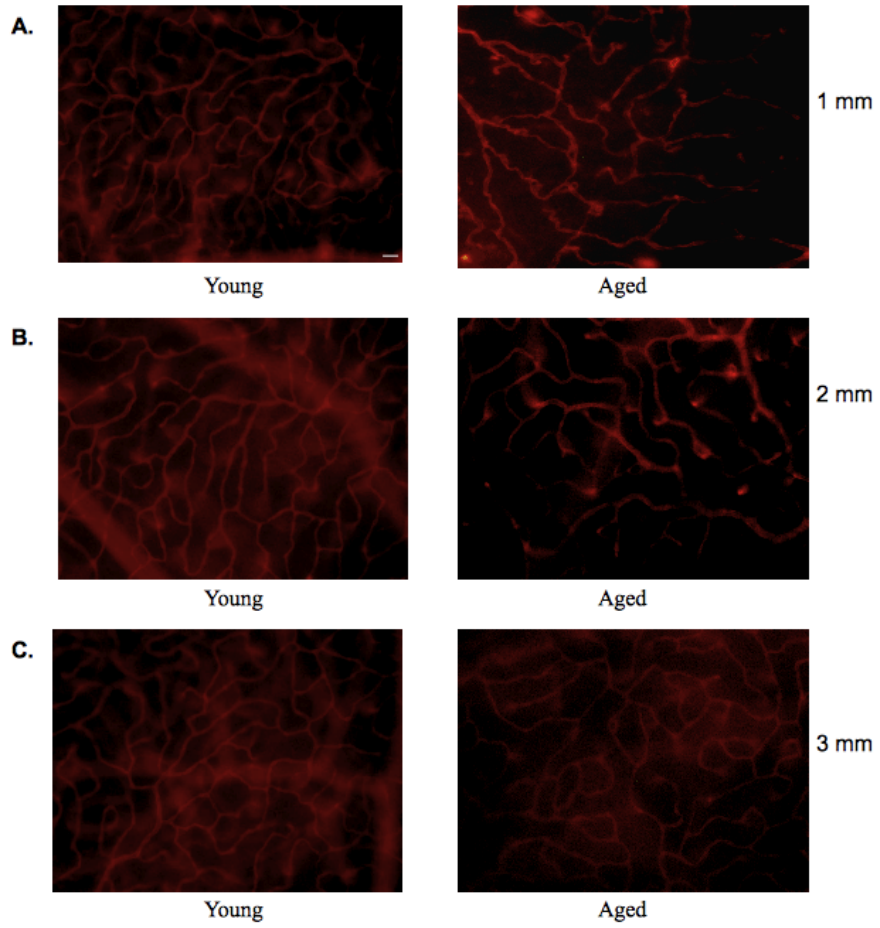


**Figure 3.4 Aged Rat Retinal Capillaries Show Differences in Lectin-Staining Compared to Young**

**A.-C.** Photomicrographs of flat-mounted young and aged lectin-stained retinal capillaries at 1, 2 and 3mm from the optic disk. Compared to young vessels, aged capillaries look thinner, less organized and overall reduced capillary density. Scale bar = 20  $\mu\text{m}$



showed broader capillaries with large areas without capillary branching in aged retina features that were not observed in the young (Figure 3.4B). Similar to results observed in ADPase stained retinas, the most drastic effects of age were observed at 3 mm from the optic disk. Lectin-stained capillaries showed reduced staining and erratic capillary patterns in aged retina in comparison to capillaries from the young retina (Figure 3.4C).

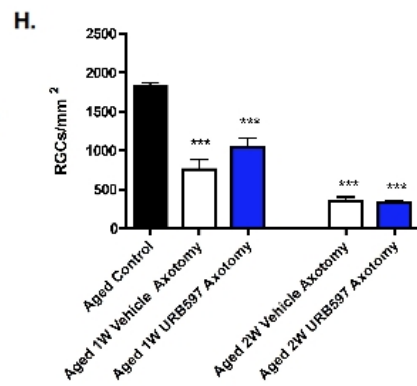
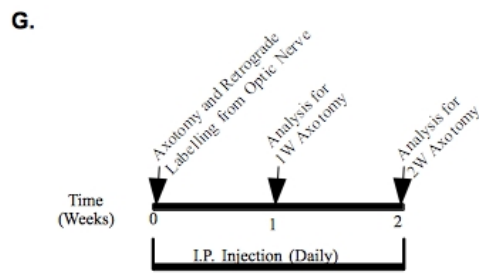
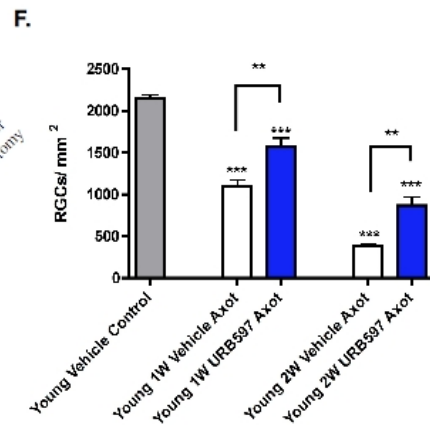
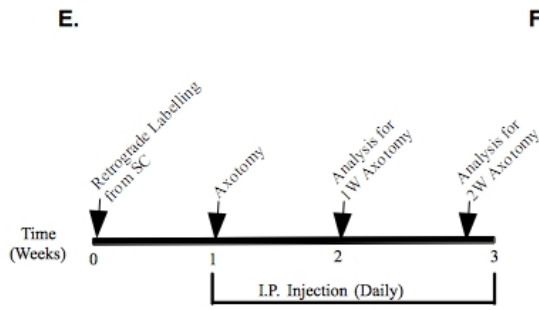
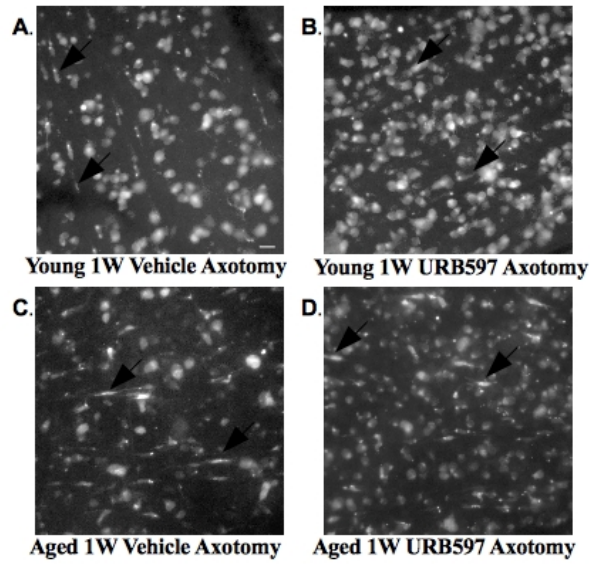
### **3.3 Retinal Ganglion Cell Density in Vehicle- and URB597-treated Young and Aged Retina Following 1 and 2 Weeks of Axotomy**

RGC density was examined after axotomy in animals treated with vehicle only, or with the FAAH inhibitor, URB597, to increase levels of the endocannabinoid, AEA. Animals were previously labelled from the SC using FG at 7 days prior to axotomy. All animals underwent axotomy in only one eye, and the contralateral eye was used as a control. Figure 3.5A-D shows representative photomicrographs of FG-labelled RGCs in young and aged vehicle-treated retina and young and aged URB597-treated retina at 1 week after axotomy. Upon analysis, it was found that at 1 week post-axotomy RGC density ( $2155 \pm 38.46$ ;  $n=5$ ) in young control retina was significantly higher ( $p<0.001$ ) than RGC density in young vehicle-treated retina ( $1097 \pm 75.31$ ;  $n=6$ ) and young URB597-treated ( $1577 \pm 98.17$ ;  $n=6$ ) retina (Figure 3.5F). Vehicle-treated retina had significantly less surviving RGCs following 1 week of axotomy than URB597-treated retinas ( $p<0.001$ ) in young animals (Figure 3.5A-B; Figure 3.5F). After 2 weeks of axotomy RGC density ( $2205 \pm 34.58$ ;  $n=5$ ) in young control retina was significantly higher ( $p<0.001$ ) than RGC density in both young vehicle-treated ( $388.70 \pm 17.68$ ;  $n=6$ )

**Figure 3.5 URB597 Provides Neuroprotection in Young Retina but not in Aged Retina Following 1 and 2 week Axotomy**

**A.-D.** Photomicrographs of FG-labelled RGC and phagocytotic MG (arrows) in flat-mounted, young and aged vehicle-treated, young and aged URB597-treated retina following 1 week (1W) of axotomy in rat retina. **E.** Schematic surgical timeline of young animals that underwent retrograde labelling from the SC prior to 1W or 2 weeks (2W) of axotomy. **F.** Bar graphs representing RGC density of young control (n=5), young 1W vehicle-treated (n=6), young 1W URB597-treated (n=6), young 2W vehicle-treated (n=6) and young 2W URB597-treated (n=6) retina following axotomy. **G.** Schematic surgical timeline showing aged animals that underwent retrograde labelling from the optic nerve stump at the time of axotomy. **H.** Bar graph representing mean RGC density following 1W of axotomy in aged control (n=6), aged vehicle-treated (n=5) and aged URB597-treated (n=5) retina (p=0.164). The bar graph also shows mean RGC density following 2 weeks of axotomy in aged vehicle-treated (n=5) and aged URB597-treated (n=4) retina (p=0.788).

Scale Bar=20  $\mu$ m; \*\*=(p<0.01) \*\*\*=(p<0.001)





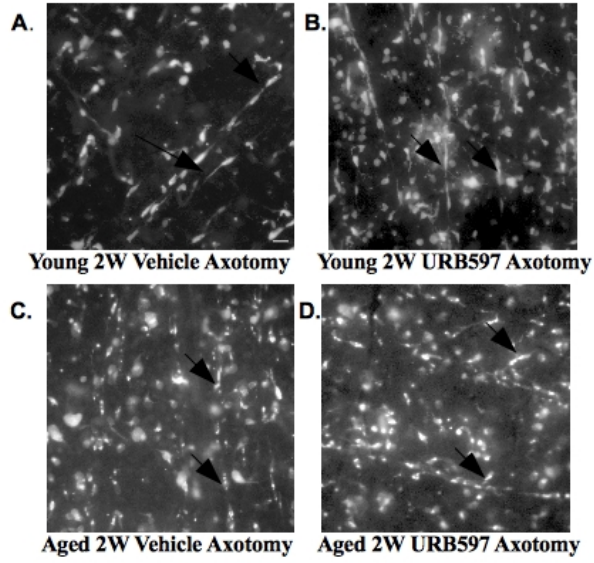
and young URB597-treated retina ( $867.7 \pm 104.7$ ;  $n=6$ ) (Figure 3.5F). Similar to the results obtained after 1 week of axotomy in young URB597-treated retina, RGC density was significantly higher than in young vehicle-treated retina following 2 weeks of axotomy ( $p<0.01$ ) (Figure 3.5).

Since aged rats were too frail to undergo retrogradely labelling from the SC as mortality with multiple surgeries was significantly higher in aged animals than young, the axotomized eye was retrogradely labelled from the optic nerve stump in each animal. Therefore, in the aged animals, vehicle-treated non-axotomized retina's were used as the axotomy controls, as apposed to the contralateral non-axotomized eye. At 1 week post-axotomy aged control rat retina ( $1833 \pm 33.84$ ;  $n=6$ ) had significantly higher ( $p<0.001$ ) RGC density than aged vehicle-treated retina ( $759.0 \pm 120.7$ ;  $n=5$ ) and aged URB597-treated retinas ( $1043 \pm 119.9$ ;  $n=5$ ). Although there appeared to be a trend for increased RGC density in aged animals treated with URB597 following 1 week of axotomy, this was not found to be significantly different ( $p=0.164$ ) (Figure 3.5H). Two weeks post-axotomy RGC density in the aged control retina ( $1833 \pm 33.84$ ;  $n=6$ ) was significantly higher than RGC density in both aged vehicle-treated ( $355.8 \pm 50.10$ ;  $n=5$ ), and aged URB597-treated retinas ( $338.5 \pm 16.41$ ;  $n=4$ ) ( $p<0.001$ ) (Figure 3.5H). RGC density in aged vehicle-treated and aged URB597-treated retina were comparable ( $p=0.788$ ) following 2 weeks of axotomy (Figure 3.5H).

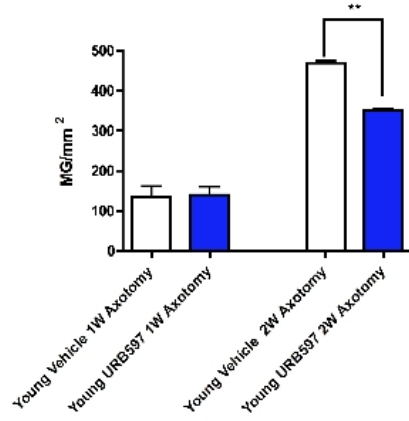
**Figure 3.6 URB597 Reduces Phagocytotic Microglia Density After 2 Weeks Axotomy in Young but not Aged Retina**

**A.-D.** Photomicrograph of FG-labelled RGC and phagocytotic MG (arrows) in flat-mount retina following 2W of axotomy in young and aged vehicle-treated, and young and aged URB597-treated retina. **E.** Bar graph representing mean phagocytotic MG density in young vehicle-treated retina (n=6) and young URB597-treated retina (n=6) following 1W of axotomy (p=0.90). The bar graph also shows young vehicle-treated rat retina (n=6) and young URB597-treated retina (n=6) following 2W of axotomy. **F.** Bar graph represents aged 1W phagocytotic MG densities after axotomy in aged vehicle-treated (n=5) and aged URB597-treated retina (n=5), (p=0.23). The bar graph also shows aged vehicle-treated phagocytotic MG density (n=5) and aged URB597-treated retinas (n=4) following 2W of axotomy (p=0.134).

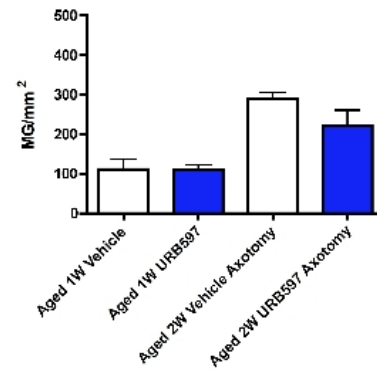
Scale Bar=20  $\mu$ m; \*\*=(p<0.01) \*\*\*=(p<0.001)



**E.**



**F.**



### **3.4 Phagocytotic Microglia Density in Vehicle- and URB597-treated Young and Aged Retina Following 1 and 2 Weeks of Axotomy.**

Phagocytotic MG were not observed in the retinas of young or aged, vehicle-treated control or URB597-treated control retina (data not shown). Figure 3.6A-D shows representative photomicrographs of FG-labelled phagocytotic MG at two weeks post-axotomy in young and aged vehicle-treated and young and aged URB597-treated retina. Vehicle-treated young retina at 1 week after axotomy had a mean phagocytotic MG density of  $135 \pm 26.98$  (n=6), which was not significantly different ( $p=0.90$ ) from young URB597-treated retina at 1 week post-axotomy,  $140 \pm 20.65$  (n=6), (Figure 3.6E). After 2 weeks of axotomy, phagocytotic MG density was significantly reduced ( $p<0.01$ ) in young URB597-treated retina ( $351 \pm 6.083$ ; n=6) compared to young vehicle-treated retina ( $469 \pm 6.36$ ; n=6) (Figure 3.6A-B; Figure 3.6E).

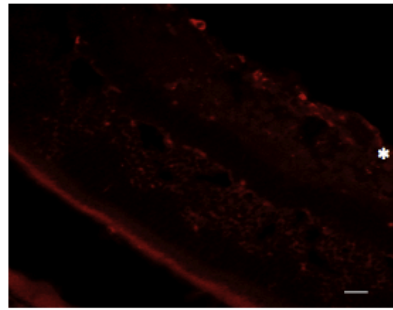
Phagocytotic MG density in the aged rat retina following 1 week of axotomy was not significantly different ( $p=0.921$ ) in vehicle-treated ( $111.3 \pm 25.71$ ; n=5) and URB597-treated aged retina ( $108.5 \pm 13.98$ ; n=5) (Figure 3.6F). Although there did appear to be a trend of reduced phagocytotic MG density in the aged retina with URB597 treatment after 2 weeks of axotomy, aged vehicle-treated ( $220 \pm 15$ ; n=5) and aged URB597-treated phagocytotic MG density ( $290 \pm 38.11$ ; n=4) were not significantly different ( $p=0.172$ ) (Figure 3.6C-D; Figure 3.6F).

Phagocytotic MG are activated MG, yet not all activated MG are phagocytotic. Therefore, we utilized an activated MG specific antibody, Iba1, to examine activated MG following axotomy (Figure 3.7). Young control retinas did not exhibit any Iba1 staining

**Figure 3.7 URB597 Localized Iba1 Staining of Activated Microglia to the Ganglion Cell Layer in Young Rat Retina Following 1 Week of Axotomy**

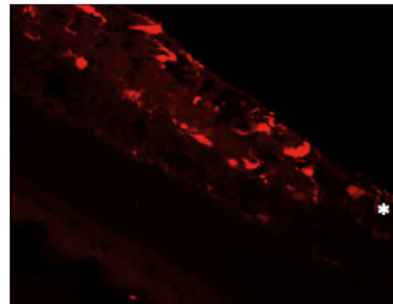
**A.-C.** Photomicrographs of sagittal sections of the retina stained with Iba1 for activated MG in young control, vehicle- and URB597-treated retina following 1 week of axotomy. Scale Bar=20  $\mu\text{m}$  \* indicates GCL

**A.**



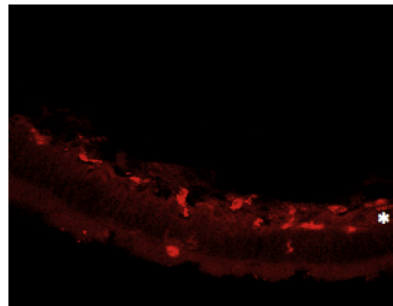
Young Control

**B.**



Young 1W Axotomy Vehicle

**C.**



Young 1W Axotomy URB597

(Figure 3.7A). However, there was a marked increase in activated MG staining with Iba1 after 1 week of axotomy in young vehicle-treated axotomized retinas (Figure 3.7B). This increase in Iba1-positive MG was also seen in young URB597-treated retinas following 1 week of axotomy (3.7C). However, while there appeared to be similar activated MG densities in both vehicle- and URB597-treated retinas, vehicle-treated Iba1 staining showed more activated MG throughout the inner retinal layers (Figure 3.7B), while in URB597-treated retina Iba1 staining demonstrated that activated MG remained localized within the GCL (Figure 3.7C).

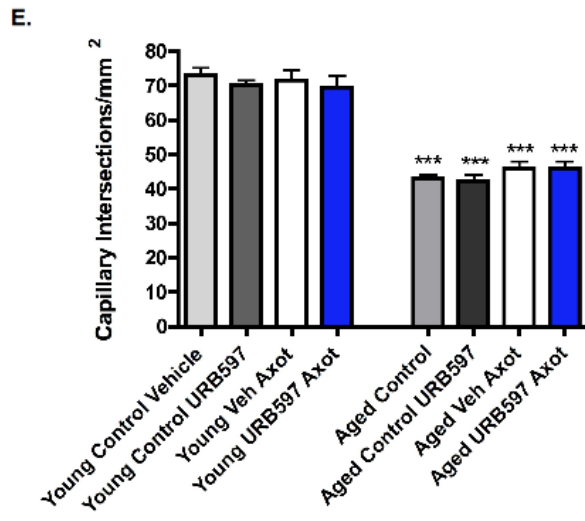
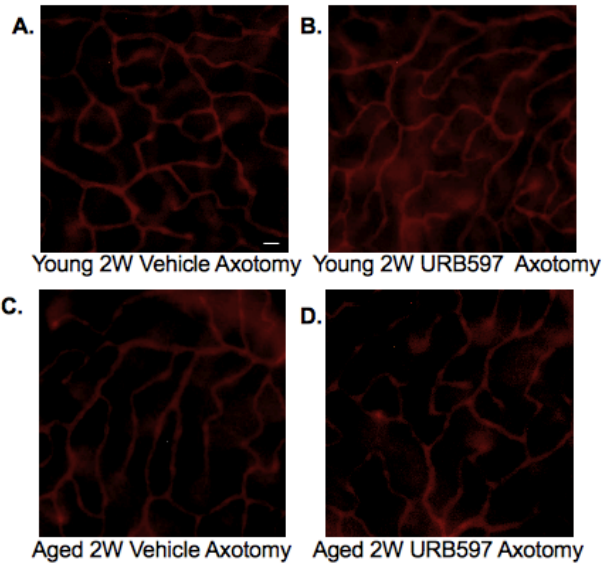
### **3.5 Capillary Intersection Density in Vehicle- and URB597-treated Young and Aged Retina Following 2 Weeks of Axotomy**

URB597 produces vasorelaxant effects on microvasculature (Ho and Randall, 2007), suggesting that a URB597-mediated increase in AEA could exert neuroprotective effects by promoting increased blood-flow to the eye or perhaps improving retinal microcirculation during ischemia or following tissue damage. Therefore, we examined the effects of axotomy plus and minus URB597 treatment on retinal vasculature to determine whether any axotomy-induced vascular changes could be identified that were mitigated by URB597 treatment. To determine alterations in retinal vascular morphology, we examined capillary intersection density at 1, 2 and 3 mm from the optic disk using lectin to visualize the capillaries. Figure 3.8A-D shows representative photomicrographs of lectin-labelled capillaries in young and aged vehicle-treated, and URB597-treated retina at 2 weeks post-axotomy. Young vehicle-treated and URB597-treated retina at 2

**Figure 3.8 Age, Not Axotomy, Produces a Significant Effect on Capillary Intersection Density**

**A.-D.** Photomicrographs of lectin-stained retinal capillaries in flat-mount young and aged vehicle-treated, and young aged URB597-treated retina following 2 weeks of axotomy. **E.** Bar graph representing mean capillary intersection density in young vehicle-treated control (n=5), young URB597-treated control (n=5), young 2W vehicle-treated axotomized (n=6), 2W URB597-treated axotomized (n=6), aged vehicle-treated control (n=5), aged URB597-treated control (n=5), 2W aged vehicle-treated axotomized (n=5) and 2W URB597-treated axotomized retina (n=4). Scale Bar=20  $\mu\text{m}$ ; \*\*\*=( $p < 0.001$ )





weeks of axotomy both show a similar capillary branching pattern with no obvious differences between experimental groups (Figure 3.8A-B). However, in contrast to young control retina, both vehicle- and URB597-treated retina post-axotomy exhibited a reduction in capillaries, and an erratic branching pattern that was similar between the two groups (Figure 3.8C-D).

Upon analysis, retinal vessel density in young vehicle-treated control eyes ( $76.22 \pm 3.14$ ;  $n=5$ ) was not significantly different from that measured in young URB597-treated control eyes ( $70.00 \pm 1.53$ ;  $n=5$ ), young 2 week vehicle-treated axotomized eyes ( $71.67 \pm 2.91$ ;  $n=6$ ), or young 2 week URB597-treated axotomized eyes ( $69.5 \pm 3.50$ ;  $n=6$ ) (Figure 3.8E). Retinas from aged vehicle-treated control eyes had a capillary intersection density of  $44.10 \pm 1.00$  ( $n=5$ ), with similar vessel density in URB597-treated control retina,  $42.33 \pm 1.095$  ( $n=5$ ). Two weeks after axotomy capillary intersection density in aged vehicle-treated retinas ( $46.00 \pm 2.00$ ;  $n=5$ ) and aged URB597-treated retinas ( $42.3 \pm 2.00$ ;  $n=4$ ) were not significantly different from vehicle and URB597-treated control retinas ( $p>0.05$ ). Taken together, no significant effect of axotomy on capillary intersections was found in either young or aged retina despite the fact that a significant difference in capillary density was found between young and aged control and axotomized retinas ( $p<0.001$ ) (Figure 3.8E).

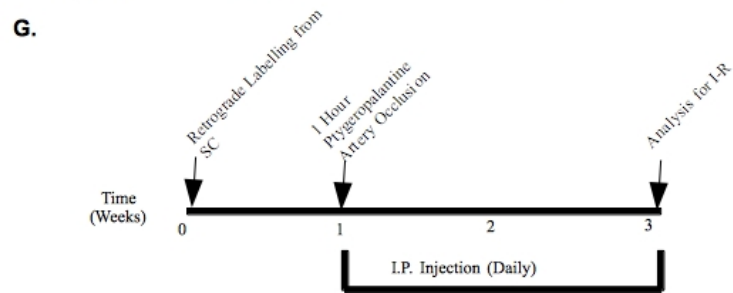
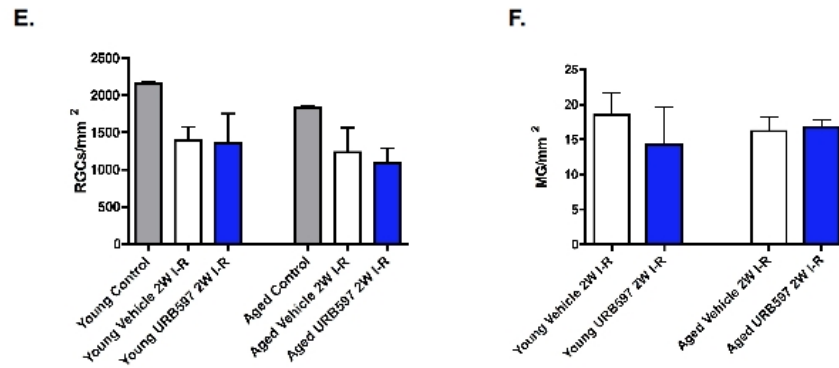
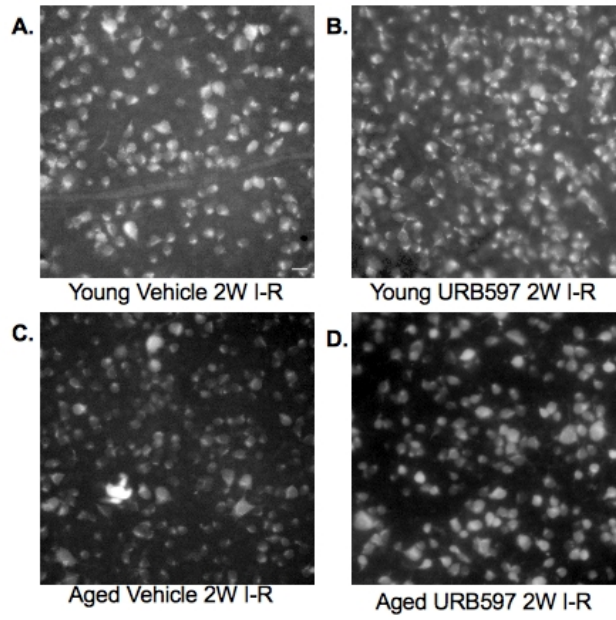
### **3.6 Retinal Ganglion Cell and Phagocytotic Microglia Density in Vehicle- and URB597-treated Young and Aged Retina after Ischemia-Reperfusion**

The transient model of ischemia followed by 2 weeks of reperfusion did not

**Figure 3.9 URB597 Does Not Alter Retinal Ganglion or Microglia Cell Density in Young and Aged Rat Retina Following Transient Ischemia-Reperfusion**

**A.-D.** Photomicrographs of FG labelled flat-mounted young and aged vehicle-treated, and young and aged URB597-treated retina following I-R. **E.** Bar graph representing mean RGC densities in young control (n=7), young vehicle-treated (n=4), young URB597-treated (n=5), aged control (n=6), aged vehicle-treated (n=4) and aged URB597-treated RGC density (n=3) following 2W of I-R. **F.** Bar graph representing mean phagocytotic MG densities in young vehicle-treated retina (n=4), young URB597-treated retinas (n=5), aged vehicle-treated retinas (n=4) and aged URB597-treated retinas (n=3) following 2W of I-R. **G.** Schematic surgical timeline showing all animals underwent retrograde labelling from the SC prior to I-R.

Scale Bar=20  $\mu$ m;



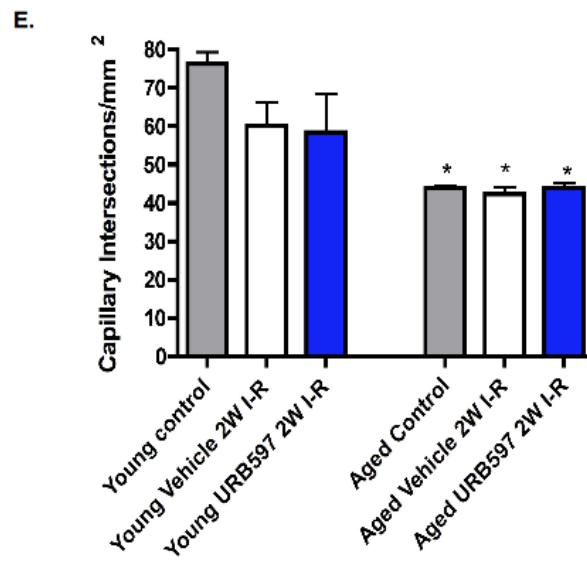
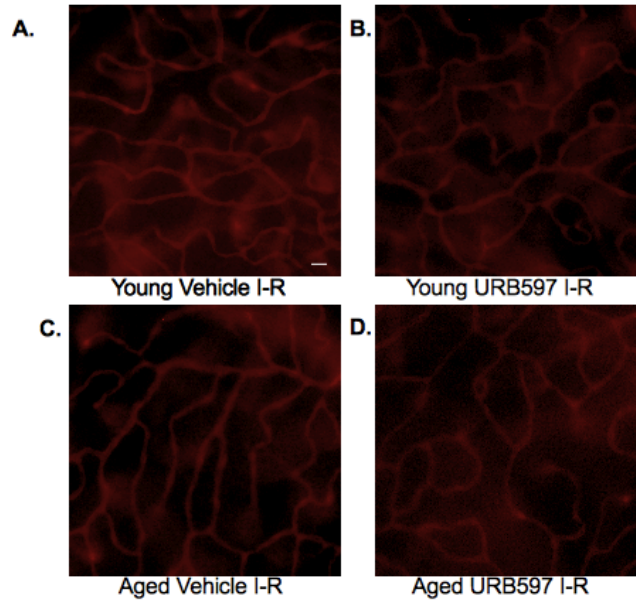
produce significant retinal RGC loss; mean RGC densities in young control retinas ( $2112 \pm 18.36$ ;  $n=7$ ), in vehicle-treated retinas ( $1392 \pm 181$ ;  $n=4$ ), and in URB597-treated retinas ( $1354 \pm 404$ ;  $n=5$ ), were not found to be significantly different from one another (3.9A-B; Figure 3.9E). When RGC loss in aged retina was examined, the results mirrored those found in the young retina. RGC density in aged control retina ( $1833 \pm 33.84$ ;  $n=6$ ), aged vehicle-treated RGC density ( $1232 \pm 336$ ;  $n=4$ ), and aged URB597-treated RGC density ( $1087 \pm 201.9$ ;  $n=3$ ), were not significantly different from one another (Figure 3.9C-D; Figure 3.9E). Analysis of RGC density between young and aged retina following I-R did not show a significant effect of age or drug (Figure 3.9A-D; Figure 3.9E). As seen in the axotomy groups, phagocytotic MG were not present in control eyes (not shown). However, at 1 week after I-R increased phagocytotic MG densities were found in young vehicle-treated retina ( $18.5 \pm 3.175$ ;  $n=4$ ) and URB597-treated retinas, ( $14.20 \pm 5.401$ ;  $n=5$ ), although MG densities between vehicle and URB597 treated groups were not significantly different ( $p=0.53$ ) following I-R (Figure 3.9A-B; Figure 3.9F). Similar results were also seen in the aged rat retina; phagocytotic MG density in aged vehicle-treated retinas ( $16.2 \pm 2.035$ ;  $n=4$ ) were not significantly different ( $p=0.83$ ) from URB597-treated aged retinas ( $16.75 \pm 1.109$ ;  $n=3$ ) (Figure 3.9C-D; Figure 3.9F) following I-R.

### **3.7 Capillary Intersections in Vehicle- and URB597-treated Young and Aged Retina Following 2 Weeks of Ischemia-Reperfusion Injury.**

Figure 3.10A-D shows representative photomicrographs of lectin-labelled retinal

**Figure 3.10 Transient Ischemia-Reperfusion Does Not Produce an Effect on Capillary Intersection Density**

**A.-D.** Photomicrograph of lectin-stained retinal capillaries in flat-mount retina in young and aged vehicle-treated and young and aged URB597-treated retinas following 2W I-R.  
**E.** Bar graph representing mean capillary intersection density in young control (n=7), young vehicle-treated (n=4), young URB597-treated (n=5), aged control (n=6), aged vehicle-treated (n=4), and aged URB597-treated (n=3) retina following 2W of I-R.  
Scale Bar=20  $\mu\text{m}$ ; \*=( $p < 0.05$ )



capillaries in young and aged vehicle- and URB597-treated retina following post-I-R. When capillary intersection density was analysed in young control, vehicle- and URB597-treated retinas at 2 weeks following I-R, there was no significant difference between these experimental groups; young control retinas had a capillary intersection density of  $76.22 \pm 3.135$  (n=7), while young vehicle- and URB597-treated retinas had densities of  $60.00 \pm 6.14$  (n=4), and  $58.5 \pm 10.04$  (n=5), respectively. Similarly, there was no effect on capillary intersection density between experimental groups in the aged rats; capillary intersection density was  $44.00 \pm 0.577$  (n=6) in aged control retinas,  $42.33 \pm 1.76$  (n=4) in aged vehicle-treated retina, and  $44.15 \pm 1.16$  (n=3) in aged URB597-treated retinas (Figure 3.10E). Taken together, only age, not drug or I-R, had a significant effect on capillary intersection density ( $p < 0.05$ ).

### **3.8 Retinal Ganglion, Phagocytotic Microglia and Capillary Intersection Density Following Chronic Ischemia in Young Retina**

RGC loss was also examined in a chronic model of ischemia in the young retina using BCCAO in which the common carotid arteries were permanently tied off to produce global chronic hypoperfusion. Figure 3.11A-B shows photomicrographs of FG-labelled young vehicle- and URB597-treated retinas following 1 week of BCCAO. Upon analysis, young control retina RGC density was reduced from  $2117 \pm 56.92$  (n=5) to  $1209 \pm 137.9$  (n=5) ( $p < 0.001$ ) and,  $1706 \pm 197.3$  (n=5) ( $p < 0.01$ ) in vehicle-treated and URB597-treated retinas, respectively, following 1 week of BCCAO (Figure 3.11D). However, comparison of vehicle- and URB597-treated retinas revealed that, as seen with



**Figure 3.11 URB597 Provides Neuroprotection Following Chronic Ischemia in Young Rat Retina**

**A.-B** Photomicrographs of FG labelled flat-mounted retina of young vehicle- and URB597-treated retina following 1W of BCCAO. **C.** Surgical timeline depicting retrograde labelling from the SC one week prior to BCCAO. Animals were injected with 0.3mg/kg or vehicle 1 hour prior to BCCAO then daily thereafter. **D.** Bar graph representing mean RGC density of young control retina (n=5), young vehicle-treated (n=5) and young URB597-treated retinas (n=5) following 1W BCCAO. Scale Bar=20  $\mu$ m; \*\*=(p<0.01) \*\*\*=(p<0.001)

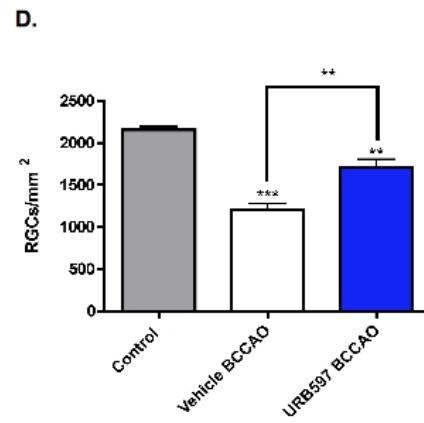
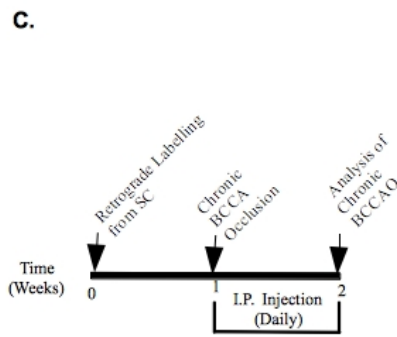
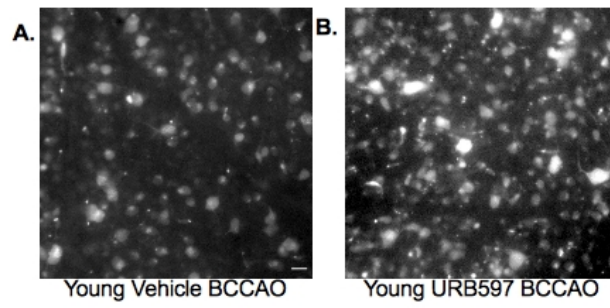
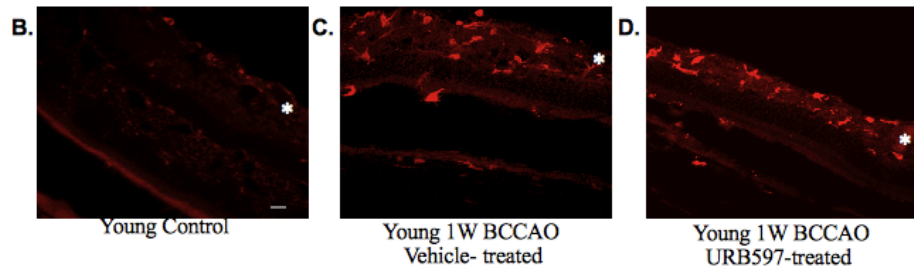
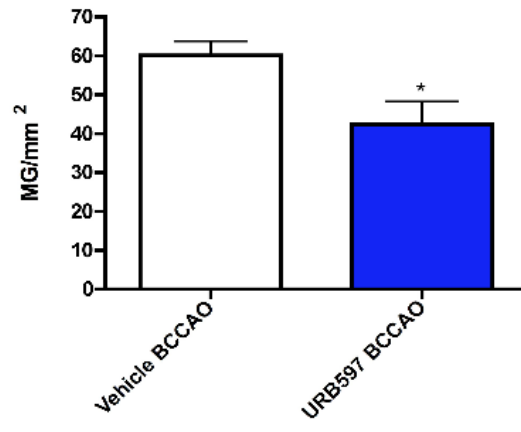


**Figure 3.12 URB597 Reduces Phagocytotic Microglia in Young Rat Retina Following Chronic Ischemia**

**A.** Bar graph representing mean phagocytotic MG densities in vehicle-treated retina (n=5) and URB597-treated retina (n=5) following 1W BCCAO. **B.-D.** Photomicrograph of Iba1-stained sagittal sections of young control, vehicle- and URB597-treated retinal sections following 1W of bilateral common carotid artery occlusion BCCAO where \* indicates GCL.

Scale Bar=20  $\mu\text{m}$ ; \*=(p<0.05) \*\*=(p<0.01) \*\*\*=(p<0.001)

A.



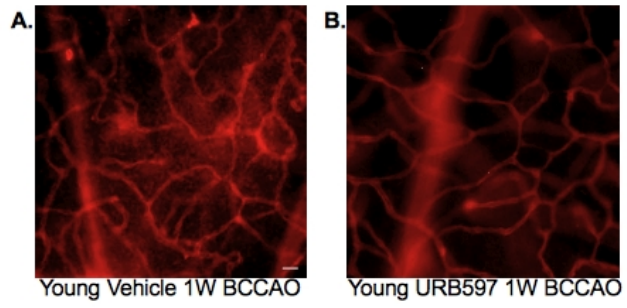
Examination of FG-labelled phagocytotic MG densities in young vehicle- and URB597-treated retina following 1 week of chronic BCCAO (Figure 3.12A) revealed a significant ( $p < 0.05$ ) reduction in phagocytotic MG with URB597 treatment ( $42.25 \pm 5.977$ ;  $n=5$ ) compared to vehicle-treated retina ( $60.08 \pm 7.27$ ;  $n=5$ ). When the effects of URB597 on activated MG were examined using Iba1 staining of retinal sections, it was found that, in comparison to control retina where there was no Iba1 staining (Figure 3.12B), there was a dramatic increase in activated MG in young vehicle-treated retina following BCCAO (Figure 3.12C). This increase in activated MG did not appear to be substantially different in URB597-treated retina (Figure 3.12D). However, similar to those results observed after 1 week of axotomy, Iba1 staining of activated MG after 1 week of BCCAO plus URB597 treatment appears to have more localized staining pattern; activated MG appeared to be segregated to the GCL in comparison to vehicle-treated retinas where activated MG staining projected throughout the inner retina (Figure 3.12B-C).

Figure 3.13A-B shows lectin-labelled capillaries in vehicle- and URB597-treated young retina following 1 week of BCCAO. In vehicle-treated retinas, capillaries were thinner and showed erratic branching patterns (Figure 3.13A) while in URB597-treated retina, capillaries appeared to have a more normal and thicker profile suggesting that URB597 was capable of reducing retinal vasculature pathology following 1 week of chronic ischemia. Upon analysis, no significant difference ( $p > 0.05$ ) in capillary

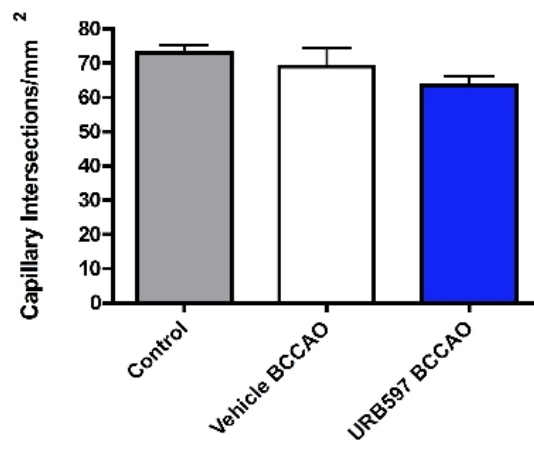
**Figure 3.13 URB597 Promotes Retinal Capillary Stability Following Chronic Ischemia**

**A.-B.** Photomicrograph of lectin-stained young vehicle- and URB597-treated flat-mount retina following 1W of BCCAO. **C.** Bar graph representing mean capillary intersection

density in young control (n=5), young vehicle-treated (n=5) and young URB597-treated retina (n=5) following 1W BCCAO.  
Scale Bar=20  $\mu$ m



**C.**



intersection density was found between control ( $73.11 \pm 2.09$ ;  $n=5$ ), vehicle-treated, ( $69.00 \pm 5.370$ ;  $n=5$ ), or URB597-treated retina, ( $63.44 \pm 2.88$ ;  $n=5$ ) (Figure 3.13C).



## **Chapter 4**

### **Discussion**

#### **4.1 Overview of Findings**

A number of progressive eye-diseases have both age and vascular dysregulation as major risk factors, suggesting that alterations that occur with age may make the aged eye more susceptible to ischemic and retinal damage. However, in order to identify appropriate therapies for these diseases, it is essential to understand the interaction of vascular damage and neuronal cell loss in age-appropriate models. My work used several different experimental models of retinal damage in order to examine effects on both neurons and vasculature. This included a model of axon injury (primarily neuronal insult) and two different models of vascular insult (transient retinal ischemia-reperfusion and chronic global retinal ischemia). These models were carried out in both young and aged animals in order to gain insight into differences between the response of young and aged retina to insult, and to identify novel therapeutic targets for treating age-related eye disease.

The eCB system has been shown to have an integral role in regulating ocular functions including regulation of vascular tone, IOP and retinal neuron activity (Adams et al., 1978; Straiker et al., 1999a; Straicker et al., 1999b; Song and Slowey, 2000; Stamer et al., 2001; Plange et al., 2007). Therefore this study investigated whether increasing levels of the endocannabinoid, AEA, would be beneficial after axotomy or retinal ischemia in both our young and aged experimental models. However, as AEA has a limited duration of action, the enzyme inhibitor, URB597, was used. URB597 inhibits degradation of

AEA by FAAH and thus can promote physiologically relevant concentrations of AEA on-demand at the site of action. The objectives of this project were: 1) to evaluate changes present with aging in the retina, 2) to determine whether the aging retina is more susceptible to insult (eg. ischemia, axotomy), and 3) to investigate whether modulation of the eCBs can provide retinal neurovascular protection in young and aged models of retinal damage (eg. ischemia, axotomy).

The results of this study showed that there was an age-related reduction in retinal capillary density throughout the retina that appeared to be independent of alterations in other physiological factors such as blood pressure, blood glucose and IOP. In comparison to the young retina, there was greater RGC loss in the aged retina following 1 week, but not 2 weeks of axotomy. URB597, was able to promote RGC survival following both 1 and 2 weeks of axotomy in young retina. However, although there was a trend toward increased RGC survival after 1 week of axotomy, URB597 did not produce significant survival effects on RGC densities in the aged retina post-axotomy. In addition to increasing RGC survival, URB597, was also able to reduce phagocytotic FG-positive MG following 2 weeks of axotomy in young retina and, while not significant, there was a trend of reduced phagocytotic MG in the aged retina with URB597 treatment following 2 weeks of axotomy. Activated MG, labelled by Iba1, like FG-positive MG, were dramatically increased following 1 week of axotomy, and while URB597 did not appear to decrease the total number of activated MG, URB597 was able to reduce migration of activated MG into other layers of the young retina post-axotomy. While phagocytotic MG density in vehicle-treated young and aged retina following 1 week of axotomy was

comparable, phagocytotic FG-positive MG were reduced in the aged retina following 2 weeks of axotomy compared to the young retina. There were no significant effects of axotomy or URB597 on retinal capillary density in young or aged retina, only an age-related reduction in retinal capillary density was observed.

In contrast to axotomy, experimental results from the model of transient I-R produced no significant effect on RGCs, phagocytotic MG or capillary density in either young or aged retina, and neither drug nor age had a significant effect on any of these parameters. On the contrary, 1 week of chronic BCCAO produced a significant reduction in RGC density, increased phagocytotic MG and disturbed retinal capillary integrity in the young retina. As seen with axotomy, URB597 treatment increased RGC cell survival, reduced phagocytotic FG-positive MG, inhibited the migration of activated MG within the retina, and reduced retinal capillary damage; URB597-treated retinal vasculature 1 week after BCCAO were indistinguishable from controls.

## **4.2 Impact of Age and URB597 treatment on the Response of Retinal Neurons, Glia and Vasculature to Axotomy and Ischemic Insult**

### *4.2.1. Retinal Vasculature*

A number of age-related alterations have been reported in the retinal vasculature that occur independent of alterations in systemic blood pressure, blood glucose and IOP (Hughes et al., 2006). These include a loss of retinal capillaries which is most pronounced in the periphery of the retina and has been shown to correlate with age-related RGC loss (Lai et al., 1978). As blood pressure and other physiological parameters in this study

remained unchanged between young and aged animals, the decrease in retinal capillary density seen in aged retina may result from impaired retinal blood-flow autoregulatory mechanisms (Hughes et al., 2006). In support of this, other studies have demonstrated that impaired retinal blood flow autoregulation and loss of capillaries precedes development of retinopathy (Mizutani et al., 1996; Kern et al., 2000) and can trigger vascular occlusive events (Kern et al., 2000), both of which increase in frequency with age.

#### 4.2.2 RGCs

Age-related alterations in retinal blood flow autoregulation and capillary loss may contribute to the increased RGC loss seen in this study following 1 week of axotomy in the aged retina, compared to the young retina. A well established pattern of RGC loss has been reported in the young adult retina following axotomy; RGC death is delayed until 3-5 days post-axotomy (Berkelaar et al., 1994; Rabacchi et al., 1994; Cellerino et al., 2000; Cordeiro et al., 2004), with peak apoptosis of RGCs occurring at 7 days, at which time 50% of all RGCs are lost (Cordeiro et al., 2004). By 2 weeks post-axotomy, RGC density is reduced to approximately 10% of controls (Berkelaar et al., 1994). In this study, increased RGC loss was found in the aged retina following 1 week of axotomy. However, by 2 weeks of axotomy, RGC loss in aged retina was comparable to that seen in the young retina, suggesting an accelerated pattern of cell loss at the initial onset of damage that then appears to plateau.

In contrast to axotomy, age-related accelerated cell loss was not observed in the model of transient I-R. However, as RGC loss in both young and aged animals was

extremely variable in this model, it was difficult to definitively determine any age-related differences in RGC survival in the response to I-R injury. A number of groups have also indicated that problems inherent in this I-R model such as high mortality rates, inconsistent infarct volume due to surgical skill, animal strain and collateral blood flow reduce the reliability of this model (Connolly et al., 1996; Tsuchiya et al., 2003; Barber et al., 2004; Tureyen et al., 2005).

Chronic BCCAO however, produced a significant reduction in RGC density with cell loss reaching approximately 40-60% of controls within 1 week of ischemia (Yamamoto et al., 2006; Kalensnykas et al., 2008). Other studies have also reported that RGC loss after BCCAO appears to maximize at 1 week with no further cell loss at 2 weeks and up to 6 months of chronic ischemia (Yamamoto et al., 2006). This arrest in the degenerative process with chronic BCCAO is thought to be due to arteriole remodelling, as the initial reduction in blood flow to the brain has been shown to gradually recover with time (Otori et al., 2003).

This study showed that URB597 was able to increase RGC survival to a similar extent following both axotomy and chronic BCCAO. While the primary insult differs between these retinal injury models, it is possible that the observed URB597-mediated neuroprotection may involve common drug targets. For example, axon damage and ischemia activates excitotoxic cascades in retina that involve excessive local glutamate release and pathological increases in intracellular  $Ca^{2+}$ . This leads to subsequent activation of pro-apoptotic protein pathways and results in neuronal apoptosis (Sucher et al., 1991; Coyle and Puttfarcken, 1993; Dreyer et al., 1996). In keeping with a central

role for glutamate in mediating RGC apoptosis, NMDA antagonists have been shown to produce neuroprotective effects in several different models of RGC damage, including axotomy, high IOP-induced ischemia and glaucoma models (Sucher et al., 1997; Adachi et al., 1998; Yoles and Schwartz, 1998; Nucci et al., 2005). The neuroprotective effects of URB597 following axotomy and ischemia in this study may be mediated via decreased glutamatergic signalling; endocannabinoids, including AEA, can act on presynaptic CB1 receptors to modify the activity of neuronal voltage-dependent  $Ca^{2+}$  channels and  $K^+$  channels (Deadwyler et al., 1995; Gomez del Pulgar et al., 2000; Galve-Roperh et al., 2002; Karanian et al., 2005; Molina-Holgado et al., 2005; Karanian et al., 2007), resulting in a decrease in neurotransmitter release. Consistent with this, increases in AEA have been shown to promote neuronal survival by reducing hippocampal excitotoxicity (Coomber et al., 2008). AEA administration also provided neuroprotection in a model of high IOP-induced ischemia where increased AEA levels resulted in decreased glutamate levels (Nucci et al., 2007). In addition to inhibition of neurotransmitter release, endocannabinoid-mediated decreases in intracellular  $Ca^{2+}$  via direct action on voltage-dependent ion channels following injury may also contribute to neuroprotection by decreasing  $Ca^{2+}$ -dependent pro-apoptotic signalling cascades (Currie et al., 2008; Liu et al., 2009; Ryan et al., 2009). Therefore, as URB597 increases levels of AEA, the neuroprotective effects associated with this drug may occur directly through a reduction of neuronal intracellular  $Ca^{2+}$  (via inhibition of  $Ca^{2+}$  influx) and by CB1-mediated inhibition of glutamate release. However, other mechanisms of neuroprotection may also include a reduction of oxidative free radicals, increased retinal blood flow and

modulatory effects on MG cells (Hampson et al., 1998; Chen and Buck, 2000; Jackson et al., 2005; Oltmanns et al., 2008; Stella, 2010).

#### 4.2.3 *MG*

Microglia, resident immune cells present in the retina, undergo a variety of structural changes based on their location, and signals from the surrounding tissue that recruit them from resting, to immunoreactive cells (Langmann, 2007). The role of activated phagocytotic MG are to enhance scavenger function and remove damaged cells and their associated debris (Langmann, 2007). Axotomy and chronic BCCAO produced an increase in phagocytotic MG in the retina after 1 week post-injury in both young and aged animals. This increase in MG was not observed following transient I-R. Also of note from our study was the observation that despite additional RGC loss at two weeks post-axotomy in aged retina, we did not find a corresponding increase in phagocytotic MG. In contrast, in young animals increased RGC loss at two weeks post-injury resulted in a reciprocal increase in phagocytotic MG. Furthermore, aged animals had fewer phagocytotic MG overall than found in the young retina. Alterations in MG activity with aging have been examined in several other studies which have demonstrated that aged retinal MG have reduced phagocytotic abilities (Njie et al., 2010), and abnormalities in MG cytoplasmic structures are increased throughout age (Streit et al., 2004). These results suggest that aged animals may have impaired MG responses in comparison to young animals, reflecting alterations in immune function with age (Xu et al., 2008).

AEA has been demonstrated to inhibit immune cell migration (Joseph et al., 2004; Oka et al., 2004). Consistent with this, URB597 administration successfully reduced

phagocytotic MG density and inhibited MG migration after both axotomy and BCCAO; sections taken from young animals treated with URB597 after 1 week of axotomy or BCCAO both showed reduced MG infiltration of retinal layers. In models where URB597 had no effect on RGC survival, such as in transient I-R, there were no significant effects on phagocytotic MG density. This may indicate that URB597 treatment alters MG response to injury to promote increased cell survival in the retina.

There is controversy surrounding the role of MG in neuronal degeneration (Langmann, 2007; Xu et al., 2008). MG are vital to digesting dying cellular debris, thereby preventing their exposure to surviving cells and also release trophic factors important to cell survival (Streit, 2002; Kohl et al., 2003; Simard et al., 2006;). However, MG are also associated with releasing neurotoxic compounds including the cytokine, tumour necrosis factor alpha (TNF $\alpha$ ). In addition to effects on MG, AEA has reported to reduce levels of TNF $\alpha$  (Sawada et al., 1989; Munro et al., 1993; Moss and Bates, 2001; Streit, 2002; Facchinetti et al., 2003). Supporting an inhibitory action of AEA on MG activation, our results show that inhibition of both phagocytotic MG and MG infiltration are associated with increased cell survival this suggests that AEA may exert neuroprotective effects in the retina as a modulator of immune cell (MG) function.

#### *4.2.3.4 Vasculature*

There was no significant retinal microvasculature pathology observed following axotomy or transient I-R in either young or aged retina. However, chronic BCCAO in young retina produced qualitative alterations of capillary morphology after 1 week that were reduced with the administration of URB597. The findings from this study are



consistent with other reports that showed that axotomy did not produce significant alterations in retinal vasculature (Baumbach et al., 1978; Bain et al., 2001), although a few studies have identified transient vascular changes following optic nerve transection (Kiernan, 1985). The lack of significant retinal vascular changes reported in these studies and in the experimental models used in this study, may reflect the post-injury time-course used; neuronal loss or ischemic vascular damage leading to vascular modifications may require an extended time-course to observe alterations (Baumbach et al., 1978; Bain et al., 2001).

Pathophysiological alterations in retinal capillaries, however, were present following chronic BCCAO. In this experimental model, capillaries exhibited thinning and a more erratic branching pattern. While we did not observe a reduction in global retinal capillary density, morphological abnormalities such as tortuosity of vessels and increased presence of microaneurysms were present in the retina after BCCAO. Other studies in the retina have shown that RGC loss precedes such vasculature alterations (Feit-Leichman et al., 2005; Zheng et al., 2007; Chen et al., 2009). The thinning of capillaries and more erratic pattern observed with chronic BCCAO was similar to findings reported for retinal arteries and arteriole alterations within hours of occluding the optic nerve sheath in a model of retinal vascular injury (Hirose et al., 2004). Thinning of the capillary wall in both clinical and experimental observations is thought to result in a reduction of blood-flow due to increase resistance. This decrease in blood flow would likely have more profound effects on vasculature over time (Steiner et al., 1965).

AEA has vasoactive actions in various different vascular beds, including those of

the eye, and increases in AEA have been associated with vasodilation and increased blood flow (Pate et al., 1995; Romano and Lograno, 2006). Of our vascular models, we observed beneficial effects of URB597 on retinal vasculature only in our chronic BCCAO model and not in the transient I-R model. Transient I-R is a model that reflects damage caused by reperfusion of blood flow resulting in an increase in oxidative free radicals and a decrease in the ability of the tissue to detoxify these compounds (Filho et al., 2004). In contrast, BCCAO involves a chronic reduction in blood flow to the retina. Therefore, it is possible that in the BCCAO model of retinal ischemic damage, URB597 is able to provide increased RGC survival and decreased vascular pathology through an AEA-mediated increase in blood-flow, thus reducing the impact of the chronic hypoperfusion that occurs in BCCAO. As I-R damage is primarily related to reperfusion injury, this might explain why URB597 was found to be more efficacious after BCCAO yet ineffective following I-R. However, this study also shows that URB597 is able to provide neuroprotection following axotomy, a model that does not appear to involve significant vascular dysregulation ( Baumbach et al., 1978; Kiernan, 1985), suggesting that URB597-mediated neuroprotection must also involve additional mechanisms independent of vascular targets.

#### **4.3 Limitations and Future Directions**

The major limitations of this study were the ability to obtain enough surviving aged animals in each of the experimental model groups to obtain significance for the drug treatment and vascular analysis. Increased frailty and attrition of the aged animals prior to

experimental induction, limited the tissue available for multiple time-points and reduced animal numbers in each group of aged animals. In addition, the costs associated with the development and maintenance of an aging colony, and the time restraints on initiating experimental procedures in order to ensure appropriate aging of animals, limited the number of animals that were available for these studies.

Future experiments that would improve the significance of these findings should include increasing the power of the study for the aged experimental groups as well as providing a vascular measure of eCB levels in young and aged animals before and after URB597 treatment. Various behavioural studies *in vivo* have now shown that 0.3 mg/kg of URB597 is sufficient to inhibit FAAH, and prolong AEA levels sufficiently to alter various behavioural parameters such as anxiety and pain threshold (Kathuria et al., 2003). Therefore, although we observed neuroprotection in our young models of axotomy and BCCAO, we do not know the exact tissue levels of AEA in our animals. Since FAAH has been shown to be up-regulated in aged animals (Maccarrone et al., 2001) and drug transport may be impaired with age, it is vital to understand if the lack of URB597 neuroprotection in aged animals reflects this increased activity of FAAH; the dose of URB597 used in this study may not sufficiently reduce FAAH and/or the neuroprotective actions of AEA may no be longer sufficient for preserving RGCs in the aged retina.

Identifying the receptor targets through which AEA exert its effects is paramount to identifying novel therapeutic targets. As URB597 may provide neuroprotection through multiple pathways ie. CB1, TRPV1 and CBx, the use of antagonists to these receptors may provide insight into which pathways are responsible for URB597-mediated

cell survival. The CB1 antagonist, AM251, has been shown *in vivo* to block certain AEA effects, while other actions of AEA are only inhibited with O-1918 administration (Kozłowska et al., 2007; Zakrzaska et al., 2010). O-1918 is a specific antagonist to CB<sub>1</sub>, the Abn-CBD-sensitive vascular cannabinoid receptor. A combination of both O-1918 and AM251 may help differentiate components of AEA neuroprotection in each model of injury.

As many cannabinoids have antioxidant abilities it has also been suggested that neuroprotective effects of URB597-mediated eCB increase may be due to antioxidant effects (Hampson et al., 1998; Chen and Buck 2000). AEA administration has been shown to increase anti-oxidant markers in a rat model of I-R (Beheshtian et al., 2008), therefore examination of anti-oxidant components such as malondialdehyde, an indicator of oxidative stress, and glutathione levels, a measure of intrinsic antioxidant capabilities of cells (Dilsiz et al., 2006) in axotomy and chronic BCCAO may provide more information on eCB antioxidant effects.

#### **4.4 Clinical Implications and the Potential of URB597 as a Therapeutic Agent**

The endocannabinoid system has been shown in experimental and clinical studies to provide protection against insult and injury, making this system a strong candidate for novel therapeutic intervention for a number of disorders (Mackie, 2008; Pacher and Hasko 2008; Vemuri et al., 2008; Janero and Makriyannis 2009). This work showed that URB597, an inhibitor of the FAAH enzyme, has the ability to prevent RGC death in models of retinal ischemia and optic nerve injury and illustrates the potential of

increasing the eCBs activity to reduce pathophysiology. In support of this approach, work in transgenic FAAH<sup>-/-</sup> mice and pharmacological blockade has shown potential in management of multiple sclerosis (Benito et al., 2007), spinal cord injury (Garcia-Ovejero et al., 2009) and high IOP-induced ischemia (Nucci et al., 2007). Enhancement of AEA has also been shown to decrease seizure severity (Karanian et al., 2007), and has been indicated in a number of age-related diseases including Alzheimer's, Parkinson's and Huntington's disease (Benito et al., 2003; Maccarrone et al., 2003; Ramirez et al., 2005; Micale et al., 2007; Bisogno and Di Marzo, 2008). Given that FAAH inhibitors are devoid of cataleptic effects (Beltramo et al., 2000; Arizzi et al., 2004; Karanian et al., 2007), do not carry an abuse potential (Justinova et al., 2008; Hwang et al., 2010), and increased AEA is produced on-demand at the site of action with actions at multiple targets, suggest that FAAH inhibitors may be safe therapeutic candidates to treat a variety of disease states. In addition, since a number of FAAH inhibitors display varied potency over time and exhibit different binding characteristics, this may provide further opportunities to regulate AEA levels and avoid off-target effects (Zhang et al., 2007; Seierstad and Breitenbucher, 2008; Hwang et al., 2010).

#### **4.5 Conclusion**

The FAAH enzyme inhibitor, URB597, showed neuroprotective potential in several models of damage in the young retina. Our results suggest that URB597-mediated neuroprotection may occur through a number of different cellular targets; URB597 had effects on RGCs, MG and retinal vasculature. In contrast, URB597 did not produce any

significant neuroprotective effects in the aged retina although some differences were apparent compared to vehicle treated controls. This illustrates the importance of understanding the mechanisms by which URB597 provides neuroprotection and how these are altered with age. Given that URB597 was able to provide neuroprotection in the young retina but had reduced efficacy in the older animals, it suggest that URB597 may only be an appropriate therapeutic compound in treatment of retinal disease in aged animals when combined with other therapies.

## References

- Adachi K, Kashii S, Masai H, Ueda M, Morizane C, Kaneda K, Kume T, Akaike A, Honda Y (1998) Mechanism of the pathogenesis of glutamate neurotoxicity in retinal ischemia. *Graefes Arch Clin Exp Ophthalmol* 236:766-774.
- Adams AJ, Brown B, Haegerstrom-Portnoy G, Flom MC, Jones RT (1978) Marijuana, alcohol, and combined drug effects on the time course of glare recovery. *Psychopharmacology (Berl)* 56:81-86.
- Ahn K, Johnson DS, Fitzgerald LR, Liimatta M, Arendse A, Stevenson T, Lund ET, Nugent RA, Nomanbhoy TK, Alexander JP, Cravatt BF (2007) Novel mechanistic class of fatty acid amide hydrolase inhibitors with remarkable selectivity. *Biochemistry* 46:13019-13030.
- Alroy J, Goyal V, Skutelsky E (1987) Lectin histochemistry of mammalian endothelium. *Histochemistry* 86:603-607.
- Arizzi MN, Cervone KM, Aberman JE, Betz A, Liu Q, Lin S, Makriyannis A, Salamone JD (2004) Behavioral effects of inhibition of cannabinoid metabolism: The amidase inhibitor AM374 enhances the suppression of lever pressing produced by exogenously administered anandamide. *Life Sci* 74:1001-1011.
- Ashton JC, Friberg D, Darlington CL, Smith PF (2006) Expression of the cannabinoid CB2 receptor in the rat cerebellum: An immunohistochemical study. *Neurosci Lett* 396:113-116.
- Bain AC, Raghupathi R, Meaney DF (2001) Dynamic stretch correlates to both morphological abnormalities and electrophysiological impairment in a model of traumatic axonal injury. *J Neurotrauma* 18:499-511.
- Barber PA, Hoyte L, Colbourne F, Buchan AM (2004) Temperature-regulated model of focal ischemia in the mouse: A study with histopathological and behavioral outcomes. *Stroke* 35:1720-1725.
- Bari M, Battista N, Fezza F, Gasperi V, Maccarrone M (2006) New insights into endocannabinoid degradation and its therapeutic potential. *Mini Rev Med Chem* 6:257-268.
- Baumbach GL, Cancilla PA, Hayreh MS, Hayreh SS (1978) Experimental injury of the optic nerve with optic disc swelling. *Lab Invest* 39:50-60.

Bayewitch M, Avidor-Reiss T, Levy R, Barg J, Mechoulam R, Vogel Z (1995) The peripheral cannabinoid receptor: Adenylate cyclase inhibition and G protein coupling. *FEBS Lett* 375:143-147.

Bear MF, Connors BW, Paradiso MA (2001) *Neuroscience exploring the brain*. Baltimore, MA: Lippincott Williams & Wilkins.

Begg M, Pacher P, Batkai S, Osei-Hyiaman D, Offertaler L, Mo FM, Liu J, Kunos G (2005) Evidence for novel cannabinoid receptors. *Pharmacol Ther* 106:133-145.

Beheshtian A, Salmasi AH, Payabvash S, Kiumehr S, Nezami BG, Rahimpour S, Rabani R, Tavangar SM, Dehpour AR (2008) Role of endogenous cannabinoids in ischemia/reperfusion injury following testicular torsion in rats. *Int J Urol* 15:449-454.

Belayev L, Busto R, Watson BD, Ginsberg MD (1995) Post-ischemic administration of HU-211, a novel non-competitive NMDA antagonist, protects against blood-brain barrier disruption in photochemical cortical infarction in rats: A quantitative study. *Brain Res* 702:266-270.

Beltramo M, de Fonseca FR, Navarro M, Calignano A, Gorriti MA, Grammatikopoulos G, Sadile AG, Giuffrida A, Piomelli D (2000) Reversal of dopamine D(2) receptor responses by an anandamide transport inhibitor. *J Neurosci* 20:3401-3407.

Benito C, Nunez E, Pazos MR, Tolon RM, Romero J (2007) The endocannabinoid system and alzheimer's disease. *Mol Neurobiol* 36:75-81.

Benito C, Nunez E, Tolon RM, Carrier EJ, Rabano A, Hillard CJ, Romero J (2003) Cannabinoid CB2 receptors and fatty acid amide hydrolase are selectively overexpressed in neuritic plaque-associated glia in alzheimer's disease brains. *J Neurosci* 23:11136-11141.

Berkelaar M, Clarke DB, Wang YC, Bray GM, Aguayo AJ (1994) Axotomy results in delayed death and apoptosis of retinal ganglion cells in adult rats. *J Neurosci* 14:4368-4374.

Bisogno T, Berrendero F, Ambrosino G, Cebeira M, Ramos JA, Fernandez-Ruiz JJ, Di Marzo V (1999) Brain regional distribution of endocannabinoids: Implications for their biosynthesis and biological function. *Biochem Biophys Res Commun* 256:377-380.

Bisogno T, Di Marzo V (2008) The role of the endocannabinoid system in alzheimer's disease: Facts and hypotheses. *Curr Pharm Des* 14:2299-3305.

Bisogno T, Howell F, Williams G, Minassi A, Cascio MG, Ligresti A, Matias I, Schiano-Moriello A, Paul P, Williams EJ, Gangadharan U, Hobbs C, Di Marzo V, Doherty P



(2003) Cloning of the first sn1-DAG lipases points to the spatial and temporal regulation of endocannabinoid signaling in the brain. *J Cell Biol* 163:463-468.

Bouaboula M, Poinot-Chazel C, Marchand J, Canat X, Bourrie B, Rinaldi-Carmona M, Calandra B, Le Fur G, Casellas P (1996) Signaling pathway associated with stimulation of CB2 peripheral cannabinoid receptor. involvement of both mitogen-activated protein kinase and induction of krox-24 expression. *Eur J Biochem* 237:704-711.

Bouaboula M, Rinaldi M, Carayon P, Carillon C, Delpech B, Shire D, Le Fur G, Casellas P (1993) Cannabinoid-receptor expression in human leukocytes. *Eur J Biochem* 214:173-180.

Breivogel CS, Griffin G, Di Marzo V, Martin BR (2001) Evidence for a new G protein-coupled cannabinoid receptor in mouse brain. *Mol Pharmacol* 60:155-163.

Buckley NE, Hansson S, Harta G, Mezey E (1998) Expression of the CB1 and CB2 receptor messenger RNAs during embryonic development in the rat. *Neuroscience* 82:1131-1149.

Cabral GA, Griffin-Thomas L (2008) Cannabinoids as therapeutic agents for ablating neuroinflammatory disease. *Endocr Metab Immune Disord Drug Targets* 8:159-172.

Cai J, Boulton M (2002) The pathogenesis of diabetic retinopathy: Old concepts and new questions. *Eye (Lond)* 16:242-260.

Cellerino A, Galli-Resta L, Colombaioni L (2000) The dynamics of neuronal death: A time-lapse study in the retina. *J Neurosci* 20:RC92.

Chauhan BC, LeVatte TL, Jollimore CA, Yu PK, Reitsamer HA, Kelly ME, Yu DY, Tremblay F, Archibald ML (2004) Model of endothelin-1-induced chronic optic neuropathy in rat. *Invest Ophthalmol Vis Sci* 45:144-152.

Chaytor AT, Martin PE, Evans WH, Randall MD, Griffith TM (1999) The endothelial component of cannabinoid-induced relaxation in rabbit mesenteric artery depends on gap junctional communication. *J Physiol* 520 Pt 2:539-550.

Chen B, Caballero S, Seo S, Grant MB, Lewin AS (2009) Delivery of antioxidant enzyme genes to protect against ischemia/reperfusion-induced injury to retinal microvasculature. *Invest Ophthalmol Vis Sci* 50:5587-5595.

Chen J, Matias I, Dinh T, Lu T, Venezia S, Nieves A, Woodward DF, Di Marzo V (2005) Finding of endocannabinoids in human eye tissues: Implications for glaucoma. *Biochem Biophys Res Commun* 330:1062-1067.

- Chen Y, Buck J (2000) Cannabinoids protect cells from oxidative cell death: A receptor-independent mechanism. *J Pharmacol Exp Ther* 293:807-812.
- Chien FY, Wang RF, Mittag TW, Podos SM (2003) Effect of WIN 55212-2, a cannabinoid receptor agonist, on aqueous humor dynamics in monkeys. *Arch Ophthalmol* 121:87-90.
- Ciulla TA, Harris A, Martin BJ (2001) Ocular perfusion and age-related macular degeneration. *Acta Ophthalmol Scand* 79:108-115.
- Cogan DG (1974) Ophthalmic manifestations of systemic vascular disease. *Major Probl Intern Med* 3:1-187.
- Connolly ES, Jr, Winfree CJ, Stern DM, Solomon RA, Pinsky DJ (1996) Procedural and strain-related variables significantly affect outcome in a murine model of focal cerebral ischemia. *Neurosurgery* 38:523-31; discussion 532.
- Coomber B, O'Donoghue MF, Mason R (2008) Inhibition of endocannabinoid metabolism attenuates enhanced hippocampal neuronal activity induced by kainic acid. *Synapse* 62:746-755.
- Cordeiro MF, Guo L, Luong V, Harding G, Wang W, Jones HE, Moss SE, Sillito AM, Fitzke FW (2004) Real-time imaging of single nerve cell apoptosis in retinal neurodegeneration. *Proc Natl Acad Sci U S A* 101:13352-13356.
- Coyle JT, Puttfarcken P (1993) Oxidative stress, glutamate, and neurodegenerative disorders. *Science* 262:689-695.
- Crandall J, Matragoon S, Khalifa YM, Borlongan C, Tsai NT, Caldwell RB, Liou GI (2007) Neuroprotective and intraocular pressure-lowering effects of (-)Delta9-tetrahydrocannabinol in a rat model of glaucoma. *Ophthalmic Res* 39:69-75.
- Croxford JL (2003) Therapeutic potential of cannabinoids in CNS disease. *CNS Drugs* 17:179-202.
- Cunha-Vaz JG, Fonseca JR, de Abreu JR, Lima JJ (1978) Studies on retinal blood flow. II. diabetic retinopathy. *Arch Ophthalmol* 96:809-811.
- Currie S, Rainbow RD, Ewart MA, Kitson S, Pliego EH, Kane KA, McCarron JG (2008) IP(3)R-mediated  $Ca^{2+}$  release is modulated by anandamide in isolated cardiac nuclei. *J Mol Cell Cardiol* 45:804-811.
- Daniel H, Crepel F (2001) Control of  $Ca^{2+}$  influx by cannabinoid and metabotropic glutamate receptors in rat cerebellar cortex requires  $K^{+}$  channels. *J Physiol* 537:793-

800.

Davies SN, Pertwee RG, Riedel G (2002) Functions of cannabinoid receptors in the hippocampus. *Neuropharmacology* 42:993-1007.

Deadwyler SA, Hampson RE, Mu J, Whyte A, Childers S (1995) Cannabinoids modulate voltage sensitive potassium A-current in hippocampal neurons via a cAMP-dependent process. *J Pharmacol Exp Ther* 273:734-743.

Delaey C, Van De Voorde J (2000) Regulatory mechanisms in the retinal and choroidal circulation. *Ophthalmic Res* 32:249-256.

Deutsch DG, Chin SA (1993) Enzymatic synthesis and degradation of anandamide, a cannabinoid receptor agonist. *Biochem Pharmacol* 46:791-796.

Devane WA, Hanus L, Breuer A, Pertwee RG, Stevenson LA, Griffin G, Gibson D, Mandelbaum A, Etinger A, Mechoulam R (1992) Isolation and structure of a brain constituent that binds to the cannabinoid receptor. *Science* 258:1946-1949.

Di Marzo V, Hill MP, Bisogno T, Crossman AR, Brotchie JM (2000) Enhanced levels of endogenous cannabinoids in the globus pallidus are associated with a reduction in movement in an animal model of parkinson's disease. *FASEB J* 14:1432-1438.

Dilsiz N, Sahaboglu A, Yildiz MZ, Reichenbach A (2006) Protective effects of various antioxidants during ischemia-reperfusion in the rat retina. *Graefes Arch Clin Exp Ophthalmol* 244:627-633.

Dodge AB, D'Amore PA (1992) Cell-cell interactions in diabetic angiopathy. *Diabetes Care* 15:1168-1180.

Dogulu FH, Ozogul C, Akpek S, Kurt G, Emmez H, Ercan S, Baykaner MK (2003) Intra-arterial simultaneous administration of anandamide attenuates endothelin-1 induced vasospasm in rabbit basilar arteries. *Acta Neurochir (Wien)* 145:579-582.

Dreyer EB, Zurakowski D, Schumer RA, Podos SM, Lipton SA (1996) Elevated glutamate levels in the vitreous body of humans and monkeys with glaucoma. *Arch Ophthalmol* 114:299-305.

Ehinger B, Falck B (1966) Concomitant adrenergic and parasympathetic fibres in the rat iris. *Acta Physiol Scand* 67:201-207.

Emre M, Orgul S, Haufschild T, Shaw SG, Flammer J (2005) Increased plasma endothelin-1 levels in patients with progressive open angle glaucoma. *Br J Ophthalmol* 89:60-63.

- Facchinetti F, Del Giudice E, Furegato S, Passarotto M, Leon A (2003) Cannabinoids ablate release of TNFalpha in rat microglial cells stimulated with lipopolysaccharide. *Glia* 41:161-168.
- Fan SF, Yazulla S (2005) Reciprocal inhibition of voltage-gated potassium currents (I<sub>K(V)</sub>) by activation of cannabinoid CB1 and dopamine D1 receptors in ON bipolar cells of goldfish retina. *Vis Neurosci* 22:55-63.
- Fan SF, Yazulla S (2004) Inhibitory interaction of cannabinoid CB1 receptor and dopamine D2 receptor agonists on voltage-gated currents of goldfish cones. *Vis Neurosci* 21:69-77.
- Fan SF, Yazulla S (2003) Biphasic modulation of voltage-dependent currents of retinal cones by cannabinoid CB1 receptor agonist WIN 55212-2. *Vis Neurosci* 20:177-188.
- Fang HC (1976) Observations on aging characteristics of cerebral blood vessels, macroscopic and microscopic features. In: *Neurobiology of aging*. (Terry RD, Gershon S, eds), pp 155–166. New York: Raven Press.
- Fechtner RD, Weinreb RN (1994) Mechanisms of optic nerve damage in primary open angle glaucoma. *Surv Ophthalmol* 39:23-42.
- Fegley D, Gaetani S, Duranti A, Tontini A, Mor M, Tarzia G, Piomelli D (2005) Characterization of the fatty acid amide hydrolase inhibitor cyclohexyl carbamic acid 3'-carbamoyl-biphenyl-3-yl ester (URB597): Effects on anandamide and oleoylethanolamide deactivation. *J Pharmacol Exp Ther* 313:352-358.
- Feit-Leichman RA, Kinouchi R, Takeda M, Fan Z, Mohr S, Kern TS, Chen DF (2005) Vascular damage in a mouse model of diabetic retinopathy: Relation to neuronal and glial changes. *Invest Ophthalmol Vis Sci* 46:4281-4287.
- Filho DW, Torres MA, Bordin AL, Crezcynski-Pasa TB, Boveris A (2004) Spermatic cord torsion, reactive oxygen and nitrogen species and ischemia-reperfusion injury. *Mol Aspects Med* 25:199-210.
- Flammer J (1994) The vascular concept of glaucoma. *Surv Ophthalmol* 38 Suppl:S3-6.
- Flammer J, Orgul S, Costa VP, Orzalesi N, Krieglstein GK, Serra LM, Renard JP, Stefansson E (2002) The impact of ocular blood flow in glaucoma. *Prog Retin Eye Res* 21:359-393.
- Forrester J, Peters A (1967) Nerve fibres in optic nerve of rat. *Nature* 214:245-247.
- Fuchsjager-Mayrl G, Wally B, Georgopoulos M, Rainer G, Kircher K, Buehl W,

Amoako-Mensah T, Eichler HG, Vass C, Schmetterer L (2004) Ocular blood flow and systemic blood pressure in patients with primary open-angle glaucoma and ocular hypertension. *Invest Ophthalmol Vis Sci* 45:834-839.

Galve-Roperh I, Rueda D, Gomez del Pulgar T, Velasco G, Guzman M (2002) Mechanism of extracellular signal-regulated kinase activation by the CB(1) cannabinoid receptor. *Mol Pharmacol* 62:1385-1392.

Garcia-Arencibia M, Gonzalez S, de Lago E, Ramos JA, Mechoulam R, Fernandez-Ruiz J (2007) Evaluation of the neuroprotective effect of cannabinoids in a rat model of parkinson's disease: Importance of antioxidant and cannabinoid receptor-independent properties. *Brain Res* 1134:162-170.

Garcia-Ovejero D, Arevalo-Martin A, Petrosino S, Docagne F, Hagen C, Bisogno T, Watanabe M, Guaza C, Di Marzo V, Molina-Holgado E (2009) The endocannabinoid system is modulated in response to spinal cord injury in rats. *Neurobiol Dis* 33:57-71.

Gawienowski AM, Chatterjee D, Anderson PJ, Epstein DL, Grant WM (1982) Effect of delta 9-tetrahydrocannabinol on monoamine oxidase activity in bovine eye tissues, in vitro. *Invest Ophthalmol Vis Sci* 22:482-485.

Gebremedhin D, Lange AR, Campbell WB, Hillard CJ, Harder DR (1999) Cannabinoid CB1 receptor of cat cerebral arterial muscle functions to inhibit L-type Ca<sup>2+</sup> channel current. *Am J Physiol* 276:H2085-93.

Gehlbach PL, Purple RL (1994) A paired comparison of two models of experimental retinal ischemia. *Curr Eye Res* 13:597-602.

Gilbert GL, Kim HJ, Waataja JJ, Thayer SA (2007) Delta9-tetrahydrocannabinol protects hippocampal neurons from excitotoxicity. *Brain Res* 1128:61-69.

Gillow JT, Gibson JM, Dodson PM (1999) Hypertension and diabetic retinopathy--what's the story? *Br J Ophthalmol* 83:1083-1087.

Glaser ST, Deutsch DG, Studholme KM, Zimov S, Yazulla S (2005) Endocannabinoids in the intact retina: 3 H-anandamide uptake, fatty acid amide hydrolase immunoreactivity and hydrolysis of anandamide. *Vis Neurosci* 22:693-705.

Glass M, Felder CC (1997) Concurrent stimulation of cannabinoid CB1 and dopamine D2 receptors augments cAMP accumulation in striatal neurons: Evidence for a gs linkage to the CB1 receptor. *J Neurosci* 17:5327-5333.

Gomez del Pulgar T, Velasco G, Guzman M (2000) The CB1 cannabinoid receptor is coupled to the activation of protein kinase B/Akt. *Biochem J* 347:369-373.

Goparaju SK, Ueda N, Yamaguchi H, Yamamoto S (1998) Anandamide amidohydrolase reacting with 2-arachidonoylglycerol, another cannabinoid receptor ligand. *FEBS Lett* 422:69-73.

Green K (1979) Marijuana in ophthalmology-past, present and future. *Ann Ophthalmol* 11:203-205.

Groh MJ, Michelson G, Langhans MJ, Harazny J (1996) Influence of age on retinal and optic nerve head blood circulation. *Ophthalmology* 103:529-534.

Grunwald JE, Riva CE, Sinclair SH, Brucker AJ, Petrig BL (1986) Laser doppler velocimetry study of retinal circulation in diabetes mellitus. *Arch Ophthalmol* 104:991-996.

Gulyas AI, Cravatt BF, Bracey MH, Dinh TP, Piomelli D, Boscia F, Freund TF (2004) Segregation of two endocannabinoid-hydrolyzing enzymes into pre- and postsynaptic compartments in the rat hippocampus, cerebellum and amygdala. *Eur J Neurosci* 20:441-458.

Haefliger IO, Zschauer A, Anderson DR (1994) Relaxation of retinal pericyte contractile tone through the nitric oxide-cyclic guanosine monophosphate pathway. *Invest Ophthalmol Vis Sci* 35:991-997.

Hammes HP (2005) Pericytes and the pathogenesis of diabetic retinopathy. *Horm Metab Res* 37 Suppl 1:39-43.

Hampson AJ, Grimaldi M, Axelrod J, Wink D (1998) Cannabidiol and (-)Delta9-tetrahydrocannabinol are neuroprotective antioxidants. *Proc Natl Acad Sci U S A* 95:8268-8273.

Hardy P, Beauchamp M, Sennlaub F, Gobeil F, Jr, Tremblay L, Mwaikambo B, Lachapelle P, Chemtob S (2005) New insights into the retinal circulation: Inflammatory lipid mediators in ischemic retinopathy. *Prostaglandins Leukot Essent Fatty Acids* 72:301-325.

Harman D (1981) The aging process. *Proc Natl Acad Sci U S A* 78:7124-7128.

Harris A, Arend O, Danis RP, Evans D, Wolf S, Martin BJ (1996) Hyperoxia improves contrast sensitivity in early diabetic retinopathy. *Br J Ophthalmol* 80:209-213.

Harris A, Kagemann L, Cioffi GA (1998) Assessment of human ocular hemodynamics. *Surv Ophthalmol* 42:509-533.

Hattar S, Liao HW, Takao M, Berson DM, Yau KW (2002) Melanopsin-containing retinal

- ganglion cells: Architecture, projections, and intrinsic photosensitivity. *Science* 295:1065-1070.
- Hayreh SS (1975) Segmental nature of the choroidal vasculature. *Br J Ophthalmol* 59:631-648.
- Hayreh SS, Bill A, Sperber GO (1994) Effects of high intraocular pressure on the glucose metabolism in the retina and optic nerve in old atherosclerotic monkeys. *Graefes Arch Clin Exp Ophthalmol* 32:745-752.
- Hayreh SS, Podhajsky PA, Zimmerman B (1997) Nonarteritic anterior ischemic optic neuropathy: Time of onset of visual loss. *Am J Ophthalmol* 124:641-647.
- Herkenham M, Lynn AB, Little MD, Johnson MR, Melvin LS, de Costa BR, Rice KC (1990) Cannabinoid receptor localization in brain. *Proc Natl Acad Sci U S A* 87:1932-1936.
- Hiley CR, Kaup SS (2007) GPR55 and the vascular receptors for cannabinoids. *Br J Pharmacol* 152:559-561.
- Hirose F, Kiryu J, Miyamoto K, Nishijima K, Miyahara S, Katsuta H, Tamura H, Honda Y (2004) In vivo evaluation of retinal injury after transient ischemia in hypertensive rats. *Hypertension* 43:1098-1102.
- Ho WS, Hillard CJ (2005) Modulators of endocannabinoid enzymic hydrolysis and membrane transport. *Handb Exp Pharmacol* (168):187-207.
- Ho WS, Randall MD (2007) Endothelium-dependent metabolism by endocannabinoid hydrolases and cyclooxygenases limits vasorelaxation to anandamide and 2-arachidonoylglycerol. *Br J Pharmacol* 150:641-651.
- Howlett AC, Qualy JM, Khachatrian LL (1986) Involvement of gi in the inhibition of adenylate cyclase by cannabimimetic drugs. *Mol Pharmacol* 29:307-313.
- Hudson BD, Hebert TE, Kelly ME (2010) Ligand- and heterodimer-directed signaling of the CB(1) cannabinoid receptor. *Mol Pharmacol* 77:1-9.
- Hughes S, Gardiner T, Hu P, Baxter L, Rosinova E, Chan-Ling T (2006) Altered pericyte-endothelial relations in the rat retina during aging: Implications for vessel stability. *Neurobiol Aging* 27:1838-1847.
- Hwang J, Adamson C, Butler D, Janero DR, Makriyannis A, Bahr BA (2010) Enhancement of endocannabinoid signaling by fatty acid amide hydrolase inhibition: A neuroprotective therapeutic modality. *Life Sci* 86:615-623.

- Jackson SJ, Diemel LT, Pryce G, Baker D (2005) Cannabinoids and neuroprotection in CNS inflammatory disease. *J Neurol Sci* 233:21-25.
- Janero DR, Makriyannis A (2009) Cannabinoid receptor antagonists: Pharmacological opportunities, clinical experience, and translational prognosis. *Expert Opin Emerg Drugs* 14:43-65.
- Jarai Z, Wagner JA, Varga K, Lake KD, Compton DR, Martin BR, Zimmer AM, Bonner TI, Buckley NE, Mezey E, Razdan RK, Zimmer A, Kunos G (1999) Cannabinoid-induced mesenteric vasodilation through an endothelial site distinct from CB1 or CB2 receptors. *Proc Natl Acad Sci U S A* 96:14136-14141.
- Joseph J, Niggemann B, Zaenker KS, Entschladen F (2004) Anandamide is an endogenous inhibitor for the migration of tumor cells and T lymphocytes. *Cancer Immunol Immunother* 53:723-728.
- Justinova Z, Mangieri RA, Bortolato M, Chefer SI, Mukhin AG, Clapper JR, King AR, Redhi GH, Yasar S, Piomelli D, Goldberg SR (2008) Fatty acid amide hydrolase inhibition heightens anandamide signaling without producing reinforcing effects in primates. *Biol Psychiatry* 64:930-937.
- Kalesnykas G, Tuulos T, Uusitalo H, Jolkkonen J (2008) Neurodegeneration and cellular stress in the retina and optic nerve in rat cerebral ischemia and hypoperfusion models. *Neuroscience* 155:937-947.
- Kaminski NE, Abood ME, Kessler FK, Martin BR, Schatz AR (1992) Identification of a functionally relevant cannabinoid receptor on mouse spleen cells that is involved in cannabinoid-mediated immune modulation. *Mol Pharmacol* 42:736-742.
- Karanian DA, Brown QB, Makriyannis A, Kosten TA, Bahr BA (2005) Dual modulation of endocannabinoid transport and fatty acid amide hydrolase protects against excitotoxicity. *J Neurosci* 25:7813-7820.
- Karanian DA, Karim SL, Wood JT, Williams JS, Lin S, Makriyannis A, Bahr BA (2007) Endocannabinoid enhancement protects against kainic acid-induced seizures and associated brain damage. *J Pharmacol Exp Ther* 322:1059-1066.
- Kathuria S, Gaetani S, Fegley D, Valino F, Duranti A, Tontini A, Mor M, Tarzia G, La Rana G, Calignano A, Giustino A, Tattoli M, Palmery M, Cuomo V, Piomelli D (2003) Modulation of anxiety through blockade of anandamide hydrolysis. *Nat Med* 9:76-81.
- Kern TS, Tang J, Mizutani M, Kowluru RA, Nagaraj RH, Romeo G, Podesta F, Lorenzi M (2000) Response of capillary cell death to aminoguanidine predicts the development of retinopathy: Comparison of diabetes and galactosemia. *Invest Ophthalmol Vis Sci* 41:3972-3978.



- Kerr NM, Chew SS, Danesh-Meyer HV (2009) Non-arteritic anterior ischaemic optic neuropathy: a review and update. *J Clin Neurosci* 16(8):994-1000.
- Kiernan JA (1985) Axonal and vascular changes following injury to the rat's optic nerve. *J Anat* 141:139-154.
- Kim DJ, Thayer SA (2000) Activation of CB1 cannabinoid receptors inhibits neurotransmitter release from identified synaptic sites in rat hippocampal cultures. *Brain Res* 852:398-405.
- Kim SH, Kim JY, Kim DM, Ko HS, Kim SY, Yoo T, Hwang SS, Park SS (2006) Investigations on the association between normal tension glaucoma and single nucleotide polymorphisms of the endothelin-1 and endothelin receptor genes. *Mol Vis* 12:1016-1021.
- Kocur I, Resnikoff S (2002) Visual impairment and blindness in europe and their prevention. *Br J Ophthalmol* 86:716-722.
- Kofuji P, Newman EA (2004) Potassium buffering in the central nervous system. *Neuroscience* 129:1045-1056.
- Kohl A, Dehghani F, Korf HW, Hailer NP (2003) The bisphosphonate clodronate depletes microglial cells in excitotoxically injured organotypic hippocampal slice cultures. *Exp Neurol* 181:1-11.
- Kohner EM, Hamilton AM, Saunders SJ, Sutcliffe BA, Bulpitt CJ (1975) The retinal blood flow in diabetes. *Diabetologia* 11:27-33.
- Kolb H, Nelson R, Ahnelt P, Cuenca N (2001) Cellular Organization of the vertebrate retina. *Prog Brain Res* 131:3-26.
- Kozak KR, Rowlinson SW, Marnett LJ (2000) Oxygenation of the endocannabinoid, 2-arachidonylglycerol, to glyceryl prostaglandins by cyclooxygenase-2. *J Biol Chem* 275:33744-33749.
- Kozłowska H, Baranowska M, Schlicker E, Kozłowski M, Laudanski J, Malinowska B (2007) Identification of the vasodilatory endothelial cannabinoid receptor in the human pulmonary artery. *J Hypertens* 25:2240-2248.
- Kuwabara T, Carroll JM, Cogan DG (1961) Retinal vascular patterns. III. age, hypertension, absolute glaucoma, injury. *Arch Ophthalmol* 65:708-716.
- Lai YL, Jacoby RO, Jonas AM (1978) Age-related and light-associated retinal changes in

fischer rats. *Invest Ophthalmol Vis Sci* 17:634-638.

Lalonde MR, Jollimore CA, Stevens K, Barnes S, Kelly ME (2006) Cannabinoid receptor-mediated inhibition of calcium signaling in rat retinal ganglion cells. *Mol Vis* 12:1160-1166.

Lam AG, Monn JA, Schoepp DD, Lodge D, McCulloch J (1999) Group II selective metabotropic glutamate receptor agonists and local cerebral glucose use in the rat. *J Cereb Blood Flow Metab* 19:1083-1091.

Lambert DM, Vandevoorde S, Jonsson KO, Fowler CJ (2002) The palmitoylethanolamide family: A new class of anti-inflammatory agents? *Curr Med Chem* 9:663-674.

Langmann T (2007) Microglia activation in retinal degeneration. *J Leukoc Biol* 81:1345-1351.

Laties AM (1967) Central retinal artery innervation. absence of adrenergic innervation to the intraocular branches. *Arch Ophthalmol* 77:405-409.

Lauckner JE, Hille B, Mackie K (2005) The cannabinoid agonist WIN55,212-2 increases intracellular calcium via CB1 receptor coupling to Gq/11 G proteins. *Proc Natl Acad Sci U S A* 102:19144-19149.

Lelong DC, Bieche I, Perez E, Bigot K, Leemput J, Laurendeau I, Vidaud M, Jais JP, Menasche M, Abitbol M (2007) Novel mouse model of monocular amaurosis fugax. *Stroke* 38:3237-3244.

Leuenberger PM (1973) Ultrastructure of the ageing retinal vascular system, with special reference to quantitative and qualitative changes of capillary basement membranes. *Gerontologia* 19:1-15.

Liu J, Wang L, Harvey-White J, Huang BX, Kim HY, Luquet S, Palmiter RD, Krystal G, Rai R, Mahadevan A, Razdan RK, Kunos G (2008) Multiple pathways involved in the biosynthesis of anandamide. *Neuropharmacology* 54:1-7.

Liu Q, Bhat M, Bowen WD, Cheng J (2009) Signaling pathways from cannabinoid receptor-1 activation to inhibition of N-methyl-D-aspartic acid mediated calcium influx and neurotoxicity in dorsal root ganglion neurons. *J Pharmacol Exp Ther* 331:1062-1070.

Lograno MD, Romano MR (2004) Cannabinoid agonists induce contractile responses through Gi/o-dependent activation of phospholipase C in the bovine ciliary muscle. *Eur J Pharmacol* 494:55-62.

Lovasik JV, Kergoat MJ, Justino L, Kergoat H (2003) Neuroretinal basis of visual

- impairment in the very elderly. *Graefes Arch Clin Exp Ophthalmol* 241:48-55.
- Lutty GA, McLeod DS (1992) A new technique for visualization of the human retinal vasculature. *Arch Ophthalmol* 110:267-276.
- Maccarrone M, Attina M, Bari M, Cartoni A, Ledent C, Finazzi-Agro A (2001) Anandamide degradation and N-acyl ethanolamines level in wild-type and CB1 cannabinoid receptor knockout mice of different ages. *J Neurochem* 78:339-348.
- Maccarrone M, Finazzi-Agro A (2003) The endocannabinoid system, anandamide and the regulation of mammalian cell apoptosis. *Cell Death Differ* 10:946-955.
- Maccarrone M, Rossi S, Bari M, De Chiara V, Fezza F, Musella A, Gasperi V, Prosperetti C, Bernardi G, Finazzi-Agro A, Cravatt BF, Centonze D (2008) Anandamide inhibits metabolism and physiological actions of 2-arachidonoylglycerol in the striatum. *Nat Neurosci* 11:152-159.
- Maccarrone M, van der Stelt M, Rossi A, Veldink GA, Vliegthart JF, Agro AF (1998) Anandamide hydrolysis by human cells in culture and brain. *J Biol Chem* 273:32332-32339.
- Mackie K (2008) Signaling via CNS cannabinoid receptors. *Mol Cell Endocrinol* 286:S60-5.
- Mackie K, Hille B (1992) Cannabinoids inhibit N-type calcium channels in neuroblastoma-glioma cells. *Proc Natl Acad Sci U S A* 89:3825-3829.
- Marinelli S, Di Marzo V, Berretta N, Matias I, Maccarrone M, Bernardi G, Mercuri NB (2003) Presynaptic facilitation of glutamatergic synapses to dopaminergic neurons of the rat substantia nigra by endogenous stimulation of vanilloid receptors. *J Neurosci* 23:3136-3144.
- Marsicano G, Goodenough S, Monory K, Hermann H, Eder M, Cannich A, Azad SC, Cascio MG, Gutierrez SO, van der Stelt M, Lopez-Rodriguez ML, Casanova E, Schutz G, Zieglgansberger W, Di Marzo V, Behl C, Lutz B (2003) CB1 cannabinoid receptors and on-demand defense against excitotoxicity. *Science* 302:84-88.
- Martinez-Orgado J, Fernandez-Lopez D, Lizasoain I, Romero J (2007) The seek of neuroprotection: Introducing cannabinoids. *Recent Pat CNS Drug Discov* 2:131-139.
- Matias I, Wang JW, Moriello AS, Nieves A, Woodward DF, Di Marzo V (2006) Changes in endocannabinoid and palmitoylethanolamide levels in eye tissues of patients with diabetic retinopathy and age-related macular degeneration. *Prostaglandins Leukot Essent Fatty Acids* 75:413-418.

- Matsuda LA, Lolait SJ, Brownstein MJ, Young AC, Bonner TI (1990) Structure of a cannabinoid receptor and functional expression of the cloned cDNA. *Nature* 346:561-564.
- Matsuda S, Kanemitsu N, Nakamura A, Mimura Y, Ueda N, Kurahashi Y, Yamamoto S (1997) Metabolism of anandamide, an endogenous cannabinoid receptor ligand, in porcine ocular tissues. *Exp Eye Res* 64:707-711.
- McAllister SD, Glass M (2002) CB(1) and CB(2) receptor-mediated signalling: A focus on endocannabinoids. *Prostaglandins Leukot Essent Fatty Acids* 66:161-171.
- McIntosh BT, Hudson B, Yegorova S, Jollimore CA, Kelly ME (2007) Agonist-dependent cannabinoid receptor signalling in human trabecular meshwork cells. *Br J Pharmacol* 152:1111-1120.
- McKinney MK, Cravatt BF (2005) Structure and function of fatty acid amide hydrolase. *Annu Rev Biochem* 74:411-432.
- Mechoulam R, Gaoni Y (1965) A total synthesis of dl-delta-1-tetrahydrocannabinol, the active constituent of hashish. *J Am Chem Soc* 87:3273-3275.
- Mechoulam R, Spatz M, Shohami E (2002) Endocannabinoids and neuroprotection. *Sci STKE* 2002:re5.
- Metaea MR, Newman EA (2007) Signalling within the neurovascular unit in the mammalian retina. *Exp Physiol* 92:635-640.
- Micale V, Mazzola C, Drago F (2007) Endocannabinoids and neurodegenerative diseases. *Pharmacol Res* 56:382-392.
- Mizutani M, Kern TS, Lorenzi M (1996) Accelerated death of retinal microvascular cells in human and experimental diabetic retinopathy. *J Clin Invest* 97:2883-2890.
- Molina-Holgado F, Pinteaux E, Heenan L, Moore JD, Rothwell NJ, Gibson RM (2005) Neuroprotective effects of the synthetic cannabinoid HU-210 in primary cortical neurons are mediated by phosphatidylinositol 3-kinase/AKT signaling. *Mol Cell Neurosci* 28:189-194.
- Moss DW, Bates TE (2001) Activation of murine microglial cell lines by lipopolysaccharide and interferon-gamma causes NO-mediated decreases in mitochondrial and cellular function. *Eur J Neurosci* 13:529-538.
- Munro S, Thomas KL, Abu-Shaar M (1993) Molecular characterization of a peripheral

receptor for cannabinoids. *Nature* 365:61-65.

Mutapcic L, Wren SM, Leske DA, Fautsch MP, Holmes JM (2005) The effect of L-thyroxine supplementation on retinal vascular development in neonatal rats. *Curr Eye Res* 30:1035-1040.

Nagata M, Katz ML, Robison WG, Jr (1986) Age-related thickening of retinal capillary basement membranes. *Invest Ophthalmol Vis Sci* 27:437-440.

Nedergaard M (1994) Direct signaling from astrocytes to neurons in cultures of mammalian brain cells. *Science* 263:1768-1771.

Newman EA (2005) Calcium increases in retinal glial cells evoked by light-induced neuronal activity. *J Neurosci* 25:5502-5510.

Njie YF, He F, Qiao Z, Song ZH (2008) Aqueous humor outflow effects of 2-arachidonylglycerol. *Exp Eye Res* 87:106-114.

Nucci C, Gasperi V, Tartaglione R, Cerulli A, Terrinoni A, Bari M, De Simone C, Agro AF, Morrone LA, Corasaniti MT, Bagetta G, Maccarrone M (2007) Involvement of the endocannabinoid system in retinal damage after high intraocular pressure-induced ischemia in rats. *Invest Ophthalmol Vis Sci* 48:2997-3004.

Nucci C, Tartaglione R, Rombola L, Morrone LA, Fazzi E, Bagetta G (2005) Neurochemical evidence to implicate elevated glutamate in the mechanisms of high intraocular pressure (IOP)-induced retinal ganglion cell death in rat. *Neurotoxicology* 26:935-941.

Nunez E, Benito C, Pazos MR, Barbachano A, Fajardo O, Gonzalez S, Tolon RM, Romero J (2004) Cannabinoid CB2 receptors are expressed by perivascular microglial cells in the human brain: An immunohistochemical study. *Synapse* 53:208-213.

Offertaler L, Mo FM, Batkai S, Liu J, Begg M, Razdan RK, Martin BR, Bukoski RD, Kunos G (2003) Selective ligands and cellular effectors of a G protein-coupled endothelial cannabinoid receptor. *Mol Pharmacol* 63:699-705.

Oka S, Ikeda S, Kishimoto S, Gokoh M, Yanagimoto S, Waku K, Sugiura T (2004) 2-arachidonoylglycerol, an endogenous cannabinoid receptor ligand, induces the migration of EoL-1 human eosinophilic leukemia cells and human peripheral blood eosinophils. *J Leukoc Biol* 76:1002-1009.

Oltmanns MH, Samudre SS, Castillo IG, Hosseini A, Lichtman AH, Allen RC, Lattanzio FA, Williams PB (2008) Topical WIN55212-2 alleviates intraocular hypertension in rats through a CB1 receptor mediated mechanism of action. *J Ocul Pharmacol Ther* 24:104-

115.

Otori T, Katsumata T, Muramatsu H, Kashiwagi F, Katayama Y, Terashi A (2003) Long-term measurement of cerebral blood flow and metabolism in a rat chronic hypoperfusion model. *Clin Exp Pharmacol Physiol* 30:266-272.

Pacher P, Hasko G (2008) Endocannabinoids and cannabinoid receptors in ischaemia-reperfusion injury and preconditioning. *Br J Pharmacol* 153:252-262.

Paradisi A, Oddi S, Maccarrone M (2006) The endocannabinoid system in ageing: A new target for drug development. *Curr Drug Targets* 7:1539-1552.

Parmentier-Batteur S, Jin K, Xie L, Mao XO, Greenberg DA (2002) DNA microarray analysis of cannabinoid signaling in mouse brain in vivo. *Mol Pharmacol* 62:828-835.

Parver LM (1991) Temperature modulating action of choroidal blood flow. *Eye (Lond)* 5 ( Pt 2):181-185.

Pate DW, Jarvinen K, Urtti A, Jarho P, Jarvinen T (1995) Ophthalmic arachidonylethanolamide decreases intraocular pressure in normotensive rabbits. *Curr Eye Res* 14:791-797.

Patterson, C. (2008). Screening for Visual Impairment in the Elderly. *Canadian Task Force On Preventative Health Care*. Retrieved from [http://www.ctfphc.org/Full\\_Text/Ch78full.htm](http://www.ctfphc.org/Full_Text/Ch78full.htm)

Pazos MR, Nunez E, Benito C, Tolon RM, Romero J (2005) Functional neuroanatomy of the endocannabinoid system. *Pharmacol Biochem Behav* 81:239-247.

Pertwee RG (2008) Ligands that target cannabinoid receptors in the brain: From THC to anandamide and beyond. *Addict Biol* 13:147-159.

Pertwee RG (1997) Pharmacology of cannabinoid CB1 and CB2 receptors. *Pharmacol Ther* 74:129-180.

Pertwee RG, Ross RA (2002) Cannabinoid receptors and their ligands. *Prostaglandins Leukot Essent Fatty Acids* 66:101-121.

Piomelli D (2003) The molecular logic of endocannabinoid signalling. *Nat Rev Neurosci* 4:873-884.

Plane F, Holland M, Waldron GJ, Garland CJ, Boyle JP (1997) Evidence that anandamide and EDHF act via different mechanisms in rat isolated mesenteric arteries. *Br J Pharmacol* 121:1509-1511.

- Plange N, Arend KO, Kaup M, Doehmen B, Adams H, Hendricks S, Cordes A, Huth J, Sponsel WE, Remky A (2007) Dronabinol and retinal hemodynamics in humans. *Am J Ophthalmol* 143:173-174.
- Pohl U, Kaas J (1994) Interactions of hormones with the vascular endothelium. effects on the control of vascular tone. *Arzneimittelforschung* 44:459-461.
- Porcella A, Casellas P, Gessa GL, Pani L (1998) Cannabinoid receptor CB1 mRNA is highly expressed in the rat ciliary body: Implications for the antiglaucoma properties of marijuana. *Brain Res Mol Brain Res* 58:240-245.
- Porcella A, Maxia C, Gessa GL, Pani L (2001) The synthetic cannabinoid WIN55212-2 decreases the intraocular pressure in human glaucoma resistant to conventional therapies. *Eur J Neurosci* 13:409-412.
- Pournaras CJ (1995) Retinal oxygen distribution. its role in the physiopathology of vasoproliferative microangiopathies. *Retina* 15:332-347.
- Quigley H, Anderson DR (1977) Cupping of the optic disc in ischemic optic neuropathy. *Trans Sect Ophthalmol Am Acad Ophthalmol Otolaryngol* 83:755-762.
- Rabacchi SA, Bonfanti L, Liu XH, Maffei L (1994) Apoptotic cell death induced by optic nerve lesion in the neonatal rat. *J Neurosci* 14:5292-5301.
- Rahmani B, Tielsch JM, Katz J, Gottsch J, Quigley H, Javitt J, Sommer A (1996) The cause-specific prevalence of visual impairment in an urban population. the baltimore eye survey. *Ophthalmology* 103:1721-1726.
- Ramirez BG, Blazquez C, Gomez del Pulgar T, Guzman M, de Ceballos ML (2005) Prevention of alzheimer's disease pathology by cannabinoids: Neuroprotection mediated by blockade of microglial activation. *J Neurosci* 25:1904-1913.
- Ramrattan RS, van der Schaft TL, Mooy CM, de Bruijn WC, Mulder PG, de Jong PT (1994) Morphometric analysis of bruch's membrane, the choriocapillaris, and the choroid in aging. *Invest Ophthalmol Vis Sci* 35:2857-2864.
- Randall MD, Alexander SP, Bennett T, Boyd EA, Fry JR, Gardiner SM, Kemp PA, McCulloch AI, Kendall DA (1996) An endogenous cannabinoid as an endothelium-derived vasorelaxant. *Biochem Biophys Res Commun* 229:114-120.
- Riva CE, Harino S, Shonat RD, Petrig BL (1991) Flicker evoked increase in optic nerve head blood flow in anesthetized cats. *Neurosci Lett* 128:291-296.
- Robinson F, Riva CE, Grunwald JE, Petrig BL, Sinclair SH (1986) Retinal blood flow

autoregulation in response to an acute increase in blood pressure. *Invest Ophthalmol Vis Sci* 27:722-726.

Romano MR, Lograno MD (2006) Cannabinoid agonists induce relaxation in the bovine ophthalmic artery: Evidences for CB1 receptors, nitric oxide and potassium channels. *Br J Pharmacol* 147:917-925.

Ronco AM, Llanos M, Tamayo D, Hirsch S (2007) Anandamide inhibits endothelin-1 production by human cultured endothelial cells: A new vascular action of this endocannabinoid. *Pharmacology* 79:12-16.

Rosenmann E, Yanko L, Cohen AM (1975) Comparative study of the pathology of sucrose-induced diabetes in the rat and adult-onset diabetes in man. *Isr J Med Sci* 11:753-761.

Rungger-Brandle E, Messerli JM, Niemeyer G, Eppenberger HM (1993) Confocal microscopy and computer-assisted image reconstruction of astrocytes in the mammalian retina. *Eur J Neurosci* 5:1093-1106.

Ryan D, Drysdale AJ, Lafourcade C, Pertwee RG, Platt B (2009) Cannabidiol targets mitochondria to regulate intracellular Ca<sup>2+</sup> levels. *J Neurosci* 29:2053-2063.

Ryan SJ, Hinton DR, Schachat AP (2005) *Retina*. USA: Mosby.

Salter JM, Cassone VM, Wilkerson MK, Delp MD (1998) Ocular and regional cerebral blood flow in aging fischer-344 rats. *J Appl Physiol* 85:1024-1029.

Sawada A, Neufeld AH (1999) Confirmation of the rat model of chronic, moderately elevated intraocular pressure. *Exp Eye Res* 69:525-531.

Sawada M, Kondo N, Suzumura A, Marunouchi T (1989) Production of tumor necrosis factor-alpha by microglia and astrocytes in culture. *Brain Res* 491:394-397.

Schatz AR, Lee M, Condie RB, Pulaski JT, Kaminski NE (1997) Cannabinoid receptors CB1 and CB2: A characterization of expression and adenylyl cyclase modulation within the immune system. *Toxicol Appl Pharmacol* 142:278-287.

Schipke CG, Kettenmann H (2004) Astrocyte responses to neuronal activity. *Glia* 47:226-232.

Schlicker E, Kathmann M (2001) Modulation of transmitter release via presynaptic cannabinoid receptors. *Trends Pharmacol Sci* 22:565-572.

Schwartz M, Yoles E (1999) Optic nerve degeneration and potential neuroprotection:



Implications for glaucoma. *Eur J Ophthalmol* 9 Suppl 1:S9-11.

Seierstad M, Breitenbucher JG (2008) Discovery and development of fatty acid amide hydrolase (FAAH) inhibitors. *J Med Chem* 51:7327-7343.

Shakib M, Cunha-Vaz JG (1966) Studies on the permeability of the blood-retinal barrier. IV. junctional complexes of the retinal vessels and their role in the permeability of the blood-retinal barrier. *Exp Eye Res* 5:229-234.

Shen M, Thayer SA (1998) Cannabinoid receptor agonists protect cultured rat hippocampal neurons from excitotoxicity. *Mol Pharmacol* 54:459-462.

Shepro D, Morel NM (1993) Pericyte physiology. *FASEB J* 7:1031-1038.

Shouman B, Fontaine RH, Baud O, Schwendimann L, Keller M, Spedding M, Lelievre V, Gressens P (2006) Endocannabinoids potently protect the newborn brain against AMPA-kainate receptor-mediated excitotoxic damage. *Br J Pharmacol* 148:442-451.

Simard AR, Soulet D, Gowing G, Julien JP, Rivest S (2006) Bone marrow-derived microglia play a critical role in restricting senile plaque formation in alzheimer's disease. *Neuron* 49:489-502.

Simionescu M, Simionescu N, Palade GE (1982) Differentiated microdomains on the luminal surface of capillary endothelium: Distribution of lectin receptors. *J Cell Biol* 94:406-413.

Skaper SD, Buriani A, Dal Toso R, Petrelli L, Romanello S, Facci L, Leon A (1996) The ALIAmide palmitoylethanolamide and cannabinoids, but not anandamide, are protective in a delayed postglutamate paradigm of excitotoxic death in cerebellar granule neurons. *Proc Natl Acad Sci U S A* 93:3984-3989.

Slipetz DM, O'Neill GP, Favreau L, Dufresne C, Gallant M, Gareau Y, Guay D, Labelle M, Metters KM (1995) Activation of the human peripheral cannabinoid receptor results in inhibition of adenylyl cyclase. *Mol Pharmacol* 48:352-361.

Song ZH, Slowey CA (2000) Involvement of cannabinoid receptors in the intraocular pressure-lowering effects of WIN55212-2. *J Pharmacol Exp Ther* 292:136-139.

Stamer WD, Golightly SF, Hosohata Y, Ryan EP, Porter AC, Varga E, Noecker RJ, Felder CC, Yamamura HI (2001) Cannabinoid CB(1) receptor expression, activation and detection of endogenous ligand in trabecular meshwork and ciliary process tissues. *Eur J Pharmacol* 431:277-286.

Steiner SH, Frayser R, Ross JC (1965) Alterations in pulmonary diffusing capacity and

pulmonary capillary blood volume with negative pressure breathing. *J Clin Invest* 44:1623-1630.

Stella N (2010) Cannabinoid and cannabinoid-like receptors in microglia, astrocytes, and astrocytomas. *Glia* 58:1017-1030.

Straiker A, Mackie K (2007) Metabotropic suppression of excitation in murine autaptic hippocampal neurons. *J Physiol* 578:773-785.

Straiker A, Stella N, Piomelli D, Mackie K, Karten HJ, Maguire G (1999a) Cannabinoid CB1 receptors and ligands in vertebrate retina: Localization and function of an endogenous signaling system. *Proc Natl Acad Sci U S A* 96:14565-14570.

Straiker A, Sullivan JM (2003) Cannabinoid receptor activation differentially modulates ion channels in photoreceptors of the tiger salamander. *J Neurophysiol* 89:2647-2654.

Straiker AJ, Maguire G, Mackie K, Lindsey J (1999b) Localization of cannabinoid CB1 receptors in the human anterior eye and retina. *Invest Ophthalmol Vis Sci* 40:2442-2448.

Streit WJ (2002) Microglia as neuroprotective, immunocompetent cells of the CNS. *Glia* 40:133-139.

Streit WJ, Sammons NW, Kuhns AJ, Sparks DL (2004) Dystrophic microglia in the aging human brain. *Glia* 45:208-212.

Stumpff F, Boxberger M, Krauss A, Rosenthal R, Meissner S, Choritz L, Wiederholt M, Thieme H (2005) Stimulation of cannabinoid (CB1) and prostanoid (EP2) receptors opens BKCa channels and relaxes ocular trabecular meshwork. *Exp Eye Res* 80:697-708.

Sucher NJ, Lei SZ, Lipton SA (1991) Calcium channel antagonists attenuate NMDA receptor-mediated neurotoxicity of retinal ganglion cells in culture. *Brain Res* 551:297-302.

Sucher NJ, Lipton SA, Dreyer EB (1997) Molecular basis of glutamate toxicity in retinal ganglion cells. *Vision Res* 37:3483-3493.

Tezel G, Siegmund KD, Trinkaus K, Wax MB, Kass MA, Kolker AE (2001) Clinical factors associated with progression of glaucomatous optic disc damage in treated patients. *Arch Ophthalmol* 119:813-818.

Thanos S (1991) Specific transcellular carbocyanine-labelling of rat retinal microglia during injury-induced neuronal degeneration. *Neurosci Lett* 127:108-112.

Thanos S, Pavlidis C, Mey J, Thiel HJ (1992) Specific transcellular staining of microglia

in the adult rat after traumatic degeneration of carbocyanine-filled retinal ganglion cells. *Exp Eye Res* 55:101-117.

Tirsi A, Bruehl H, Sweat V, Tsui W, Reddy S, Javier E, Lee C, Convit A (2009) Retinal vessel abnormalities are associated with elevated fasting insulin levels and cerebral atrophy in nondiabetic individuals. *Ophthalmology* 116:1175-1181.

Tjon-Fo-Sang MJ, de Vries J, Lemij HG (1996) Measurement by nerve fiber analyzer of retinal nerve fiber layer thickness in normal subjects and patients with ocular hypertension. *Am J Ophthalmol* 122:220-227.

Tsuchiya D, Hong S, Matsumori Y, Kayama T, Swanson RA, Dillman WH, Liu J, Panter SS, Weinstein PR (2003) Overexpression of rat heat shock protein 70 reduces neuronal injury after transient focal ischemia, transient global ischemia, or kainic acid-induced seizures. *Neurosurgery* 53:1179-87; discussion 1187-8.

Tureyen K, Vemuganti R, Sailor KA, Dempsey RJ (2005) Ideal suture diameter is critical for consistent middle cerebral artery occlusion in mice. *Neurosurgery* 56:196-200; discussion 196-200.

Twitchell W, Brown S, Mackie K (1997) Cannabinoids inhibit N- and P/Q-type calcium channels in cultured rat hippocampal neurons. *J Neurophysiol* 78:43-50.

van der Stelt M, Veldhuis WB, Maccarrone M, Bar PR, Nicolay K, Veldink GA, Di Marzo V, Vliegthart JF (2002) Acute neuronal injury, excitotoxicity, and the endocannabinoid system. *Mol Neurobiol* 26:317-346.

Van Sickle MD, Duncan M, Kingsley PJ, Mouihate A, Urbani P, Mackie K, Stella N, Makriyannis A, Piomelli D, Davison JS, Marnett LJ, Di Marzo V, Pittman QJ, Patel KD, Sharkey KA (2005) Identification and functional characterization of brainstem cannabinoid CB2 receptors. *Science* 310:329-332.

Veldhuis WB, van der Stelt M, Wadman MW, van Zadelhoff G, Maccarrone M, Fezza F, Veldink GA, Vliegthart JF, Bar PR, Nicolay K, Di Marzo V (2003) Neuroprotection by the endogenous cannabinoid anandamide and arvanil against in vivo excitotoxicity in the rat: Role of vanilloid receptors and lipoxygenases. *J Neurosci* 23:4127-4133.

Vemuri VK, Janero DR, Makriyannis A (2008) Pharmacotherapeutic targeting of the endocannabinoid signaling system: Drugs for obesity and the metabolic syndrome. *Physiol Behav* 93:671-686.

Venkataraman ST, Hudson C, Fisher JA, Flanagan JG (2006) Novel methodology to comprehensively assess retinal arteriolar vascular reactivity to hypercapnia. *Microvasc Res* 72:101-107.

- Vidal-Sanz M, Villegas-Perez MP, Bray GM, Aguayo AJ (1988) Persistent retrograde labeling of adult rat retinal ganglion cells with the carbocyanine dye diI. *Exp Neurol* 102:92-101.
- Villegas-Perez MP, Vidal-Sanz M, Rasminsky M, Bray GM, Aguayo AJ (1993) Rapid and protracted phases of retinal ganglion cell loss follow axotomy in the optic nerve of adult rats. *J Neurobiol* 24:23-36.
- Walter L, Franklin A, Witting A, Wade C, Xie Y, Kunos G, Mackie K, Stella N (2003) Nonpsychotropic cannabinoid receptors regulate microglial cell migration. *J Neurosci* 23:1398-1405.
- Walter L, Stella N (2004) Cannabinoids and neuroinflammation. *Br J Pharmacol* 141:775-785.
- Wang L, Fortune B, Cull G, Dong J, Cioffi GA (2006) Endothelin B receptor in human glaucoma and experimentally induced optic nerve damage. *Arch Ophthalmol* 124:717-724.
- Weinreb RN, Khaw PT (2004) Primary open-angle glaucoma. *Lancet* 363:1711-1720.
- Weinreb RN, Shakiba S, Zangwill L (1995) Scanning laser polarimetry to measure the nerve fiber layer of normal and glaucomatous eyes. *Am J Ophthalmol* 119:627-636.
- Weisse I (1995) Changes in the aging rat retina. *Ophthalmic Res* 27 Suppl 1:154-163.
- Werner EB, Drance SM (1977) Progression of glaucomatous field defects despite successful filtration. *Can J Ophthalmol* 12:275-280.
- Woolf D (1956) A comparative cytological study of the ciliary muscle. *Anat Rec* 124:145-163.
- Xu H, Chen M, Forrester JV (2009) Para-inflammation in the aging retina. *Prog Retin Eye Res* 28:348-368.
- Yamaji K, Sarker KP, Kawahara K, Iino S, Yamakuchi M, Abeyama K, Hashiguchi T, Maruyama I (2003) Anandamide induces apoptosis in human endothelial cells: Its regulation system and clinical implications. *Thromb Haemost* 89:875-884.
- Yamamoto H, Schmidt-Kastner R, Hamasaki DI, Yamamoto H, Parel JM (2006) Complex neurodegeneration in retina following moderate ischemia induced by bilateral common carotid artery occlusion in wistar rats. *Exp Eye Res* 82:767-779.

- Yan DB, Coloma FM, Metheetrairut A, Trope GE, Heathcote JG, Ethier CR (1994) Deformation of the lamina cribrosa by elevated intraocular pressure. *Br J Ophthalmol* 78:643-648.
- Yazulla S, Studholme KM (2001) Neurochemical anatomy of the zebrafish retina as determined by immunocytochemistry. *J Neurocytol* 30:551-592.
- Yazulla S, Studholme KM, McIntosh HH, Deutsch DG (1999) Immunocytochemical localization of cannabinoid CB1 receptor and fatty acid amide hydrolase in rat retina. *J Comp Neurol* 415:80-90.
- Yazulla S, Studholme KM, McIntosh HH, Fan SF (2000) Cannabinoid receptors on goldfish retinal bipolar cells: Electron-microscope immunocytochemistry and whole-cell recordings. *Vis Neurosci* 17:391-401.
- Yoles E, Schwartz M (1998) Elevation of intraocular glutamate levels in rats with partial lesion of the optic nerve. *Arch Ophthalmol* 116:906-910.
- Young RW (1987) Pathophysiology of age-related macular degeneration. *Surv Ophthalmol* 31:291-306.
- Yu DY, Cringle SJ (2001) Oxygen distribution and consumption within the retina in vascularised and avascular retinas and in animal models of retinal disease. *Prog Retin Eye Res* 20:175-208.
- Yu DY, Su EN, Cringle SJ, Yu PK (2003) Isolated preparations of ocular vasculature and their applications in ophthalmic research. *Prog Retin Eye Res* 22:135-169.
- Yu M, Ives D, Ramesha CS (1997) Synthesis of prostaglandin E2 ethanolamide from anandamide by cyclooxygenase-2. *J Biol Chem* 272:21181-21186.
- Zakrzaska A, Schlicker E, Baranowska M, Kozłowska H, Kwolek G, Malinowska B (2010) A cannabinoid receptor, sensitive to O-1918, is involved in the delayed hypotension induced by anandamide in anaesthetized rats. *Br J Pharmacol* 160:574-584.
- Zeng HY, Zhu XA, Zhang C, Yang LP, Wu LM, Tso MO (2005) Identification of sequential events and factors associated with microglial activation, migration, and cytotoxicity in retinal degeneration in rd mice. *Invest Ophthalmol Vis Sci* 46:2992-2999.
- Zhang D, Saraf A, Kolasa T, Bhatia P, Zheng GZ, Patel M, Lannoye GS, Richardson P, Stewart A, Rogers JC, Brioni JD, Surowy CS (2007) Fatty acid amide hydrolase inhibitors display broad selectivity and inhibit multiple carboxylesterases as off-targets. *Neuropharmacology* 52:1095-1105.
- Zheng L, Gong B, Hatala DA, Kern TS (2007) Retinal ischemia and reperfusion causes

capillary degeneration: Similarities to diabetes. *Invest Ophthalmol Vis Sci* 48:361-367.

Zimmer A, Zimmer AM, Hohmann AG, Herkenham M, Bonner TI (1999) Increased mortality, hypoactivity, and hypoalgesia in cannabinoid CB1 receptor knockout mice. *Proc Natl Acad Sci U S A* 96:5780-5785.

Appendix i: License for Figure 1.1 and 1.3



Contracts, Copyrights  
and Permissions

Two Penn Plaza  
New York, NY 10121-2298  
212 904 1674 ext.  
252 904 6883 Fax

PERMISSION LICENSE: COMMERCIAL PRINT AND ELECTRONIC USE

Request ID/Invoice Number: JDA48630

Date: July 29, 2010

To Joanna E. Slusar  
Dalhousie University  
Department of Pharmacology  
5850 College Street  
Halifax NS B3H 1X5  
CANADA  
"Licensee"

McGraw-Hill Material

Author: Riordan-Eva, Paul and Whiteher, John  
Title: Vaughan & Asbury's General Ophthalmology, 17th © 2008  
ISBN: 0071443142  
Description of material: Figures 1-7, 1-17, 1-26, and 1-13 (ONLY)

Fee: WAIVED

Licensee Work

Author: Joanna E. Slusar  
Title: *Examination of neuroprotective effect of URB597 in the young and aged rat retina*  
[Thesis]  
Publisher: Dalhousie University  
Format: Print and Electronic  
Distribution/territory: Canada  
Languages: English

Permission for the use described above is granted under the following terms and conditions:

1. McGraw-Hill hereby grants Licensee the non-exclusive right to include the McGraw-Hill Material in the Licensee Work and to reproduce and distribute the McGraw-Hill Material as part of the Licensee Work. The McGraw-Hill Material may be used only in the Licensee Work. All use of the McGraw-Hill Material is subject to the terms and conditions of this Agreement.

## Appendix ii: License for Figure 1.2

### ELSEVIER LICENSE TERMS AND CONDITIONS

Aug 18, 2010

---

This is a License Agreement between Joanna E Slusar ("You") and Elsevier ("Elsevier") provided by Copyright Clearance Center ("CCC"). The license consists of your order details, the terms and conditions provided by Elsevier, and the payment terms and conditions.

**All payments must be made in full to CCC. For payment instructions, please see information listed at the bottom of this form.**

Supplier	Elsevier Limited The Boulevard, Langford Lane Kidlington, Oxford, OX5 1GB, UK
Registered Company Number	1982084
Customer name	Joanna E Slusar
Customer address	5850 College Street Halifax, NS 3JH 4HK
License number	2492060963550
License date	Aug 18, 2010
Licensed content publisher	Elsevier
Licensed content publication	Molecular and Cellular Endocrinology
Licensed content title	Physiology and pathology of somatostatin in the mammalian retina: A current view
Licensed content author	Davide Cervia, Giovanni Casini, Paola Bagnoli
Licensed content date	14 May 2008
Licensed content volume number	286
Licensed content issue number	1-2
Number of pages	11
Type of Use	reuse in a thesis/dissertation
Requestor type	Not specified
Intended publisher of new work	n/a
Part on	figures/tables/illustrations
Number of figures/tables / illustrations	1



## Appendix iii: License for Figure 1.4



**Education**

Contracts, Copyrights  
and Permissions

Two Penn Plaza  
New York, NY 10121-2298  
212 904 2574 Tel  
212 904 6265 Fax

### PERMISSION LICENSE: COMMERCIAL PRINT AND ELECTRONIC USE

Request ID/Invoice Number: JQA42048

Date: July 29, 2010

To: Joanna E. Slusar  
Dalhousie University  
5850 College Street  
Halifax NS B3H 1X5  
CANADA  
"Licensee"

McGraw-Hill Material

Author: Junqueira, Luiz and Carneiro, Jose  
Title: Basic Histology: Text & Atlas, 12/e  
Description of material: Figures 11-11, 11-10, 11-16, and 23-9 (ONLY)

Fee: WAIVED

Licensee Work

Author: Joanna F. Slusar  
Title: *Examination of the neuroprotective effect of URB597 in the young and aged rat retina [thesis]*  
Publisher: Dalhousie University  
Format: Print and Electronic  
Distribution/territory: Canada  
Languages: English

Permission for the use described above is granted under the following terms and conditions:

1. McGraw-Hill hereby grants Licensee the non-exclusive right to include the McGraw-Hill Material in the Licensee Work and to reproduce and distribute the McGraw-Hill Material as part of the Licensee Work. The McGraw-Hill Material may be used only in the Licensee Work. All use of the McGraw-Hill Material is subject to the terms and conditions of this Agreement.

## Appendix iv: License for Figure 2.1

### WOLTERS KLUWER HEALTH LICENSE TERMS AND CONDITIONS

Aug 18, 2010

---

This is a License Agreement between Joanna E Slusar ("You") and Wolters Kluwer Health ("Wolters Kluwer Health") provided by Copyright Clearance Center ("CCC"). The license consists of your order details, the terms and conditions provided by Wolters Kluwer Health, and the payment terms and conditions.

**All payments must be made in full to CCC. For payment instructions, please see information listed at the bottom of this form.**

License Number	2492061158175
License date	Aug 18, 2010
Licensed content publisher	Wolters Kluwer Health
Licensed content publication	Stroke
Licensed content title	Novel Mouse Model of Monocular Amaurosis Fugax
Licensed content author	Dominique Claude Lelong
Licensed content date	Dec 1, 2007
Volume Number	38
Issue Number	12
Type of Use	Dissertation/Thesis
Requestor type	Individual
Title of your thesis / dissertation	Examination of the Neuroprotective Effects of URB597 in Young and Aged Rat Retina
Expected completion date	Sep 2010
Estimated size(pages)	100
Billing type	Invoice
Billing Address	5850 College Street St Charles Upper Building Halifax, NS B3H 4H4 Canada
Customer reference info	
Total	0.00 USD
Terms and Conditions	